Investigation of the Stability of Clay/Basalt Packing Materials

Prepared by D. R. Peacor, E. J. Essene, J. H. Lee

Department of Geological Sciences
University of Michigan

NOTICE

Availability of Reference Materials Cited in NRC Publications

Most documents cited in NRC publications will be available from one of the following sources:

1. The NRC Public Document Room, 1717 H Street, N.W.
   Washington, DC 20555

2. The Superintendent of Documents, U.S. Government Printing Office, Post Office Box 37082, Washington, DC 20013-7082

3. The National Technical Information Service, Springfield, VA 22161

Although the listing that follows represents the majority of documents cited in NRC publications, it is not intended to be exhaustive.

Referenced documents available for inspection and copying for a fee from the NRC Public Document Room include NRC correspondence and internal NRC memoranda; NRC Office of Inspection and Enforcement bulletins, circulars, information notices, inspection and investigation notices; Licensee Event Reports; vendor reports and correspondence; Commission papers; and applicant and licensee documents and correspondence.

The following documents in the NUREG series are available for purchase from the GPO Sales Program: formal NRC staff and contractor reports, NRC-sponsored conference proceedings, and NRC booklets and brochures. Also available are Regulatory Guides, NRC regulations in the *Code of Federal Regulations*, and *Nuclear Regulatory Commission Issuances*.

Documents available from the National Technical Information Service include NUREG series reports and technical reports prepared by other federal agencies and reports prepared by the Atomic Energy Commission, forerunner agency to the Nuclear Regulatory Commission.

Documents available from public and special technical libraries include all open literature items, such as books, journal and periodical articles, and transactions. *Federal Register* notices, federal and state legislation, and congressional reports can usually be obtained from these libraries.

Documents such as theses, dissertations, foreign reports and translations, and non-NRC conference proceedings are available for purchase from the organization sponsoring the publication cited.

Single copies of NRC draft reports are available free, to the extent of supply, upon written request to the Division of Technical Information and Document Control, U.S. Nuclear Regulatory Commission, Washington, DC 20555.

Copies of industry codes and standards used in a substantive manner in the NRC regulatory process are maintained at the NRC Library, 7920 Norfolk Avenue, Bethesda, Maryland, and are available there for reference use by the public. Codes and standards are usually copyrighted and may be purchased from the originating organization or, if they are American National Standards, from the American National Standards Institute, 1430 Broadway, New York, NY 10018.

Investigation of the Stability of Clay/Basalt Packing Materials

Prepared by
D. R. Peacor, E. J. Essene, J. H. Lee

Department of Geological Sciences
University of Michigan
Ann Arbor, MI 48109

LIST OF CONTRIBUTING SCIENTISTS

Jung Ho Ahn

Michael A. Cosca

Eric J. Essene

Carl Henderson

Lung Chuan Kuo

Jung Hoo Lee

Donald R. Peacor

Lu-Chyi Yau

ABSTRACT

Geological systems analogous to proposed packing materials have been
reviewed and investigated and approximate temperature limits for smectite,
mixed layer smectite/layer smectite/illite and illite have been found to be
100, 200 and 250°C respectively. All phases are metastable, with reaction
rates being controlled by factors influencing kinetics, principally temperature
and rock/water ratio. Even over geological time periods the phases may exist
metastably at low temperatures with low water/rock ratios. Experiments with
bentonite/basalt mixtures confirm that there is little change at 300°C
and below in simulated packing conditions for experimental durations of up to a
year and a half. Data are consistent with a lack of equilibrium, such that
experimental reactions occur at much higher temperatures than in geologic
systems, and cannot be used to reliably predict the state of such systems over
long time periods. Analysis of geological systems suggests that a suitable
continuous clay matrix can minimize the degree of transition of clays and
clay/basalt mixtures.

TABLE OF CONTENTS

LIST OF FIGURES

EXECUTIVE SUMMARY

Storage of high level nuclear wastes in subsurface repositories may
utilize a packing material as a physical/chemical barrier between solid waste
cannisters and the host rock. Packing materials may be subject to reactions
with actively circulating ground water at temperatures estimated to be up to
300°C and pressures of several hundred bars. Chemical, structural and textural
changes due to reactions with such hydrothermal solutions may degrade packing
performance such that, for example, porosity and permeability are increased,
thus accelerating cannister/ground water reactions. In order to evaluate the
potential for such reactions, we have:

(1) carried out hydrothermal experiments on candidate packing phases
(bentonite, illite, basalt and smectite/basalt mixtures) under conditions
analogous to those anticipated for the repository;

(2) thoroughly characterized both reactant and product experimental phases
using EMPA, XRD, SEM/EDS, and TEM/AEM techniques in order to evaluate
changes;

(3) reviewed and analyzed geologic systems which are analogous to the
repository packing systems; and

(4) integrated the data for both experimental and synthetic systems. This
is essential in that experimental reaction rates are notoriously slow for
systems at such low temperatures, but geologic systems exist for many
millions of years and therefore serve as natural experimental systems
which more accurately express an approach to equilibrium, and therefore of
the long term (10,000 years) state of the packing systems.

Basalt, smectite and illite have all been characterized and found to be
heterogeneous. Smectite and illite samples not only are contaminated by other
phases to be expected from their geologic origins, but are also found to be

1

locally heterogeneous in chemistry, structure and texture at TEM/AEM levels of resolution. Basalt contains both secondary phases on fractures (e.g. nontronite, opal and zeolites) and up to 25% of immiscible, two-phase glasses, one of which is K-rich; the latter may provide K to groundwater.

Experiments up to and including 300°C resulted in changes in starting materials only on an irregular basis and then only in limited ways, despite the apparent metastability of starting materials and the very long durations for the experiments, of up to approximately 1 1/2 years. These limited changes, and those occurring above 300°C (up to 460°C) are compatible with those occurring in geologic systems at much lower temperatures.

Analogous geologic systems are reviewed, and transitions in Gulf Coast and Salton Sea argillaceous sediments are examined in detail, as type examples of systems approaching closure and openness with respect to solutions. In general, smectite may exist at temperatures up to ca. 100°C, mixed layer illite/smectite up to ca. 200°C, and illite (relative to ideal muscovite) up to ca. 250°C. High porosities and permeabilities in the presence of fluids cause reactions to occur at lower temperatures, such that discrete, authigenic illite is found at temperatures as low as 115°C in Salton Sea sediments.

Experiments with clay minerals imply that reaction temperatures are higher than for natural systems, due simply to the relatively short times for such experiments. These and other data all imply that the reactions involve unstable phases, with reaction progress constrained by temperature, time, and mediating fluids. Even in geologic systems where reaction temperatures are significantly lower than those expected for the repository (300°C), closure to hydrothermal solutions caused by an appropriate impermeable clay mineral fabric causes reaction progress to be significantly decreased.

2

1. INTRODUCTION

1.1 General Framework

One concept of high level nuclear waste disposal involves the use of packing and backfill materials which fill the space between the container with solid-form waste and the host bedrock. Potential packing and backfill materials include natural geologic materials such as smectite, illite and basalt. A major function of the packing material is to isolate the container system from fluid present in the host rock. In an anhydrous environment the integrity of the cannister is enhanced. In addition, migration of all elements, including any radionuclides which may be freed through breaching of the cannister, is dramatically retarded in a fluid-free environment. The packing material is therefore evaluated on factors such as mechanical strength, porosity, permeability, swelling (crack-sealing) properties, ion-exchange properties, etc.

Whatever desirable properties are represented in the original packing material, long-term stability is essential in retaining those properties and thus maintaining its usefulness as a physical and chemical barrier. An ideal packing material would therefore be one whose properties do not change or which, if changed, cause an improvement in performance. It is therefore essential to determine the relative stabilities of candidate packing materials under the repository conditions, which include estimated temperatures up to 300°C, pressures up to several hundred bars, and saturation by fluids (principally H_2O).

Determination of relative stabilities may be carried out in two ways:

1. Laboratory experiments using candidate packing materials under repository conditions. This approach is essential, but conclusions may be problematic in that experimental conditions are at such low temperatures

3

that reaction is often difficult or impossible to obtain in the short times possible in experimental research. Therefore it is essential to interpret such experiments in light of the second major thrust of this report, viz.:

2. a review of the geologic literature relating to analogous systems, and research on those systems serving as models for packing materials and conditions. Geologic systems change over time periods of millions of years. Therefore, changes which may be significant over the proposed lifetime of the repository (10,000 years) are detectable in geologic systems, even though they may be undetectable under laboratory conditions.

It is essential, therefore, to integrate the results of both kinds of systems. Two major components of this report, therefore, concern both experimental and geologic systems, and their mutually integrated significance.

Lastly, it is essential to properly characterize the reactants and products in experiments, so that the changes and processes of change, if any, can be characterized. We have therefore undertaken a program of careful and complete characterization of selected candidate starting packing materials, in order to define their properties to serve as a reference for possible change in materials used in experiments. The products of those experiments have likewise been carefully characterized in order to detect changes. Although an integrated approach to characterization is utilized we have emphasized the results of Transmission Electron Microscopy (TEM) and Analytical Electron Microscopy (AEM) because these methods are capable of detecting changes at the highest levels of resolution (approximately 5 $\overset{o}{A}$ for TEM, and 300 $\overset{o}{A}$ for AEM). Therefore, small changes in experimental charges, which may not be detectable in bulk samples by the usual methods of characterization, but which when

4

integrated over the life of the repository have a significant effect on properties, may be detected. It is essential that such changes also be compared with those of natural geologic systems in order to test their validity and significance.

1.2 Materials and Range of Conditions Studied

Two candidate packing materials are crushed basalt and bentonite, either separately or in combination. These materials have already been extensively studied (e.g. Sasaki, 1982; Wood, 1983), and it has been concluded that bentonite is a suitable packing material up to temperatures of 300°C. The basalt is a candidate if the proposed repository in basalts at Hanford, Washington is ultimately selected. Smectite is the general name for a family of clay minerals of which montmorillonite is a specific Na and Al-rich variety. Bentonite is a rock rich in montmorillonite derived through alteration of volcanic ash which is mined in commercial quantities. In this report the terms smectite and bentonite will be used interchangeably. A third potential packing material is the clay mineral illite. It is to be preferred for backill and packing because smectite is known to change to illite under conditions similar to those of the repository (see Section 2.1). Smectite is known to be unstable under repository conditions, but systems with illite are much closer to being in equilibrium. Illite is thus much less likely to undergo change. Certain mixed layer illite/smectite clays retain a significant fraction of the expandability possessed by smectite, and thus have desirable engineering properties. Such clays are the principal component of certain shales and are thus available in larg. volume. However, such shales have significant proportions of other phases from which illite cannot be separated, but whose significance is in part addressed later in this report.

The characterized materials will be used in experiments that approximate, as nearly as possible, repository conditions. These include:

(1) A temperature range of up to 300°C, as this upper limit represents the maximum and long-term temperatures expected in the repository (Apted and Myers, 1982). Temperatures above 300°C will be used in order to accelerate reaction rates.

(2) A pressure near 300 bars, as this is the pressure equivalent to 1 km depth.

(3) A solution chemistry corresponding to either distilled water or an artificial solution having ion concentrations and pH equal to those of the BWIP proposed repository groundwater (Ferguson, 1982) (Table 4.2).

(4) Water/rock (W/R) ratios of 50 to 0.4 which are typical of natural hydrothermal fields (e.g., Savage and Chapman, 1982).

The geological literature will be reviewed for aspects of diagenesis of chemically and mineralogically similar systems over equivalent ranges of conditions, and the results integrated with those of the experiments.

1.3 Summary of Methodology

1.3.1 General Geologic Framework

Sedimentary or volcanic geological materials, following deposition at the surface of the earth, may be subject to burial under succeeding generations of such materials. Over periods of tens of millions of years, continued deposition of materials at the surface causes a given layer of material to become progressively more deeply buried. Such materials are thus subject to a series of changes in texture, chemistry, and mineralogy which is referred to by the term "diagenesis", and the general process of change is referred to as "burial metamorphism". Principal factors affecting those changes are:

(1) Temperature. The normal crustal geothermal gradient naturally causes an increase in temperature with increasing depth of burial. Such an increase in temperature results in an increase in the rate of chemical reactions, therefore causing changes in materials not originally in chemical equilibrium (including most materials in such an environment) toward a state of equilibrium. In addition, changes in temperature may cause phases which were initially in a state of chemical equilibrium to no longer be so related, such that changes toward a new equilibrium state will occur. An increase in temperature may also be initiated through unusual subsurface processes such as the intrusion of a magma or the introduction of circulating hydrothermal fluids.

(2) Pore solutions. All rocks, and especially sediments, have measurable porosities. Such pore space is generally filled by water-rich solutions which may have been part of the original sedimentary environment, water lost during diagenetic chemical reactions and which was initially included as part of the structure of originally deposited minerals (principally clays), or introduced as circulating waters from external sources. The sediments of the Salton Sea, for example, have been affected by circulating brines which are driven by thermal anomalies. Pore water is a primary factor in chemical reactions because it serves as a mediator for chemical reactions. Where pore water is known not to have been present, unstable mineral assemblages have been retained over hundreds of millions of years. In addition, circulating pore waters are the principal medium for transport of chemical (ionic) species. Addition or loss of components generally promotes chemical change as it causes a system to move away from an equilibrium state.

(3) Pressure. Burial metamorphism results in an increase in pressure due to the weight of accumulating overburden. Such increases in pressure have a negligible effect on equilibrium relations, as compared with the dramatic

7

effects of temperature. Pressure may affect reaction rates due to increases in solubility via pressure solution, but the effects are expected to be inconsequential under the relatively low pressure conditions of the repository.

In summary, the prime factors affecting diagenesis through burial metamorphism are temperature and pore solutions. The approximate temperature interval for diagenesis through a transition to low grade metamorphism in geological systems ranges up to approximately 300°C, after which changes are described within the regime of metamorphism. This range correponds approximately to the proposed limits of the repository (up to 300°C). Such geological systems are therefore appropriate as models of changes in packing materials. In addition, as packing materials may be contacted by pore solutions, (e.g., ground water, or water derived by dehydration of minerals due to increase in temperature), the natural geologic systems subject to such pore solutions (either static or convecting) are especially appropriate as models.

1.3.2 Hydrothermal Experiments

Although natural geologic systems are analogous to the packing systems, they are imperfect models for several reasons. First, they are exceedingly complex, compared to most synthetic systems. For example, shale may consist of major proportions of as many as six minerals, with clay minerals representing less than half of the total. The textural relations, types and proportions of pores and other variables are ill-defined. Secondly, although changes may occur in geologic systems over tens of millions of years, such times are inappropriate for a repository; when similar materials exist over repository storage intervals, they might remain unaltered, albeit in a metastable state.

Synthetic systems do offer the opportunity to control the variables which act independently in geologic systems, and to maintain relative simplicity in starting materials. If changes do occur in experimental materials it is possible to at least qualitatively determine the relative effect of different variables and the rates of change. Changes occurring in geologic systems may therefore be placed on a more predictable basis. We emphasize, however, that the results of either experimental or natural geological systems are, separately, subject to misinterpretation. It is therefore essential that the results of each be interpreted in an integrated manner.

There are some general problems associated with laboratory experiments as carried out under repository conditions. First, these experiments are carried out at relatively low temperatures. As 300°C is the projected maximum temperature to which packing materials are subjected, this is the normal upper temperature limit for experiments. It is well known after many decades of experimentation on geologic materials over temperatures extending to those of igneous melts, that it is difficult if not impossible to reach equilibrium at temperatures at or below 300°C. Indeed, it is difficult to even induce small changes in some phases even though they are known to be unstable. This is particularly true of silicates (e.g. clay minerals, minerals of basalts), whose reaction rates are exceedingly slow. Therefore, the lack of change, or the presence of small changes, in experiments must be viewed with extreme caution. Furthermore, the results of such changes cannot generally be viewed as the final, equilibrium system to be expected under the times proposed for a repository. We are especially concerned, for example, that Wood (1983) has concluded that bentonite is "sufficiently stable" at 300°C to serve as a packing material. This conclusion was based on relatively short-term laboratory experiments involving basalt and bentonite without proper regard for

evidence from the geological record. Indeed, smectite is not "stable" at 300°C, and even the small changes observed by Wood, when extrapolated over the durations planned for the repository, are significant.

Secondly, laboratory experiments commonly occur over time intervals of weeks or months, and a year is a very long experiment. The geological literature is replete with examples of systems which are known to change over the geological time scale, but for which equivalent laboratory experiments show no change. Experiments over long time periods may result in changes which are so small as to be undetectable, yet changes which when extrapolated over thousands of years are significant.

In summary, then, we note that although laboratory experiments provide data that are unique relative to natural geological systems, such data must be treated with caution, and only by analogy with geologic systems which are known to generally display a closer approach to equilibrium conditions.

1.3.3 Characterization of Materials

The changes attendant to diagenesis in geological systems or to synthetic hydrothermal systems are primarily concerned with three different aspects of the component phases, or minerals, and include textural, chemical and structural changes. It is essential to characterize the materials used in synthetic runs as completely as possible to detect any changes in run products. Insofar as starting materials in experimental runs, or actual packing materials, are not pure, it is necessary to identify all components of the sample; otherwise changes which are observed may be incorrectly ascribed to an apparently pure starting material. We therefore have undertaken a complete mineralogical characterization of both starting and product run materials using a variety of techniques. These include polarizing microscope techniques on both crushed fragments and thin sections, powder X-ray diffraction, Scanning

10

Electron Microscopy (SEM) including qualitative energy dispersive analyses, and TEM and AEM techniques. AEM is emphasized because:

(1) It is essential to determine the characteristics of phases present at the trace to minor amounts.

(2) Candidate phases such as smectite and illite occur in grain sizes too small to be resolved by conventional techniques. SEM may resolve textural relations for only some grains, while AEM is the only technique capable of providing chemical analytical data on single phases, especially of the clay minerals. Other characterizing techniques such as X-Ray Diffraction (XRD) only yield data on bulk samples which are indirectly a function of individual grain features and directly an average over a large volume.

(3) Laboratory experiments occur over relatively short (on the order of months) time periods, relative to geological conditions, and occur at relatively low temperatures (300°C), at which reaction rates are slow and equilibrium difficult to obtain. Reactions which may go to completion over geological time spans may be incomplete or hardly occur at all, therefore. Only by examining such materials at the TEM/AEM scale may subtle changes be observed, which when extrapolated over the life of the repository, may be significant.

1.3.4 Integration of Data for Natural and Synthetic Systems

In the above sections we have pointed out the principal advantages and disadvantages of geological versus synthetic systems as models for packing materials and conditions. The geological systems tend to approach an equilibrium state and thus to provide a model for changes over the long time periods required for the repository. On the other hand, the complex variables

associated with geological systems can be carefully controlled and the relative effects of separate variables may be identified.

We maintain that data from either experimental or geologic systems is subject to serious error and/or misinterpretation when separately considered, but that data of both types are mutually supportive. Integration of data from both types of systems is therefore a prime goal of this project, and our conclusions are based on such mutually inclusive interpretations.

2. REVIEW OF GEOLOGICAL SYSTEMS

2.1 Smectite/Ilite/Muscovite Transitions

Characterization of the changes in mineralogy, chemistry, structure, and texture (collectively referred to as the process of diagenesis) of argillaceous and clastic sediments has been and continues to be a major goal of sedimentary petrologists, and a vast and growing literature exists on the subject. Comprehensive reviews have been given by Singer and Muller (1983) and by Kisch (1983) with additional references by Larsen and Chilinger (1983). Such studies are concerned, in part, with changes in the clay minerals smectite and illite in response to increasing temperature (up to approximately 300°C), geologic time, pressure and factors relating to pore solutions, including chemistry of solutions, rock/water ratio and fluid flow. As smectite and illite are prime candidates for packing materials, and as the geological paramaters are equivalent to those of the repository, such geologic systems are natural analogues of the repository. Because times of formation of many tens of millions of years are available for geological systems, they represent long-term experiments wherein the lack of reaction due to limited laboratory experiment durations is obviated.

Smectite is one of the principal minerals of clastic, argillaceous sediments (muds), having been derived by surface weathering of preexisting silicates (commonly volcanic tuff), and transported by water to a site of sedimentation. Progressive burial of such sediments by additional sediments (to depths of tens of thousands of feet) in part causes changes in temperature, pressure and other variables resulting in the progressive conversion of smectite into mixed layer smectite/illite (I/S) and eventually to 100% illite. This transformation has a dominant influence on major changes in the properties of the sediments. It has therefore been studied in detail by many investigators, e.g. Weaver (1959), Burst (1959, 1969), Powers (1959, 1967), Dunoyer de Segonzac (1964, 1969, 1970), Muffler and White (1969), Perry and Hower (1970, 1972), Weaver and Beck (1971), Eslinger and Savin (1973), Hower et al. (1976) and Boles and Franks (1979). Of this sampling of a vast literature, Hower et al. and Boles and Franks review the essential data and conclusions of clay diagenesis.

Smectite is the name applied to a large family of expandable clay minerals with common crystal structure features, but variable chemistry. Montmorillonite is a specific member of the family, which is the variety proposed as a packing material and is common in argillaceous sediments. Its composition is approximately

$$Na_x(Al,Mg,Fe)_2(Si,Al)_4O_{10}(OH)_2 \cdot nH_2O; \quad x < 0.3; \quad Mg,Fe \ll Al.$$
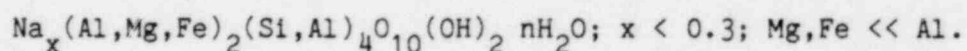
The structure consists of two layers of tetrahedra (principally Si with minor Al) sandwiched to the top and bottom of a layer of octahedrally coordinated cations (principally Al, but with some Mg and Fe). The latter is the so-called dioctahedral layer of montmorillonite. In other varieties of smectite this layer is dominantly a trioctahedral layer principally occupied by Mg and Fe. Smectite basically consists of stacks of such basic T-O-T layers, each of which

13

extends infinitely in two dimensions, but with one important addition. Because such T-O-T layers have a small excess of negative charge, additional cations are required for charge balance. Alkali and alkaline earth cations such as Na and Ca occupy interlayer sites. In part because bond forces between adjacent T-O-T layers are weak, such large alkali and alkaline earth cations may attract coordination spheres of H_2O molecules, thus effectively forming continuous layers of large cations and H_2O which alternate with T-O-T layers. As water pressure changes in the environment, H_2O may be gained or lost with concomitant expansion or contraction of the cation-water layer. Complete dehydration under vacuum leads to complete loss of H_2O with "collapse" of the layers to an H_2O-free basic layer thickness of $10\overset{\circ}{A}$ (effectively the thickness of a single T-O-T layer); addition of H_2O may cause gain of H_2O with concomitant expansion of the cation-H_2O layer to a characteristic thickness of approximately $14\overset{\circ}{A}$ at ambient conditions, but increasing H_2O-pressure may cause expansion to much higher layer thicknesses. Even the "normal" state of expansion is 40% greater than that of the collapsed state, and much higher values are possible at relatively low $P(H_2O)$. The expansion of smectite with addition of H_2O with concomitant loss of porosity and decrease in permeability in clay aggregates is of course a principal reason why bentonite is considered to be a potential packing material.

Illite is derived from smectite principally by substitution of K in interlayer sites in substitution for Na, and of Al for Si. The overall change can be written, to a first approximation, by the reaction smectite + K + Al = illite + Si + Na. Illite derived from smectite has the approximate composition $K_{0.5}(Al,Mg,Fe)_2(Si_{3.5}Al_{0.5})O_{10}(OH)_2$ with Al $\gg$ Mg,Fe.

14
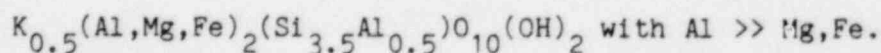
These substitutions collectively result in "collapse" of the structure to its characteristic 10Å, T-O-T layer repeat; i.e. the potential for gain of H_2O associated with interlayer cations is lost and the resulting clay mineral, illite, is not expandable or collapsible. This is in large part due to the fact that increasing substitution of Al for Si results in a higher negative layer charge, which in turn results in a higher proportion of interlayer K (relative to, say Na), with greater interlayer bonding forces.

The transition of smectite to illite generally occurs gradually with increasing depth, from 100% smectite through a series of so-called mixed-layer illite/smectite phases to 100% illite with the proportion of illite increasing continuously. One theory holds that intermediate phases consist of alternating, ordered sequences of illite and smectite (ordered mixed-layer phases) (e.g., Hower et al., 1976) while some research indicates that illite occurs as discrete domains whose size and proportion increases with increasing degree to transition. This has little relevance to potential packing materials however. The principal point here is that the transition occurs gradually, and continuously over depth, time and other geologic variables; the change is permanent and results in a proportional permanent decrease in the expansion/contraction properties of the clay.

Illite is itself subject to further change. Further substitution, primarily of Al for Si and concomitant substitution of K in vacant interlayer sites ($K + Al = \square + Si$) results in transition toward the endmember phase, muscovite. Muscovite has the ideal composition $KAl_2(Si_3Al)O_{10}(OH)_2$, and it is the stable, final product in the transformation of smectite (assuming that K + Al are available and disregarding the role of other elements such Mg and Fe). The change in composition from illite to muscovite is accompanied by loss of H_2O from some interlayer sites occupied by K, change in mode of stacking of

layers from a disordered to an ordered sequence, and decrease in the concentration of structural imperfections with an increase in so-called "crystallinity" as detected by X-ray diffraction.

This sequential change from smectite to mixed layer I/S to illite to muscovite is idealized. In actual samples various domains of different clay mineral grains may display a variety of transition states, with some average state dominating. Thus a sample of so-called illite inevitably will retain some proportion of expandable smectite-like layers. Illite samples, then, may retain a minimum potential for drastic change, while retaining a potential for limited expansion. The Fithian illite described elsewhere in this report is such a material and is being studied in large part because its potential for change in the packing environment is minimal relative to smectite, and it retains some of the desirable engineering properties of smectite.

Weaver (1967) suggested that the K needed for the transitions is produced from breakdown of detrital K-feldspar and/or mica. This interpretation was supported by Hower et al. (1976), who observed a gradual disappearance of K-feldspar with increasing depth in Gulf Coast sediments. They suggested that K-feldspar may also be the source for Al. Weaver and Beck (1971) stressed the possible importance of the K supply from nearby shale formations during sandstone diagenesis. On the other hand, Boles and Franks (1979) proposed that the Al component of illite during the smectite-illite transition is entirely supplied from smectite layers and, therefore, some smectite must be consumed to form I/S. This implies that the smectite-illite transformation can proceed without Al from the pore solution. However, the supply of K (or other interlayer cations) is critical to the smectite-illite transition (or breakdown of smectite into a non-expandable phase), and these ions must be primarily

16

supplied from pore solution because their amounts are lower in smectite than in illite.

The presence of K is essential to the smectite-illite transition. However, it is possible for K to substitute for Na in bentonite to form an expandable K-bentonite. The transition to illite is primarily dependent on the substitution of Al for Si. As this is a sluggish process compared with the alkali substitution, it is the rate-determining step. Furthermore, smectite may transform to a variety of other phases, such as kaolinite, in geologic systems, and changes in it and in the properties of the aggregates within which it is included are therefore not entirely dependent on a supply of K.

The kinetics of the smectite-illite transformation have been studied experimentally in the temperature range of 150-400°C by Eberl and Hower (1976, 1977). They reported an activation energy of around 20 kcal/mole for the I/S transition, indicating the breaking of chemical bonds in tetrahedral/octahedral layers. They found that this transition is more rapid in K-saturated than in Na-saturated smectite. Eberl (1978) further showed that the inhibitory strength of monovalent ions for the smectite-I/S transition follows the order Li, Na, Cs, and K and of divalent ions, Ca, Mg, Sr, and Ba, which is positively correlated to the magnitude of dehydration energy of these ions. A higher negative charge in smectite layers is required to incorporate a cation with higher hydration energy into the interlayer site. Eberl and Hower (1977) showed that when reacted with water, Na-smectites typically break down into paragonite-bearing assemblages whereas K-smectite typically produces I/S. The inhibition of the smectite-I/S transition by Na, Ca, and Mg ions in the solution has also been demonstrated by Roberson and Lahann (1981).

17

Temperature ranges of the smectite-illite transition have been inferred from various field studies (Steiner, 1968; Burst, 1969; Muffler and White, 1969; Dunoyer de Segonzac, 1970; Perry and Hower, 1970, 1972; Eslinger and Savin, 1973; Foscolos and Kodama, 1974; Hower et al., 1976; Boles and Franks, 1979). Most of these results indicate a temperature of about 100°C for the onset of I/S formation (e.g., Perry and Hower, 1970; Foscolos and Kodama, 1974). Lower temperatures have also been reported (e.g., 60°C, Hower et al., 1976; Boles and Franks, 1979). Complete conversion of smectite to illite is estimated to occur at temperatures as low as 200°C (from experiments: Khitarov and Pugin, 1966; Sabatier, quoted by Dunoyer de Segonzac, 1969; Hiltabrand et al., 1973). The range of temperatures for the transformation of illite to muscovite is large (approximately 100-350°C). Oxygen isotope thermometry of coexisting quartz and illite from the Belt Series (Eslinger and Savin, 1973) indicates that 50% of the illite of the <0.5 m size fraction would have been converted from the $1M_d$ to the 2M polytype at a temperature of about 290°C. Coal-rank (references in Kisch, 1974) and illite crystallinity (Weaver, 1961; Kubler, 1964, 1967; Weber, 1972a, 1972b; for additional references see Kisch, 1983) are widely used as indicators of temperature, and thus degree of burial metamorphism (increasing depth, time, temperature) in a diagenetic sequence, and confirm this approximate temperature range.

Because the transitions occur at low temperatures, laboratory experiments which attempt to establish stability relations are inconclusive due to the slowness of reactions. It is not established that either smectite or illite has a true stability field under geologic conditions. The detailed textural and chemical relations between them indicate that smectite and illite are metastable, with the state of transition being kinetically controlled. Thus availability of large fluid volumes, which promote solution and

18

crystallization, as well as increasing temperature or any other factor which influences reaction rate, promote the transitions. Because smectite is uniformly observed to transform to illite and other phases when kinetic factors are favorable is itself evidence for the metastability of smectite. Nevertheless its continued existence in argillaceous sediments which are many millions of years in age point out that the expandable component of argillaceous sediments can be retained over geologic time at low temperatures where kinetic factors are unfavorable for the transition.

In summary, in geologic systems it appears that the smectite to illite conversion is complete at temperatures of approximately 200°C and that illite to muscovite conversion is complete at temperatures approaching 300°C. The reactions require a source of K and Al. The reacting clays are apparently metastable phases with reaction rates primarily controlled by temperature, the availability of fluids and concentrations of reacting cations in solution. However, under geological conditions which are analogous to the repository, smectite and illite may remain largely unaltered up to temperatures of 150 and 300°C, respectively. The relative significance of the factors affecting the reactions under the specific conditions of the repository remain to be determined.

2.2 Hydrothermal Experiments on Basalt

Many workers have experimented on basalt-water systems at low to moderate temperatures and for a variety of pressures and aqueous compositions (Liou et al., 1974; Seyfried and Bischoff, 1977, 1981; Mottl and Holland, 1978; Pohl and Dickson, 1979; Mottl and Seyfried, 1980; Spear, 1981; Moody et al., 1983; Apted and Liou, 1983). Several of these researchers started with natural or synthetic basalt glass presumably to speed reaction (Seyfried and Bischoff, 1977, 1981; Pohl and Dickson, 1979; Apted and Liou, 1983). However, this

19

starting material may yield highly metastable crystalline run products at low P-T, and in any case may not reproduce the reaction of a crystalline starting basalt. Some of the workers examined the reaction of basalt with seawater presumably to mimic seafloor alteration of freshly extruded ocean basalt (Seyfried and Bischoff, 1977, 1981; Mottl and Holland, 1978; Pohl and Dickson, 1979; Mottl and Seyfried, 1980). The greatly increased alkali chloride and alkaline earth bicarbonates may well be expected to yield different run products, particularly with respect to clay minerals whose chemistry is strongly controlled by exchange with aqueous fluids. Many of the workers conducted experiments at higher pressures (> 1 kb) and/or higher temperatures (> 400°C) in order to mimic regional metamorphism and to promote detectable reaction (Liou et al., 1974; Pohl and Dickson, 1979; Spear, 1981; Apted and Liou, 1983; Moody et al., 1983). Such experiments, while probably attaining a closer approach to equilibrium assemblages (at a given P, T, X, fO_2, fH_2O, etc.) provide less information on intermediate steps in the hydrothermal alteration of basalt precisely because of the approach to equilibrium. Experiments are needed with crystalline basalt and appropriate groundwaters if one is to hope to predict expected mineral assemblages for a given P, T, time, aqueous system, and interactive backfill material. For these reasons, it was decided that experiments on natural Umtanum basalt + H_2O, + high-T groundwater, + clay backfill would be useful in constraining the alteration history of Umtanum basalt. Although the solutions were analyzed after the experimental runs for alkalis, and alkaline earths, it was decided that a greater emphasis would be placed on the proper characterization of the alterations of the solids.

20

2.3 Analogous Geologic Systems

The results described in this section represent, in part, results of our studies of diagenesis of sediments over the range of temperature (below 300°C) of the repository, focusing on the smectite/illite/muscovite transitions, and have been carried out emphasizing STEM/AEM techniques (references to our work include Lee et al., 1982a, 1982b, 1983, 1985a, 1985b, 1986c; Lee and Peacor, 1983, 1986, 1988; Ahn et al., 1983; Yau et al., 1983; Ahn and Peacor, 1985, 1986). The systems described here are representative of the range of conditions postulated for the repository and are generally representative of the large number of geologic systems for which clay mineral transitions have been studied. Furthermore, although these systems have been studied by a number of other investigators using a variety of techniques, and thus serve as valid type cases on that basis alone, we have studied them using STEM/AEM techniques which have been emphasized in this project as applied to experimental materials in Section 4. The results can therefore be directly correlated and integrated with experimental results.

Three sequences are described below. These include an approximately 3000 m depth interval of Gulf Coast sediments and a transitional sequence of mudstone to slate in the Martinsburg Formation at Lehigh Gap, Pennsylvania. These two sequences, when combined, represent a continuous sequence of diagenesis for temperatures up to approximately 250°C. As shown below, the changes in mineralogy apparently occur under closed system conditions; i.e., fluids are excluded by the impermeable clay matrix. By contrast, a sequence from the Salton Sea geothermal field represents a completely open system, with geothermal waters flowing through permeable sediments, with temperatures exceeding 300°C. These contrasting systems thus represent limiting cases in water/rock ratios relative to the repository conditions.

2.3.1 Gulf Coast Sequence

The changes that occur in the Gulf Coast sediments were described by Hower et al. (1976). Smectite is the original detrital clay mineral at shallower depths. The major changes in mineralogy and chemistry which occur at the depth interval between 2000 and 3700 m are an increase in the illite proportion of mixed-layer I/S from 20 to 80%, a decrease of calcite from 20% to 0%, a decrease of K-feldspar to 0% and an increase of chlorite with increasing depth. However, the bulk chemical composition shows no major changes with depth except for a decrease in CaO concomitant with the decrease in calcite. On the other hand, the <0.1 m fraction (virtually pure I/S) exhibits a large increase in K_2O, Al_2O_3 and a decrease in SiO_2, implying the reaction:

$$\text{smectite} + K^+ + Al^{3+} = \text{illite} + Si^{4+}.$$
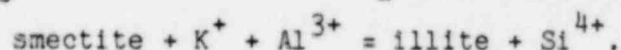
The K and Al appear to be derived from the decompositon of K-feldspar (and mica) and the excess Si forms quartz. Below the 3700 m depth, no further major changes in mineralogy and chemistry are observed.

TEM observations (Ahn and Peacor, 1985, 1986) using the same samples as in Hower et al. (1976) reveal the nature of the transitions. Transformation from smectite to illite in beginning stages at shallow depths occurs on a small scale. Illite layers appear as small domains (usually less that 100 Å, or 10 illite layers, in thickness) within smectite crystals (Fig. 2.1a). Smectite crystals are imperfect and irregular with a characteristic appearance of undulating and anatomosing layers with high concentrations of defects such as dislocations and general heterogeneities in both local chemistry and structure. Illite, in contrast, generally shows much more regular, straight and well crystallized structure layers. As the smectite to illite conversion proceeds in deeper sections, the domains of illite layers become thicker and longer and finally become dominant over smectite layers below 3700 m

22
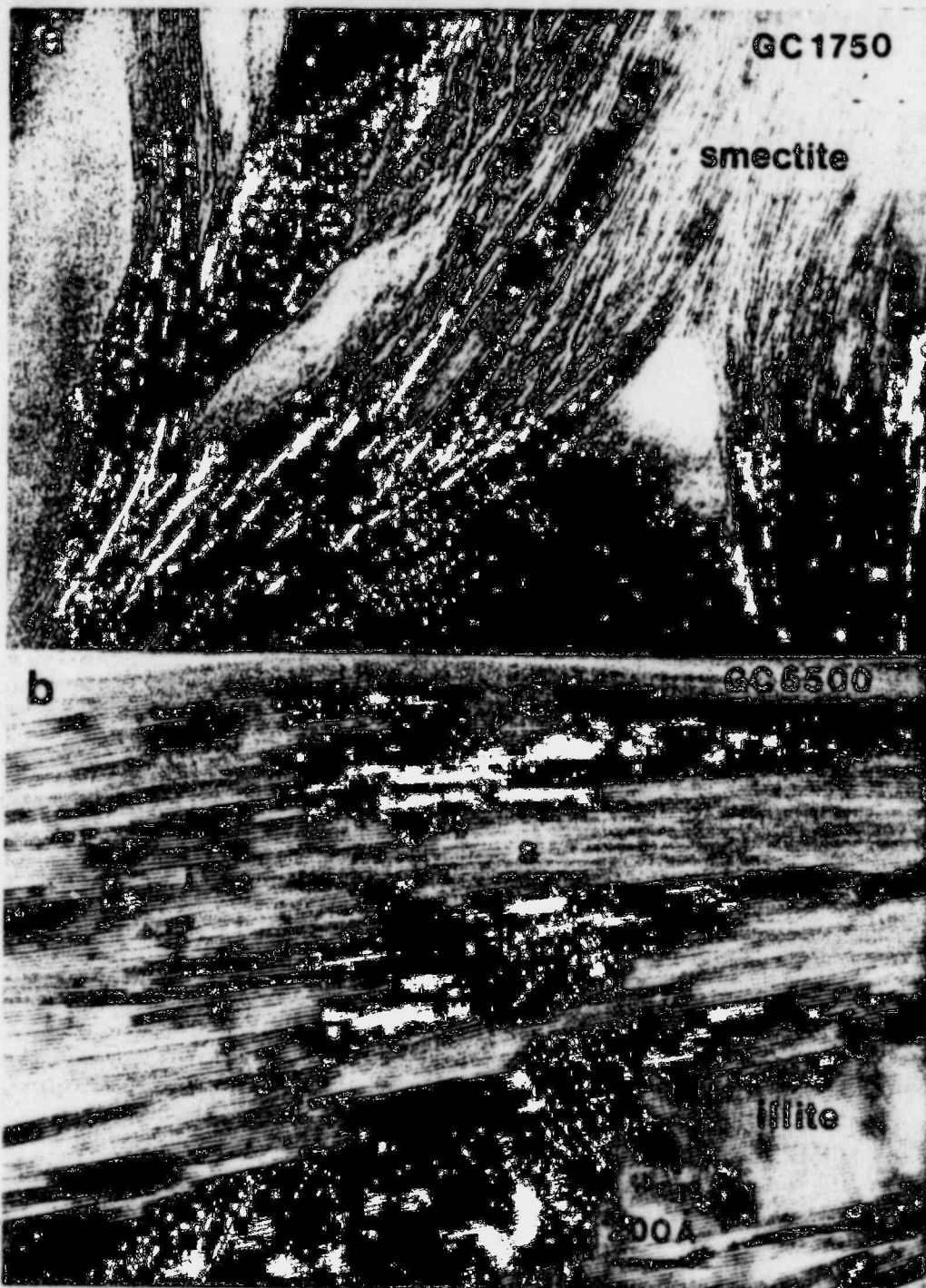
Figure 2.1. TEM lattice-fringe images of samples from Gulf Coast sediments at two different depths, (a) 1750 m and (b) 5500 m showing changes in smectite and illite layer proportions: (a) At 1750 m depth, smectite is dominant over illite. Smectite layers are characteristically very irregular and imperfect. Small packets of illite (i) occur within smectite. (b) At 5500 m depth, illite is the dominant mineral. The layers are relatively regular and well crystallized but show some imperfections along grain boundaries (packet boundaries) with mottled contrast features. Smectite (s) is rare and shows very little contrast because it is easily damaged by the electron beam relative to illite. (photos from Lee et al., 1985a)

(Fig. 2.1b). As smectite transforms to illite, the proportion of trioctahedral chlorite (and berthierine) also increases, occurring as packets of layers intergrown with or closely associated with smectite and illite. Ahn and Peacor (1985) showed that the illite has a lower proportion of Mg and Fe than the smectite from which it is derived, and that the chlorite (or berthierine) is largely derived from this Mg and Fe. In addition, kaolinite is also locally derived from parent smectite, and Ahn and Peacor propose that this occurs where the K necessary to form illite is not available.

An important feature of the smectite to illite transformation in Gulf Coast sediments is that the illite forms as a direct replacement of parent smectite. Transformed illite layers are parallel to and contiguous with smectite (Fig. 2.1). Hower et al. (1976) envisioned a transformation mechanism where the T-O-T layers of smectite were effectively retained in the transition. Boles and Franks (1979) called on destruction of at least some of the original T-O-T layers, to serve as a source of Al. Ahn and Peacor (1985, 1986) showed, however, that the transition mechanism is one which involves virtually complete solution and recrystallization of original smectite at the interface with expanding domains of illite. The distinction is important relative to kinetic factors. The activation energy for the actual solution and recrystallization mechanism must be orders of magnitude greater than one in which the T-O-T units are largely retained. It is easy to understand, then, how smectite can exist metastably even with K locally available, rather than transform to illite. The mechanism thus explains the sluggishness of the reaction and confirms that the rate-determining feature involves disruption of the T-O-T bonds (and is thus related to increase in tetrahedrally coordinated Al relative to Si) rather than simple exchange of K for Ca or Na; i.e. saturation of bentonite by K-rich solutions will not in and of itself result in

a transition to illite. The Al must also be made available from external sources (contrary to the hypothesis of Boles and Franks, 1979) and the structure must locally be destroyed and reconstituted.

One other important feature of the reaction mechanism as shown by Ahn and Peacor (1985, 1986) involves the scale over which components essential to the reaction must diffuse. The illite, kaolinite, berthierine and chlorite derived from original smectite directly replace original smectite. Diffusion of components thus can be shown to occur only over distances of the order to magnitude of the size of the clay mineral grains; i.e. over thousands of Angstroms. Abundant chemical and structural data attest to a lack of pervasive, through-flowing solutions which would give rise to dramatic solution/recrystallization effects. The amount of water necessary to act as a catalyst for the smectite to illite transition need only exist at the structural discontinuity at the reaction front at any given time. Such a quantity of water may be vanishingly small; the structural water contained within smectite may itself be sufficient to serve as the vehicle for solution/recrystallization. Smectite is partially retained to depths up to 3000 meters because the compacted sediment is apparently closed with respect to water. The Gulf Coast sediments dramatically show the significance of H_2O as a catalyst to the reaction and show that exclusion of H_2O contributes to retention of smectite. The Salton Sea system as described below sharply contrasts with the Gulf Coast system in that regard, and further confirms the role of water.

2.3.2 Lehigh Gap Shale to Slate Sequence

The (Ordovician) Martinsburg Formation at Lehigh Gap, Pennsylvania represents a diagenetic sequence whose least deformed rock corresponds to the deepest section of the Gulf Coast sequence (Wintsch, 1978; Lee et al., 1985b). The outcrop of Lehigh Gap displays a transition of rock type from mudstone to slate which is paralleled by a gradual development of slaty cleavage perpendicular to the original bedding (Holeywell and Tullis, 1975). The least deformed mudstone is at the contact with the overlaying Shawangunk Formation. Illite and chlorite are the dominant clay-size minerals and no mixed-layer I/S is present in the outcrop. The Martinsburg Formation (approximately 4 km thick) is slate deformed by a (post-Silurian) tectonic event (Epstein and Epstein, 1969). The occurrence of undeformed mudstone is due to a pressure shadow caused by the competent quartzitic Shawagunk Formation (Epstein and Epstein, 1969) and the release of strain by the fault (Wintsch, 1978). No major changes in bulk composition (Wintsch, pers. comm.) and in mineralogy (Lewis, 1980) occur across the entire sequence. XRD studies (Lewis, 1980) show that the mudstone to slate transition is associated with a reaction of $1M_d$ illite toward well-crystallized, ordered 2M muscovite.

STEM/AEM observations reveal the chemical, structural and textural changes in the clay minerals in four significant ways:

1) The change in illite polytypism ($1M_d$ to 2M) is paralleled by an increase in K and Al and a decrease in Si. The composition of illite in the slate is close to that of muscovite; 2) Illite layers in mudstone samples generally are highly imperfect with small angle grain boundary-like features where structural defects (layer terminations and dislocations) are concentrated (Fig. 2.2a). Such imperfections decrease in concentration as the transition to slate proceeds (Fig. 2.2b); 3) Random interlayering between illite and chlorite

26
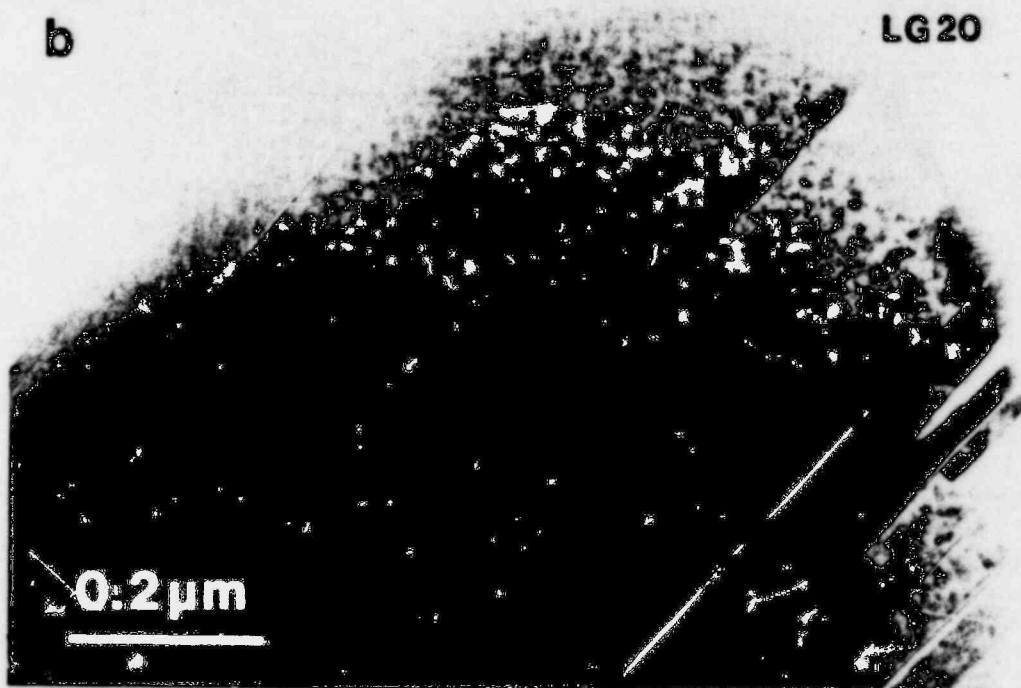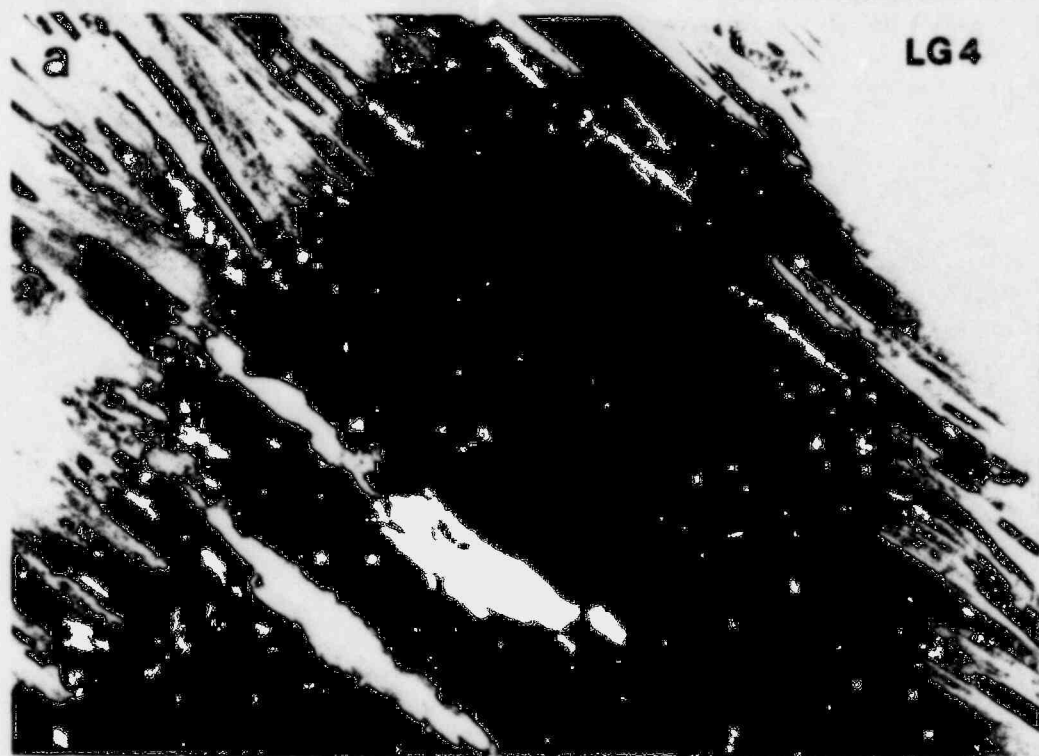
Figure 2.2. TEM images of samples from the Lehigh Gap outcrop showing changes in perfection of layer texture and structure in illite. Notice the increase in the thickness of layer packets and regularities along the packet boundaries from (a) mudstone near the Shawangunk-Martinsburg contact to (b) slate 120 m further from the contact. There are parallel changes in composition (see text). (Photos from Lee et al., 1985a)

27

occurs commonly in mudstones and intermediate samples but disappears in slate
samples and changes to discrete packets of two different layers (Figs. 2.3a and
2.3b); 4) Kaolinite layers which only rarely occur as packets interleaved with
illite, decrease in packet thickness and frequency with the transformation of
mudstone to slate (Lee et al., 1985b). Chemical compositions of illite and
chlorite analyzed by AEM are highly variable from one grain to another,
probably due to a highly variable composition of their precursor smectite.

The clay mineral rock-fluid reactions in the Gulf Coast sequence become
apparent at a depth of approximately 2000 m and at the temperature of
approximately 60°C (Hower et al., 1976). Most of the pore water had been
expelled from the sediment by that depth (about 10% pore water remaining;
Burst, 1969) and the sediments were well lithified. Many of the detrital
minerals (calcite, mica, K-feldspar and most importantly smectite) underwent
reactions under these changing conditions. Most of the components from the
breakdown of the detrital minerals were actively redistributed within the
system except Ca and water. Ca was completely expelled from the system while
the pore water content decreased further (to around 5%) along with the
interlayer water released by smectite dehydration. In a filtration experiment,
Benzel and Graf (1984) showed that Ca passes through smectite membranes
preferentially relative to Na. The K and Al from K-feldspar and mica react
with smectite which is converted to illite and excess Si which forms quartz
(Hower et al., 1976).

As the depth approaches 3700 m at (approximately 110°C) conditions for the
reactions are no longer favorable due apparently to lower permeability and lack
of pore waters (about 5%, Burst, 1969) relative to temperature conditions. At
this stage, the reaction rate becomes too slow even on a geologic time scale
(Burst, 1969). This is evidenced by the fact that most young diagenetic
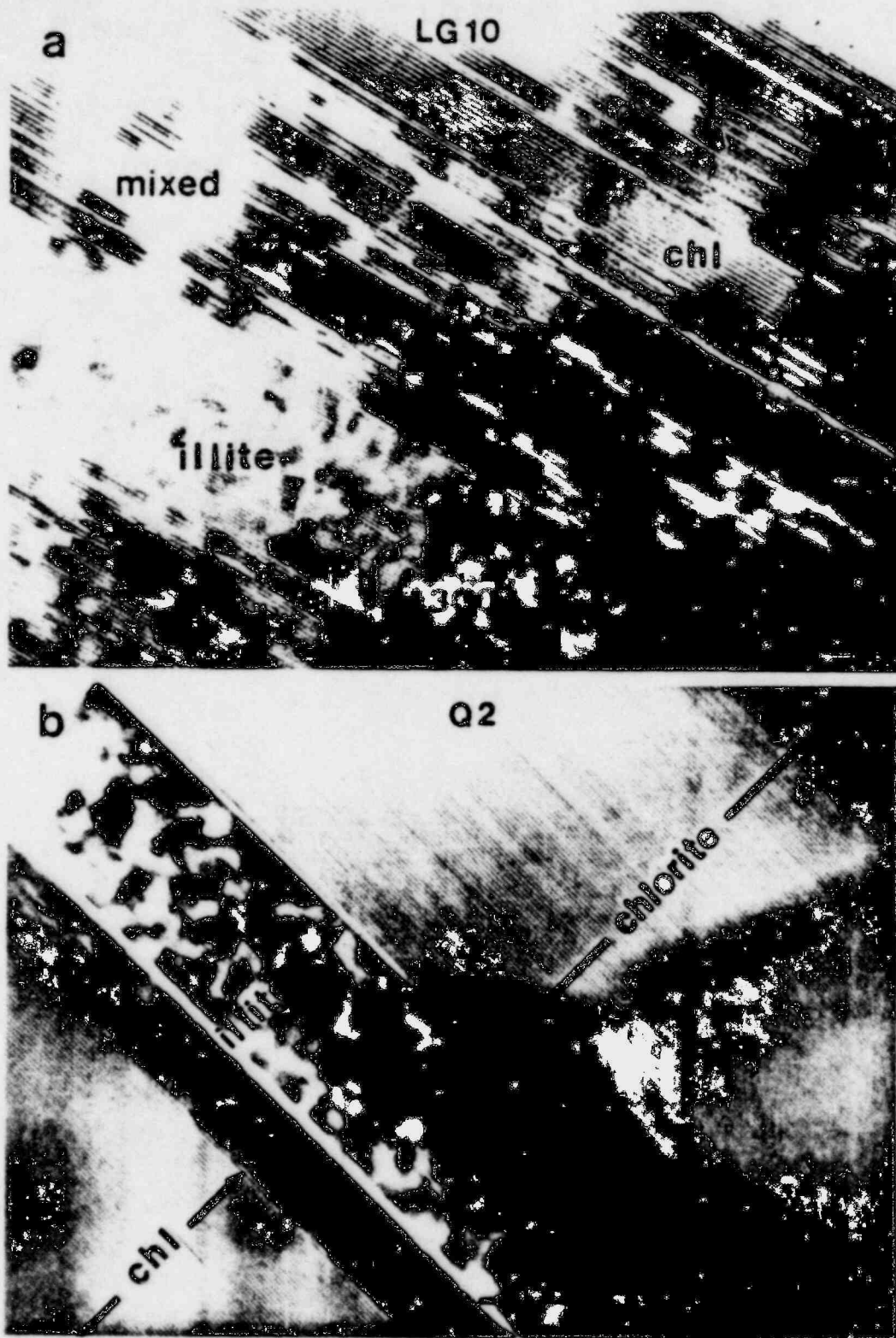
Figure 2.3. TEM lattice-fringe images of samples from the Lehigh Gap outcrop showing changes in illite-chlorite interlayering from (a) random interlayering in a sample closer to the Shawangunk-Martinsburg contact to (b) complete separation of the two minerals into well defined packets in slate samples. (Photos from Lee et al., 1985b)

sequences (Tertiary) extend only to approximately 80% illite in mixed-layer I/S (Velde and Hower, 1963; Maxwell and Hower, 1967). STEM and SEM data also indicate that the changes occur on a small scale and at a slow rate even in the depth interval with the active mineral reactions. Therefore, the systems have reached a point where reaction rate is so slow that no major change can be detected within 10-20 million years (Burst, 1969).

Compared to the Gulf Coast sediments, Lehigh Gap samples represent a higher degree of diagenesis with further dehydration evidenced by absence of smectite and lower Ca content (Wintsch, 1978) and by lack of bulk chemical and mineralogical changes. It is inferred that the system was already closed at the time of deformation with a very low pore water content. Reactions in the Lehigh Gap system occurred very slowly on a local scale (only around hundreds of Angstroms: Lee et al., 1985b). Temperatures in the sequence are estimated, although imprecisely, to have been 200-250°C (Epstein and Epstein, 1969; Lewis, 1980; Lee et al., 1985b), but isothermal throughout the outcrop (Lee et al., 1985b). Under these conditions, reactions in the Martinsburg Formation were promoted by tectonic compression to produce the regionally developed slaty cleavage. However, the reaction rates near the Martinsburg-Shawangunk contact were still too slow (due to a local lack of stress) to result in a transformation to slate and, as a consequence, a diagenetic sequence displaying a gradual transition from illite (mudstone) to muscovite (slate) was developed.

The mineralogical transitions observed in both Gulf Coast and Lehigh Gap apparently occurred with systems that were closed to an influx of H_2O. There is abundant evidence for solution/recrystallization effects but only for those requiring transport of components over distances of the order of magnitude of microns. There is no evidence for the occurrence of pervasive, through-flowing solutions which could give rise to mass transfer over large distances and of

30

large volumes of materials. For example, Hower et al. (1976) and Lee et al. (1985c) show that the compositions of the sediments in each case remain effectively constant during diagenesis (except for some loss of H_2O). This, and the detailed textural/chemical/structural data derived from STEM studies show that the effect of pore solutions has been minimal.

An apparent cause of the lack of through-flowing solutions can be seen in the textural relations. For example, Figure 2.1a shows typical relations among clay minerals and non-clay minerals. The layers of smectite structure have very different orientations in different areas of the image (on the order of tens of degrees). However, if a path is chosen along any given layer of structure, or if a shift is made from one contiguous layer to another (where the structure is locally periodic, with only minor distortion), a route along apparently continuous structure can be traced, even between domains which are extremely misoriented relative to one another. This is especially evident where clay structure layers bend around grains of non-phyllosilicates. The clay minerals thus form a matrix of continuous structure which surrounds and includes grains of non-phyllosilicates. There is, effectively, a single, large continuous unit of clay structure. The term "grain" with its implication of well-defined grain boundaries, surface area, and intergrain pore space has little meaning insofar as the clay is concerned. Such a continuous matrix must serve, effectively, as a barrier to fluid flow and its existence readily explains the closure of the systems to water. The only mechanism for fluid flow would appear to be diffusion through the clay minerals, probably using the high density of dislocations as pathways. Such diffusion is clearly orders of magnitude less efficient than migration along grain boundaries where no clay matrix is present. Formation of an efficient clay matrix may therefore be a prime objective in a packing material.

31

The clay matrix described above is present in all of the Gulf Coast and Lehigh Gap samples studied. However, the shallowest and least altered sample in these studies has still been subject to effects of early diagenesis. The original sediments, for example, clearly consisted of separate, well-defined grains of detrital clay and non-clay minerals. The clay matrix then, must be the result of compaction and local recrystallization along grain boundaries, as a precursor to other more profound mineralogical transitions. The original compacted packing material must consist of separate grains, but the first interaction with pore fluids might well have a beneficial effect of promoting production of a clay matrix and causing a decrease in porosity and permeability. These factors are further discussed in a later section.

2.3.3 Salton Sea Sequence

The Salton Sea geothermal field represents extreme contrasting conditions relative to the Gulf Coast sediments insofar as fluid flow is concerned. An unusually high geothermal gradient (over 300°C/km: Helgeson, 1968) and actively circulating brine water (major elemental components Cl, Na, K and Ca; Muffler and White, 1969) promote reactions at relatively shallow depths in the Pliocene and Pleistocene sediments (Muffler and Doe, 1968) compared to most other diagenetic systems. The mineralogical relations of coarse-grained clasticshave been described in detail by McDowell and Elders (1980, 1983) while our work (Yau et al., 1983) is primarily on finer grained argillaceous sediments.

The mineralogy and petrology of Salton Sea materials have been studied as a function of depth by McDowell and Elders in the well Elmore 1 (1980, 1983). The original sediments have a high proportion of detrital clay minerals, which consist in large part of mixed-layer illite/smectite with approximately 70% illite. With increasing depth the smectite is converted to illite, and at a

32

depth of approximately 700 m (275°C; McDowell and Elders, 1980) there is no smectite detectable even in mixed-layer illite/smectite.

TEM images show that there are three kinds of illite present in the samples from well IID #2. One consists of original detrital grains of well crystallized illite/muscovite. As this constitutes a minor component of the sediment, we do not consider it further. A second type includes detrital smectite. Such material in near-surface sediments consists of smectite with domains of illite. The appearance of this material is nearly identical to that of Gulf Coast smectite/illite in an intermediate state of transition. As temperature (depth) increases, the size of illite domains increases until no smectite can be detected at a temperature of approximately 200°. The sequence of transition textures also is equivalent to these of the Gulf Coast sequence. As the proportion of such material decreases with depth we propose that the smectite not only is transforming to illite in some domains, but that it also must be subject to partial dissolution.

The third type of illite, the most abundant and significant, consists of subhedral crystals which in cross-section have a lath-like shape (Figure 2.4.). These crystals are flattened parallel to (001), and are approximately 250 A thick and 1 um in diameter. Detailed TEM/AEM data confirm that they are well-defined crystals of illite with morphologies which dramatically contrast with the morphology of Gulf Coast illite (Figures 2.5 and 2.6). The TEM images also show abundant pore space between grains of both illite and other minerals (preserved and occupied by epoxy). Such crystals have clearly formed by direct precipitation from pore solutions. The chemical components may have been derived at great distances from the crystals formed by precipitation, and have sources in the dissolution of a variety of original detrital grains including smectite, feldspar and quartz. We observe no direct

33

Figure 2.4. A TEM image of a sample from the Salton Sea geothermal field (250 m depth) showing lath-shaped authigenic illite crystals. (Courtesy of Y.C. Yau).
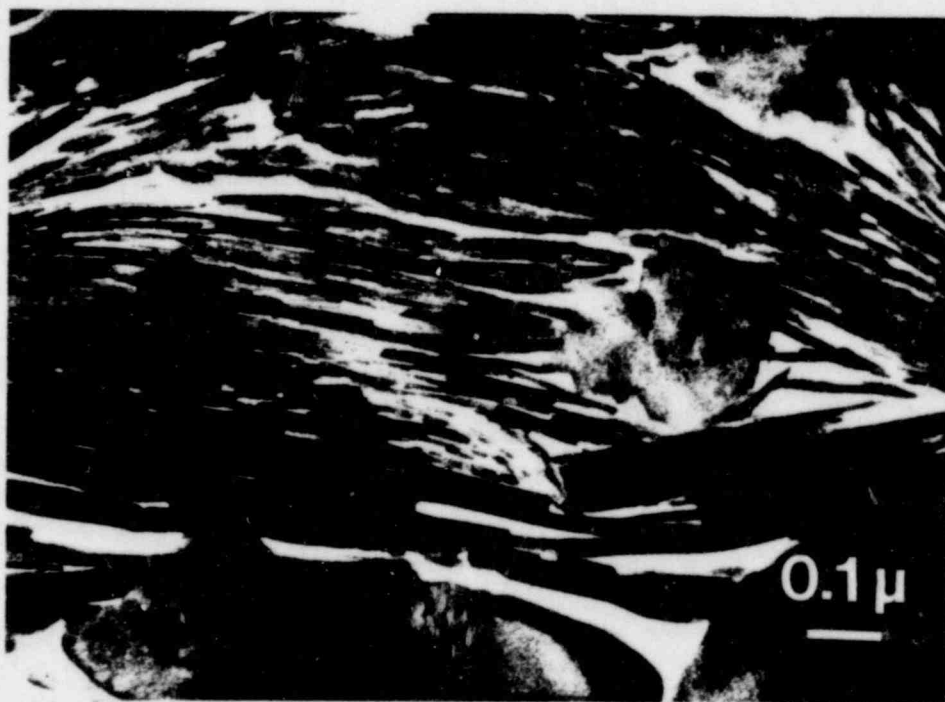
Figure 2.5. Euhedral illite crystals with interconnected pore space and
non-phyllosilicate detrital grains at a depth of 535 m feet (220°C),
Salton Sea. (Courtesy of Y.C. Yau).

35

Figure 2.6. Subhedral, subparallel illite crystals forming a semi-continuous
framework with a small proportion of pore space at a depth of 730 m
(260°C), Salton Sea.

relation between precipitated phases and any detrital phases so we have no way of directly identifying specific sources of components or of determining distances over which ion transport has been accomplished by flow of ascending solutions. We refer to such illite as being authigenic - sensu strictu.

Authigenic illite is first detected, with increasing depth and intensity of diagenesis, at 256 m (115°C; Yau, pers comm.). These illite laths tangentially fill interstices between detrital grains of non-phyllosilicates. With increasing depth the proportion of pore space decreases, but is still readily identifiable (Figure 2.6). However, illite laths become subparallel, as if they undergo reorientation through compaction. At the greatest depth at which such illite occurs (approximately 730 m), grains have coalesced into larger "mega-grains" presumably through a process of recrystallization along semiparallel grain boundaries, leaving low-angle-grain-boundary-like features defined by linear arrays of edge dislocations (layer terminations) as traces of original grain boundaries. In this fashion a semicontinuous matrix of clay minerals (primarily illite) is formed which is analogous to the continuous matrix in Gulf Coast sediments. Nevertheless, considerable connecting pore space is always observed.

At greater depths illite is entirely replaced by chlorite, and chlorite in turn by biotite at a temperature of approximately 315°C. The latter two phases likewise form well defined platy crystals. At depths which are transitional from illite to chlorite, or chlorite to biotite, single crystals consisting of separate packets of two different phases may be found.

The presence of an actively convecting system, then, causes flow-through of brines along intergranular pore space which dramatically contrasts with the Gulf Coast sediments, within which we have yet to positively identify any pore space at all. Detrital minerals undergo dissolution, with transport of ions by

convecting brines, with direct crystallization of brine components as illite (or phases such as chlorite or biotite at greater depth) in open pore space.

Although smectite is largely transformed to illite to depths with a temperature of 200°C, illite fails to react completely to muscovite at temperatures up to 250°C with increasing depth. The conversion of smectite to well-defined authigenic illite at temperatures (< 115°C) less than in the Gulf Coast sequence is interpreted as being due to the catalyzing influence of water, which promotes solution and recrystallization. The lack of a continuous clay matrix to minimize permeability, thus facilitating dramatic solution and recrystallization effects, is especially significant in relation to the role of packing materials in impeding fluid transport.

2.3.4 Summary of Specific Geologic Systems

In summary, these geologic systems imply the following relations concerning smectite/illite/muscovite reactions in relation to repository conditions:

(1) Argillaceous sediments such as Gulf Coast shales generally act as nearly closed systems; i.e., when compacted through burial, the clay fabric forms a closed network which forms a barrier to fluid flow. Even at the highest levels of TEM resolution pore space is not seen in such sediments.

(2) The smectite to illite to muscovite reactions are kinetically controlled, with active water flow through permeable rocks greatly increasing reaction rate. The effect may be more significant than that of temperature, although both factors are significant. At Lehigh Gap, the temperature was constant (approximately 200-250°C) across the entire sequence for geological times. The entire range of transformation from illite to muscovite is still preserved, however. Even though smectite, I/S and illite are thermodynamically

38

unstable these phases may be retained in geological systems, with smectite or I/S retained up to 150° and 200°C, respectively and illite up to approximately 300°C.

(3) STEM studies show that the transformations involve three factors: a) addition of K; b) substitution of Al for Si; c) reconstruction of entire layers or packets of layers of structure. Thus, smectite does not transform to illite only by substitution of K. The Al/Si ratio and other chemical bonds must be broken with at least small units of structure undergoing local solution/recrystallization. Such processes are inherently sluggish. They therefore require that the reaction of smectite to illite is basically sluggish. This explains why unstable clays such as I/S may be retained at elevated temperatures even over geological time periods.

3. CHARACTERIZATION OF STARTING MATERIALS

3.1. Definition of Starting Materials

There are three starting materials to be considered: smectite, illite, and basalt. Smectite (bentonite) is available in bulk through several commercial sources. We have characterized several commercial bentonites using XRD. All were found to be subject to contamination by other minerals (e.g. quartz, feldspar, calcite and even gypsum in one case). In addition, the principal 001 diffraction peak was of variable width in different materials, indicating the presence of some inhomogeneity in the bentonite itself. The material known as Envirogel was found to have both a minimum of contaminating phases and to have a sharp, well-defined 001 diffraction peak. It was therefore chosen as the standard bentonite. However, we have made no attempt to compare different samples of Envirogel, mined for example at different

times, and we therefore cannot guarantee homogeneity among diferent bulk samples. The basalt was a portion of a drill core, provided by Nuclear Regulatory Commission staff, which was obtained by drilling into the Umtanum Formation. This particular basalt flow considered as a target for the repository and was therefore sampled. Illite is a relatively poorly defined clay mineral which is quite variable from sample to sample. Different samples of "illite" may consist of several other minerals in variable proportions, and the "illite" component may vary in structure and chemistry. We have therefore obtained samples of illite through Ward's Natural Science Establishment which in turn came from the outcrop of "type" illite from Fithian, Illinois. This material is from the outcrop serving as the source of the material defined originally as illite and is available as a reproducable standard for research.

As shown in the following sections, even these carefully chosen samples of illite, smectite and basalt were found to be heterogeneous. Because such geologic materials are generally variable in composition we emphasize the necessity for different investigators to use the same, standard starting materials. Only in this way can experimental results be directly compared with a minimum of ambiguity.

Following procurement of each of these materials, approximately 1 kg of each was crushed and mixed, in order to guarantee homogeneity. All these materials were subsequently obtained from these source batches.

3.2 Characterization Procedures

3.2.1 XRD Analysis

Samples of both experimental products and starting materials were finely powdered and dispersed on glass slides. The XRD analyses were carried out using CuK_α radiation. The samples were scanned from $2°$ to $50°$ 2θ at a rate of

1° 2θ/min. Samples containing clays were generally treated with standard expanding agents when appropriate.

3.2.2 SEM/EDX Analysis

The analyses were conducted using a JEOL JSM-U3 instrument equipped with an energy dispersive X-ray detector operated at 15 kV. Samples were spread on aluminum blocks and were coated with gold film. Mineral identification was made using qualitative energy dispersive analyses when morphological data was not definitive.

3.2.3 STEM/AEM Analysis

Characterization by scanning transmission electron microscopy (STEM) was emphasized because it is potentially capable of detecting changes in experimental charges which may remain entirely undetected by unconventional methods. STEM provides high resolution TEM images (up to 1.5 $\overset{\circ}{A}$ point-to-point resolution) while also yielding quantitative chemical analytical data (resolution of 300 $\overset{\circ}{A}$ in ideal cases) on the same areas. Variations in structure, texture and chemistry can be characterized, therefore, in single areas.

Lattice-fringe images of 7 $\overset{\circ}{A}$ resolution or less were routinely obtained in this study, especially for clay minerals. For greater resolutions, defocus conditions must be calibrated in order to obtain valid structure images (Allpress et al., 1972; Anderson, 1978; Spence, 1981). As 001 spacings of clay minerals in this study are all equal to or greater than 7 $\overset{\circ}{A}$, images could simply by obtained under optimum contrast conditions in order that they reflect true lattice periodicities.

41

Analytical data are obtained by measuring peak intensity ratios of energy dispersive spectra for particular elements from thin edges of the sample. This is the "ratio method" (Cliff and Lorimer, 1972, 1975; Lorimer and Cliff, 1976) in contrast with the "absolute count method" as in EMPA. For silicate samples, peaks are ratioed to Si. This ratio is measured by comparison with that of a standard with a well-known composition. The ZAF correction can be avoided because these analyses are conducted only on thin edges of specimens generally less than 0.5 μm in thickness (Goldstein et al., 1977).

Since powdered samples are mainly used in this study, two different sample preparation techniques were used for STEM/AEM studies. First, powder samples were settled on a flat surface, embedded in epoxy, and cut perpendicular to the surface so that the (001) layers of clay minerals could be observed. Procedures for the preparation of ion-thinned samples (Blake et al., 1980) were then followed. Second, finely crushed samples were sparsely deposited on a C film on a Be grid. The first method (ion-thinned sample) was used for high resolution TEM observation of lattice fringes of clay minerals. The second method (crushed sample) was more frequently used especially for experimental run products because it requires less effort and uses smaller volumes of material.

The electron microscope used in this study is a JEOL JEM 100CX instrument modified for high-resolution analysis (Blake et al., 1980; Allard and Blake, 1982) using the analytical procedure of Isaacs et al. (1981) with conditions of STEM analysis from Lee and Peacor (1985a).

3.2.4 Optical and Electron Microprobe (EMPA) Analysis

Standard optical studies were carried out using polished thin sections of original geologic materials. Luminoscope observations were also made of all sections. Following complete optical characterization those same polished

42

sections were analyzed by electron microprobe techniques. Both qualitative energy dispersive and quantitative wavelength dispersive techniques were used under conditions of Isaacs et al. (1981). In the case of the basalt glass samples, thin sections used for EMPA were also submitted for ion milling, and analyzed by STEM.

3.2.5 Bulk Chemical Analysis

Following acquisition of bulk source materials, several kilograms of each were crushed and thoroughly mixed in order to obtain a source of homogeneous material for all further studies. Samples of each were submitted for chemical analysis by X-ray fluorescence analysis (XRF).

3.3 Results of Characterization

3.3.1 Smectite

Chemistry - Bulk chemical analytical data are given in Table 3.1. The data are typical for a bentonite. All elements, with the exception of P, are compatible with substitution in the smectite structure. Ahn and Peacor (1985) have recently shown by direct AEM analysis of individual grains of bentonite that Fe, Mg, Mn, Ti and K commonly occur in solid solution in smectite and need not be due to separate contaminating phases. Figure 3.4 includes a typical energy dispersive AEM pattern of smectite verifying the presence of Mg, K and Ca directly in the smectite. The portion of the pattern containing Ti and Fe peaks is not shown, but contains small peaks due to these elements. The Mg and Na peaks appear to be small, but nevertheless reflect relatively large proportions of these elements (peak intensities in the low energy portion of the spectrum are diminished in intensity relative to those at higher energy). The smectite is thus shown to have a complex composition, including the

43

Table 3.1 XRF analysis[+] of Wyoming bentonite and Fithian illite standard samples. (weight percent)

Oxide	Bentonite	Illite
SiO_2	59.8	54.8
TiO_2	0.20	0.91
Al_2O_3	17.7	18.6
Fe_2O_3[@]	3.79	7.63
MgO	2.11	1.69
MnO	0.02	0.01
CaO	1.71	0.61
Na_2O	2.24	0.49
K_2O	0.73	0.25
P_2O_5	0.08	0.25
LOI[&]	11.8	9.93
Total	100.2	99.8

[+]Analyzed by X-ray Assay Laboratories Ltd., Don Mills, Ontario

[@]Total iron as Fe_2O_3.

[&]LOI = Loss on ignition.

presence of some K, which presumably would facilitate the transformation to illite. The formula derived from the analysis, normalized to 4 Si, is

$$(Na_{.29}K_{.06}Ca_{.12})(Mg_{.21}Fe_{.21}Al_{1.53})Si_4O_{10}(OH)_2 \cdot nH_2O$$
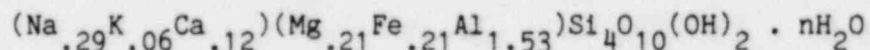
X-ray Diffraction - XRD patterns show a sharp 001 peak with d=12.5 Å as typical of well ordered bentonite. The peak was slightly asymmetric toward higher d-values. Approximately 15% of the sample consisted of subequal amounts of calcite, quartz, and a 10 Å mica (illite, as characterized by STEM/AEM data). The proportions of minerals were determined using ratios of integrated intensities of characteristic peaks of given minerals as compared with separately prepared standard curves. The proportions of these minerals, when combined with the AEM data for smectite, are compatible with the bulk chemical analytical data; i.e. calcite and illite account for a part of the Ca and K respectively. Treatment with ethylene glycol resulted in expansion of 001 layers to 16.6 Å, as typical bentonite.

In order to cause expansion of layers which is retained in the vacuum of the STEM, smectite was expanded with 0.1 N laurylamine HCl solution following the technique introduced by Yoshida (1973). The expansion of smectite was monitored at each step until no significant changes in the X-ray diffraction pattern occurred. The principal 001 peak splits into two separate peaks indicating a variable degree of structure expansion. As no further significant changes occurred with further treatments, it was concluded that the maximum expansion possible had occurred, and that the samples were suitable for TEM observations.

STEM-Data - Quartz appears in TEM images as sub-micron, subhedral crystals. The 10 Å phyllosilicate was shown to be illite by qualitative AEM analysis and through 10 Å lattice-fringe images. Calcite was not detected by STEM. Lastly, SEM images and qualitative EDX analytical data showed the

45

presence of some zeolite grains, as well as rare grains of a phase appearing to be amorphous silica.

Figures 3.1 and 3.2 show typical untreated (unexpanded) smectite at different scales. The electron diffraction patterns (insets) leading to these images have $d(001) = 13.0$ Å, in good agreement with the X-ray diffraction results. The patterns are generally streaked parallel to c^*, however, indicating the presence of a range of spacings.

Figure 3.1 shows typical smectite layers. They are severely distorted and imperfect in a variety of ways. Figures 3.2a and 3.2b are both lattice-fringe images at high resolution. The lines shown are images of the layers of structure, several Angstroms in width, and are typical of all smectites that we have observed. Individual layer spacings can been seen to differ from one another. Detailed analyses shows that most are 13.0 Å in width on average, as consistent with a normal, hydrated smectite, but others have a width of 10 Å. This is presumably due to collapse, with loss of water in the vacuum of the TEM of an original 13 Å layer. Imperfections in smectite structure such as undulating layers and variable layer spacings (Figs. 3.2a and 3.2b) are also commonly observed in natural smectite (Lee et al., 1985a).

Figures 3.3a and 3.3b show typical images of the expanded smectite (by laurylamine HCL). The electron diffraction patterns leading to these images show 001 layer spacings of 13 to 16 Å, as consistent with expanded layers as measured by X-ray diffraction. The same doubled 001 reflections are seen as in X-ray diffraction, and there is significant streaking parallel to c^*, as indicative of stacking disorder.

Figures 3.3a and 3.3b are both high resolution lattice fringe images showing individual layers of structure. Most layers have widths of 14 to 16 Å, with very few approaching 10 Å, verifying the permanent expanding ability of

46

Figure 3.1. A low magnification TEM image of an untreated Wyoming bentonite embedded in epoxy shows the form of smectite grains and their (001) structure layers oriented normal to the plane of the figure. The inset electron diffraction pattern shows an 001 layer stacking periodicity of 13.0 A on average.
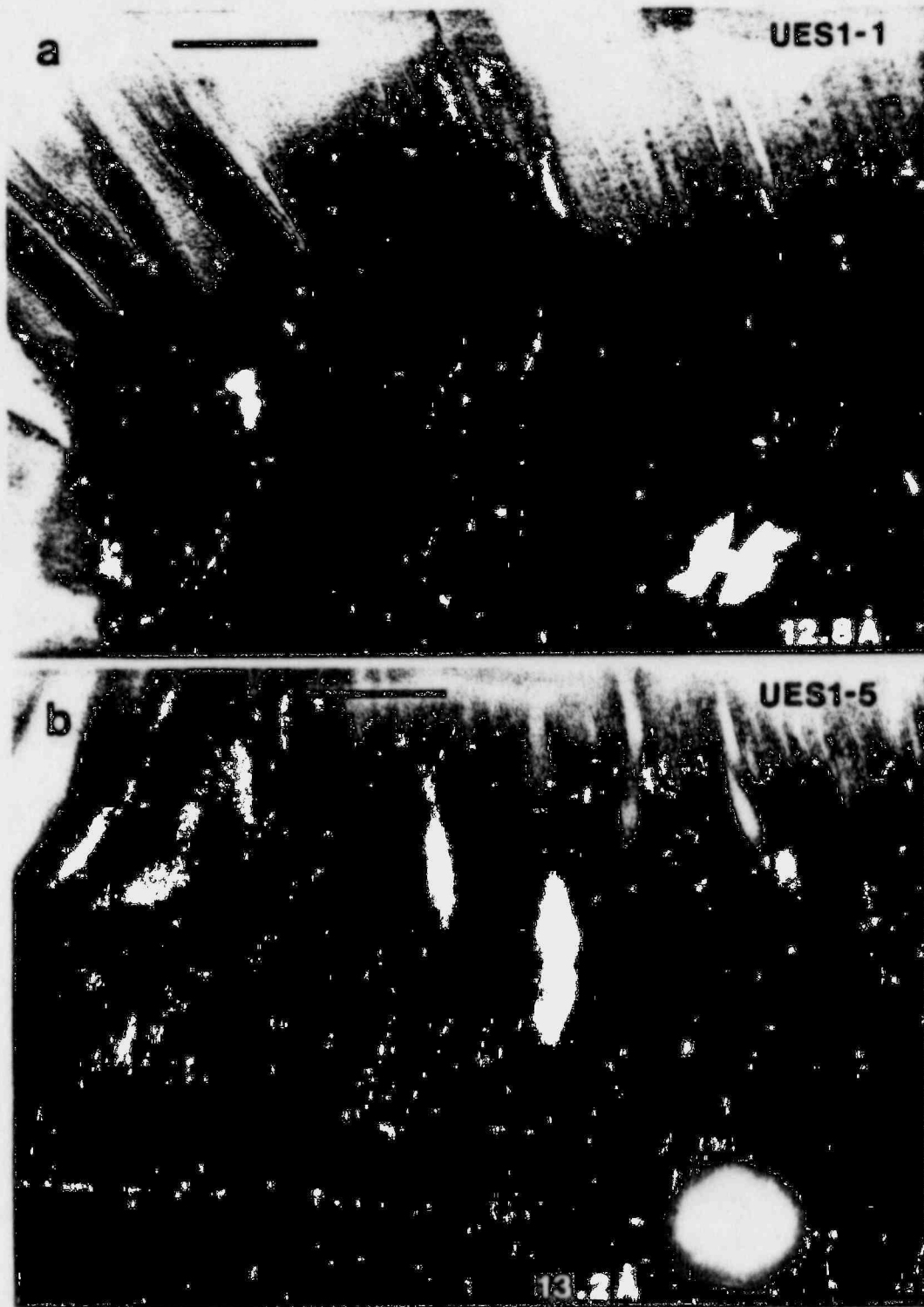
Figure 3.2. a. A TEM lattice-fringe image of untreated Wyoming bentonite shows partial collapse of layers. The average value of d(001) is 12.8 Å.
b. Same sample as in a. The scale bar is approximately 500 Å. The sample is embedded in epoxy.
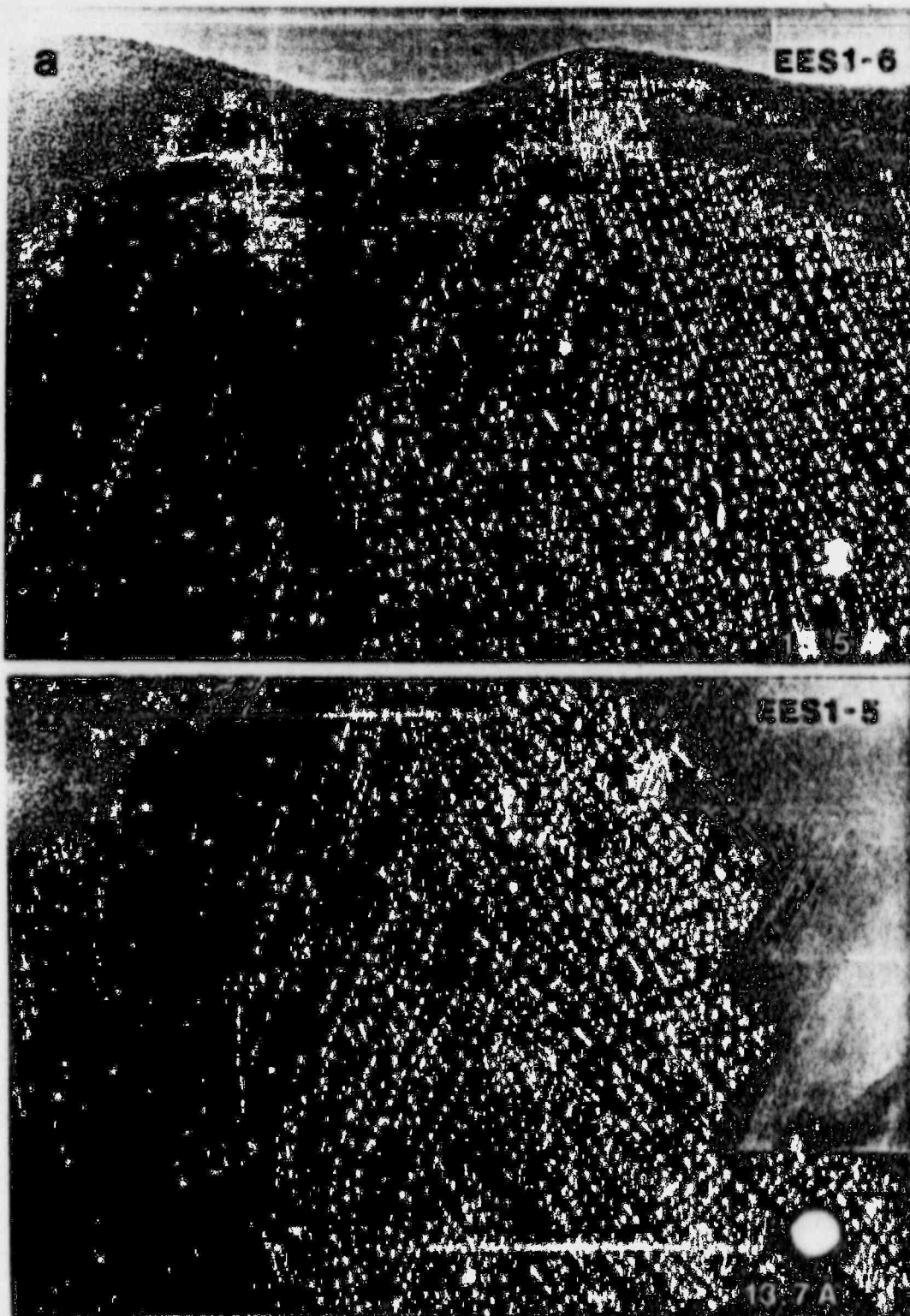
Figure 3.3. TEM lattice-fringe images of Wyoming bentonite expanded with
0.1 N laurylamine HCl indicating larger d values. d(001) of smectite
layers is highly variable as shown in (a) 15.5 Å and (b) 13.7 Å. The
sample is embedded in epoxy. The scale bar is approximately 500 Å.

laurylamine HCL. The layers show the same high degree of imperfection as shown in Figures 3.1 and 3.2.

The qualitative AEM data, for which the spectrum shown in Figure 3.4 is representative, show considerable variation from area to are, especially in the Fe and Al contents, but also in the relative amounts of Na, K and Ca. This cannot be due to contamination by other phases, because analyses are only obtained from sample areas shown to be bentonite by TEM observation. The dominant composition is that of an Al-rich bentonite, but a smaller population has relatively high Mg and Fe content relative to Al.

SEM Data - Figure 3.4 is a typical image of smectite and the EDS spectrum obtained from it. The smectite occurs as homogeneous grains that have the appearance of stacks of layers. The EDS spectrum confirms that Na is the major interlayer cation, with subordinate K and Ca, and that Fe and Mg occur in measurable quantities, substituting in octahedrally coordinated sites.

The formula of smectite given above, based on bulk chemical analysis, is slightly Si-rich as compared with an ideal formula. Because quartz was shown by XRD to occur as a contaminant, the excess Si is at least in large part explained. However, bentonite forms by alteration of volcanic tuff, which is in part non-crystalline. In addition, it is well known that bentonite may have considerable amounts of cristobalite. Although cristobalite is crystalline (and was not detected in XRD patterns) it may be an inversion product of non-crystalline silica. Some bentonite may be composed of significant proportions of non-crystalline, silica-rich material, therefore. Such a phase would be very reactive in the backfill environment.

Accordingly, we have carried out several tens of hours of SEM/EDX observations in order to detect the possible existance of non-crystalline silica. During the course of these observations, grains of phases such as
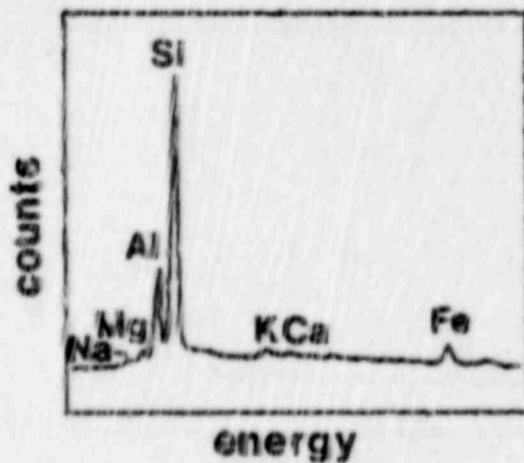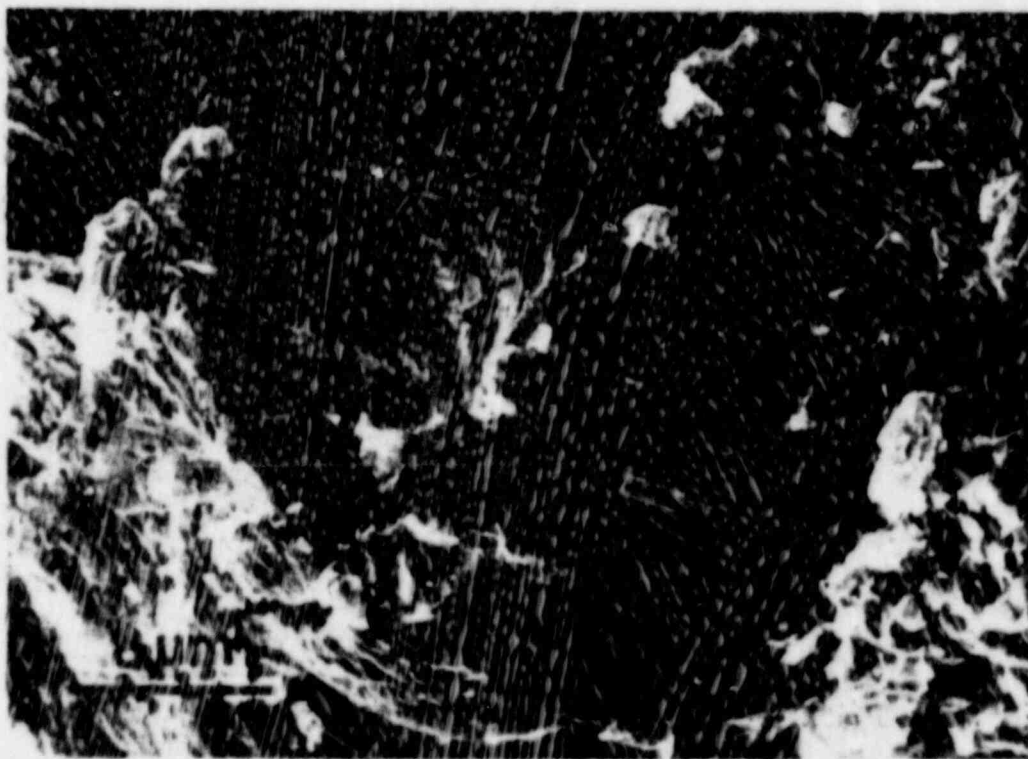
Figure 3.4.   SEM image of bentonite, showing layered appearance (above), and an EDX spectrum of the same grain (below).

feldspar and quartz, and euhedral crystals of apparent zeolites were observed, but only trace amounts of possible glass was detected. We conclude that, if present, it occurs in trivial amounts, and the excess Si in the bulk chemical analysis is entirely attributable to contaminating quartz.

3.3.2 Illite

The illite is even more heterogeneous than the smectite, but this is not unexpected as the samples are shale rock samples which typically contain several minerals. The heterogeneities fall into two categories discussed below.

(1) The illite is itself heterogeneous. X-ray diffraction shows that it is a mixed-layer illite-smectite, with approximately 20-30% expandable layers so that structurally it exhibits a range of spacings from 10 to approximately 14 $\overset{\circ}{A}$. Typical TEM images of Fithian illite samples (Figs. 3.5a and 3.5b) also demonstrate the presence of 14 $\overset{\circ}{A}$ smectite layers interlayered within 10 $\overset{\circ}{A}$ illite layers (Fig. 3.5a). AEM analyses show two kinds of grains, although all have K as the dominant interlayer cation. One type has up to 20% (Ca + Na) K. The other kind has approximately less than 5% Ca + Na. There is approximately twice as much of the Ca, Na-rich phase. Although there are two general categories, there is considerable variation in K, Ca and Na within each one.

(2) Additional phases are present. These include: a) Quartz (43%), which is a major component of the shale; b) Plagioclase feldspar (2%, variety albite with minor Ca, K) has been identified as a minor phase by both AEM and XRD; c) K-rich feldspar was identified in a single grain by AEM; d) Calcite was identified by XRD in Fithian illite samples obtained from a Clay Minerals society standard sample (50% illite, 30% quartz, 14% calcite and 6% plagioclase feldspar), but has not been detected in our

Figure 3.5. TEM lattice-fringe images of Fithian illite starting material embedded in epoxy. Areas of (a) mixed-layer I/S and (b) regular 10 A illite layers without smectite.

standard samples. The standard Fithian illite was treated with hydrogen-peroxide in order to remove organic material and was also submitted for X-ray fluorescence chemical analysis. The analytical values in Table 3.1 are in reasonable agreement with those predicted on the basis of the mineralogical analysis by X-ray diffraction.

3.3.3 Basalt

The core samples available to us (Umtanum Formation, well DC-6, Hanford Site, Washington) are dark gray, fine-grained, homogeneous basalts. XRD analysis and norm calculation (Table 3.2) show that it is a typical tholeiite. In thin section, Umtanum basalt displays hyalo-ophitic texture characterized by the presence of up to 30% of silicate mesostasis interstitial to plagioclase laths (typically less than 0.1 mm in width) as well as euhedral to subhedral augites (analysis in Table 3.2). Magnetite microphenocrysts are ubiquitous.

The core samples have several exposed fissure surfaces as well as ellipsoidal vesicles. The surfaces of these fissures are ubiquitously coated with a layer of black, earthy, fine-grained clay material. The coating is usually decorated with yellowish-brown streaks manifesting the precipitation of Fe-bearing opaline material from Si-saturated solution. Large grains of opal, showing corchoidal fracture, are occasionally present. In several cases, patches of white, thin layers of zeolites are sandwiched between black clay layers. Zeolites and quartz are dominant in vesicles.

Figure 3.6 shows SEM images of these fracture materials. The XRD analysis indicates that the black clay in nontronite, an Fe-rich smectite. The grains are homogeneous and compact (e.g., Fig. 3.6a). Opaline material occurs as linear arrays of spheroidal particles with relatively uniform size (about 0.1 mm in diameter), as contrasted with the blocky nontronite sandwiching it
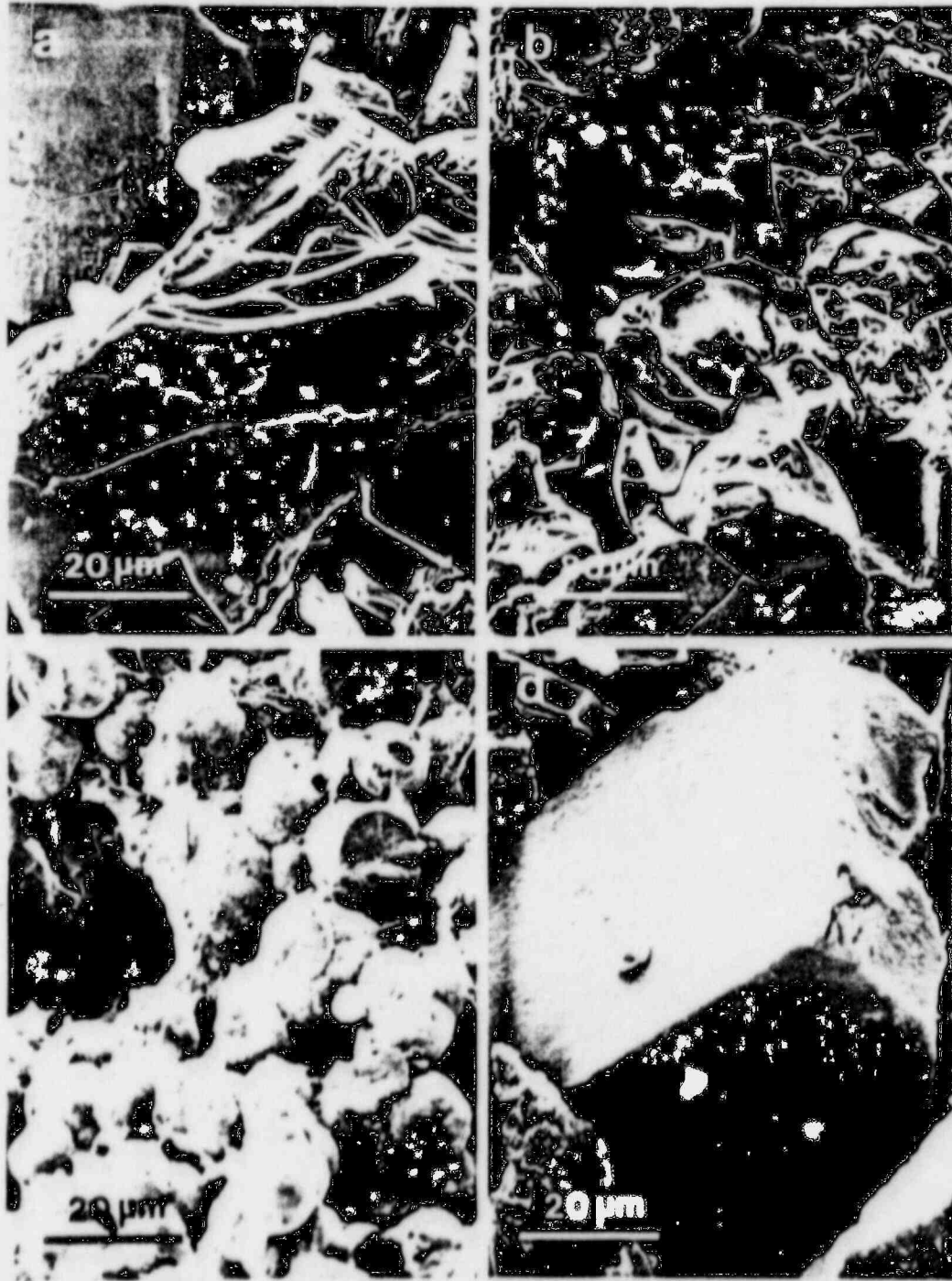
Figure 3.6. SEM images showing the morphology and occurrence of phases in the
fractures of the Umtanum basalt. (a) Platy, homogeneous nontronite.
(b) Spheroidal aggregate of opaline material sandwiched between nontronite
layers. Note the conchoidal fracture. (c) Aggregate of spherical
epistilbite in an amygdule. (d) Heulandite crystal showing one perfect
face (lower).

Table 3.2 Analyses of the bulk rock and augite in the Umtanum Basalt

	Bulk rock*	augite**			
SiO_2	53.1	50.67		*CIPW norm	
TiO_2	2.10	0.92	qz	7.6	
			zr	0.0	
Al_2O_3	12.8	2.85	or	8.2	
			ab	26.7	
Fe_2O_3@	3.6	-	an	16.6	
			di	6.3	
FeO	11.0	16.85	hd	7.5	
			en	6.2	
CaO	7.11	13.01	fs	8.3	
			mt	5.2	
MgO	3.65	15.66	il	4.0	
			ap	0.8	
MnO	0.22	nd#			
Na_2O	3.15	nd			
K_2O	1.39	nd			
P_2O_5	0.33	nd			
LOI	1.00	nd			
total	99.5	99.96			

** Calculated formula:

$$(Ca_{0.53}Mg_{0.98}Fe_{0.53}Ti_{0.03}Al_{0.04})(Al_{0.09}Si_{1.91})O_6$$
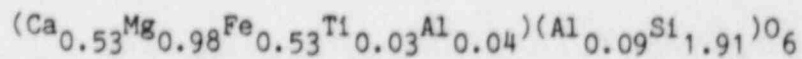
which corresponds to $En_{46}Fs_{27}Wo_{27}$

@ Fe_2O_3 calculated as $Fe_2O_3 = TiO_2 + 1.5$.

not determined

(Fig. 3.6b). Concentric fractures are characteristic. The EDX spectrum indicates tha Fe is the major impurity in these grains, which is consistent with their yellowish-brown color. Epistilbite is found as aggregates of spherical crystals in an ellipsoidal amygdule (Fig. 3.6c) characterized by its spherical habit and its higher Ca/Si and Al/Si ratios than heulandite. Heulandite is found to be the major zeolite coexisting with the nontronite in the fractures. A typical heulandite crystal is presented in Figure 3.6d.

We have directed special attention to high resolution STEM/AEM characterization of the interstitial glass in the basalt because this glass is much more reactive than crystalline phases upon hydrothermal alteration, and its breakdown will modify the groundwater chemistry and consequently the nature of alteration products.

Figure 3.7a shows the TEM image of the glass and shows that it consists of two-phase, immiscible glasses. It consists of randomly distributed, dark glass globules (globular glass) in a transparent glass interstitial to plagioclase laths (matrix glass). The globular glasses show a bimodal size distribution: either 0.5-1.5 μm or less than 0.1 μm in diameter. Larger glass globules display various degrees of optical and chemical heterogeneity. Those labelled A (Fig. 3.7b) are compositionally homogeneous throughout the globule and have very smooth globular surfaces without appreciable variations in contrast. Those labelled B are extremely heterogeneous in composition and have irregular outlines with strong contrast changes within the globule. They contain domains of crystal-like phases which give rise to powder-like electron diffraction patterns. Those labelled C show lesser degrees of optical and chemical heterogeneities and surface irregularities than type B. The matrix glass typically show higher contrast.
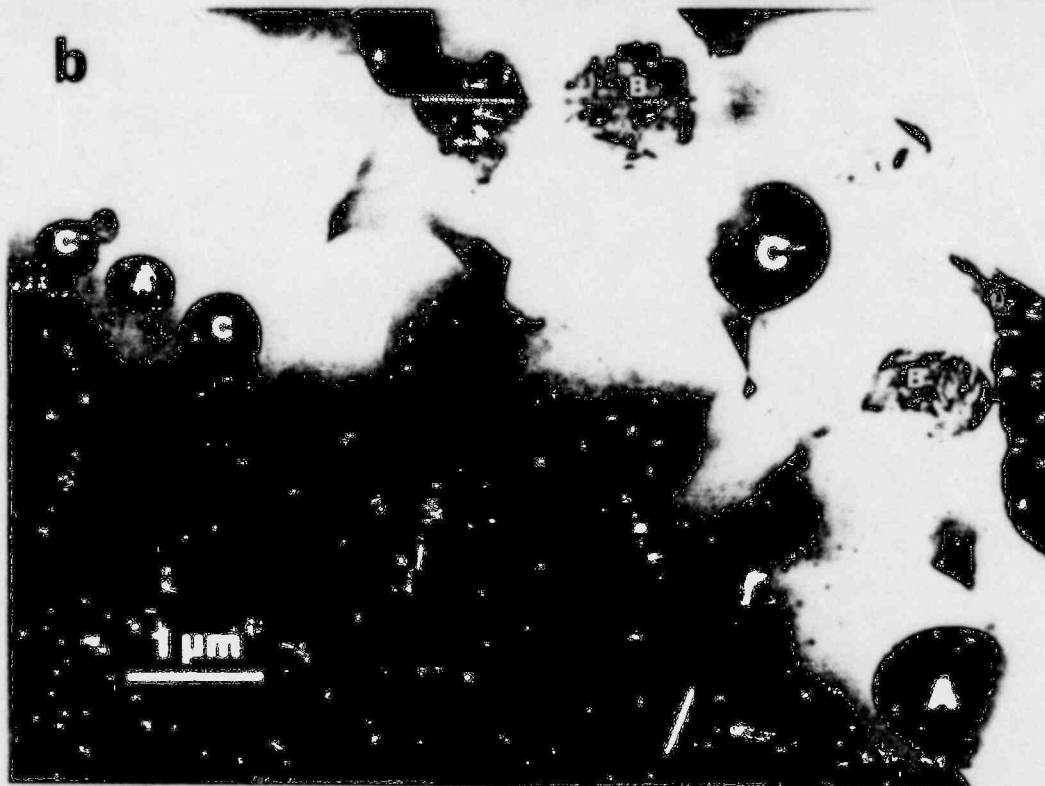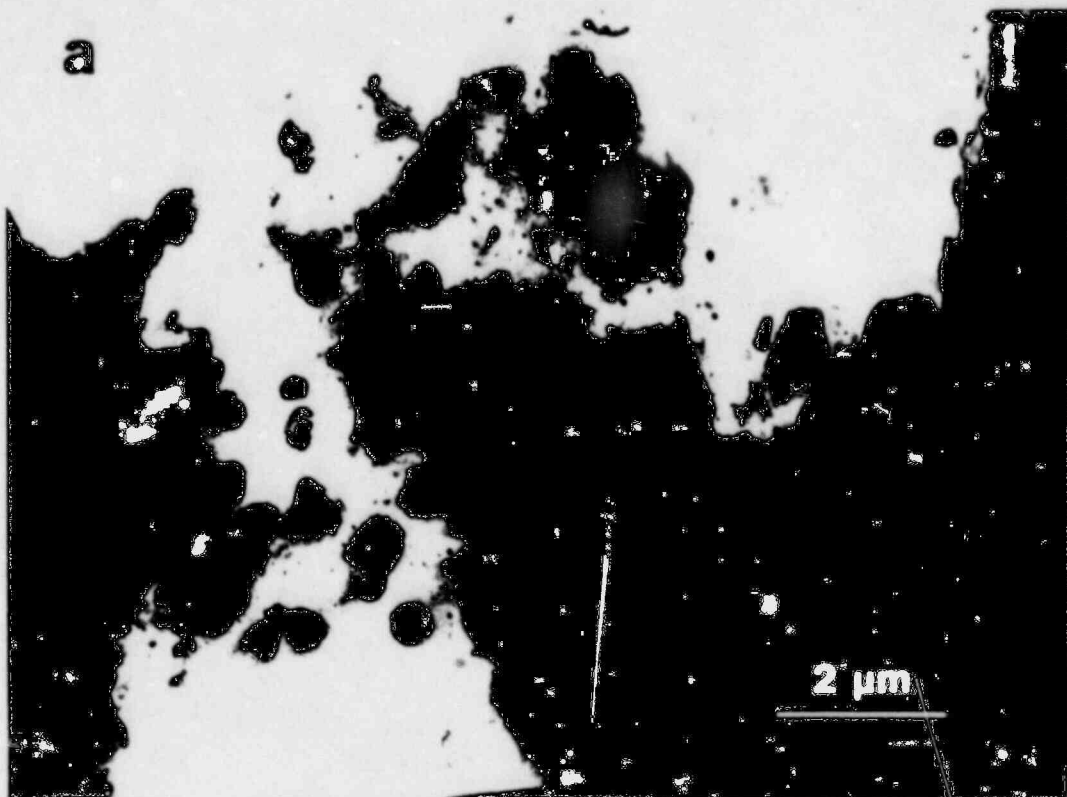
57

Figure 3.7. a. A TEM image of the immiscible glass in the Umtanum basalt
showing randomly distributed, dark glass globules in light matrix glass.
b. An enlarged view of the immiscible glass showing the variations in
chemistry and in optical homogeneity of globules; A, maximum homogeneity;
B, maximum heterogeneity; and C, intermediate.

Energy dispersive spectra indicate that the globular glasses are characterized by high Si, Ca, and Fe contents with subordinate Mg, Al, P, S, Cl, K, Ti, and Mn (Fig. 3.8a). In one of the type B globular glasses a covariation of Ca and P was detected, indicating the possible presence of apatite as a crystalline phase. The bulk chemistry of type B glasses is very similar to that of type A globules. The matrix glass, on the other hand, consists mostly of Si with less Al and minor amounts of Na, Mg, K, Ca, Ti, and Fe (Fig. 3.8b). If the composition of the small globular glasses is similar to that of the larger ones, Fe, Ca, and Ti in the matrix glass may be partially contributed from these small globules.

Quantitative chemical analyses of the globular and matrix glasses were performed using AEM techniques. The size of the electron beam was about 0.1 um for point analyses and 0.5-2 um for bulk analyses. Typically several point analyses were averaged to obtain the composition of a homogeneous globular glass. Table 3.3 presents representative results. It can be seen that homogeneous (type A) globular glasses also show narrow compositional ranges (columns 1 and 2, Table 3.3), whereas heterogeneous ones display a more diverse compositional range (columns 5 and 6, Table 3.3). The matrix glasses (columns, 3, 4, Table 3.3) are typically rich in Si and Al, yielding high quartz and feldspar components in the CIPW norm, as contrasted with the high pyroxene, olivine, ilmenite, and apatite components for the globular glasses.

Both morphologic and chemical properties are consistent with the interpretation of subsolidus phase separation origin of these glasses. This is illustrated by a triangular plot (Fig. 3.9) in which the compositions of globular and matrix glasses are separated by a region of silicate liquid immiscibility (Roedder, 1978). Our compositions of matrix glasses are comparable with those of published data, but the globular glasses show lower Si

59
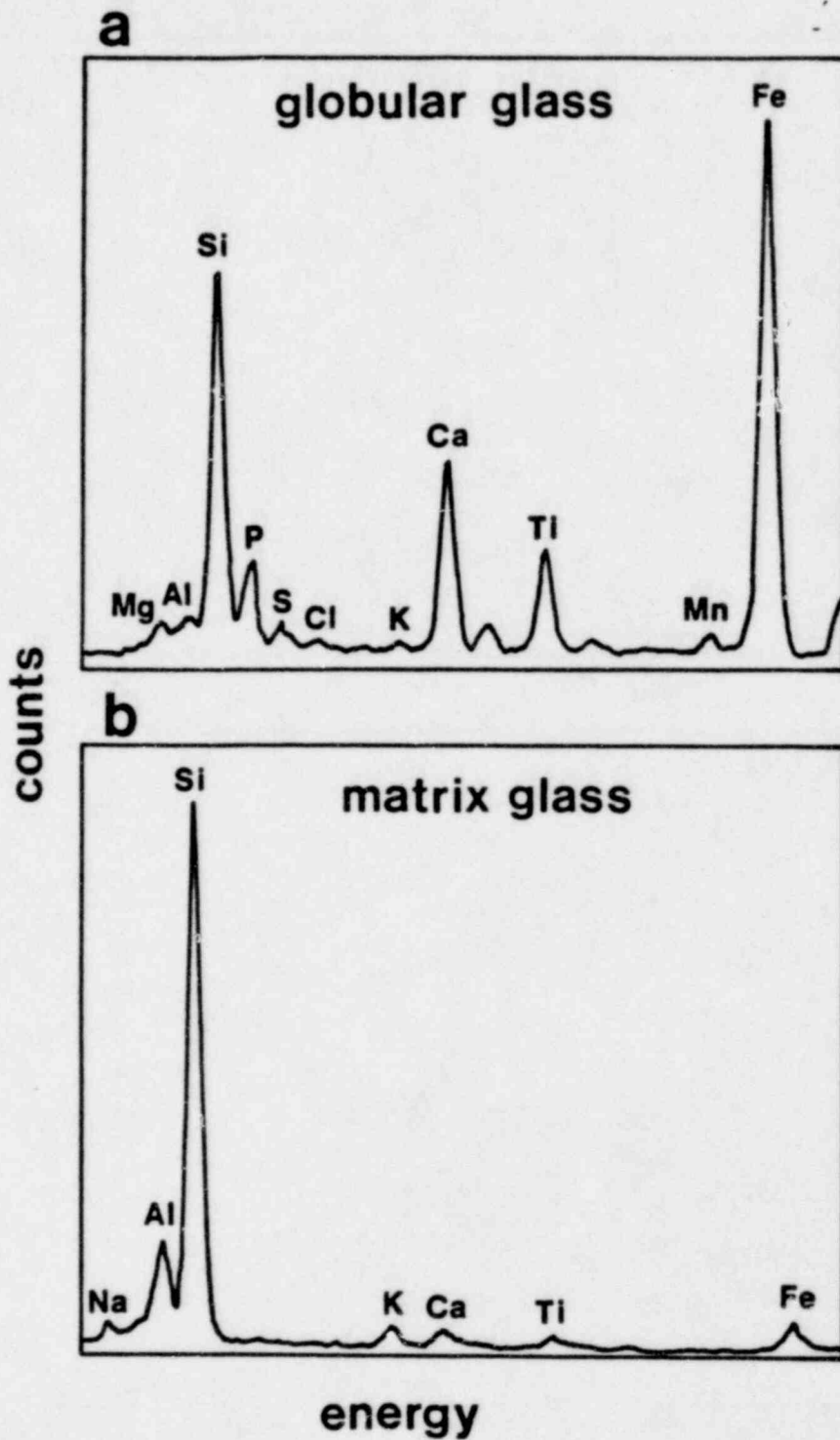
Figure 3.8. EDX spectra showing the chemistries of typical (a) globular, and (b) matrix glass. Note the enrichment of Si-Ca-Fe in the globules in contrast with the high Si-Al-K contents in the matrix glass.

Figure 3.9. Triangular plot (in wt % oxides) of compositions of two immiscible glasses from Umtanum basalt in comparison to those of lunar and terrestrial basalts and to the experimentally determined immiscible gap (stippled area) in the simplified system, leucite-fayalite-silica.

61

Table 3.3 Representative AEM analyses of two immiscible glasses

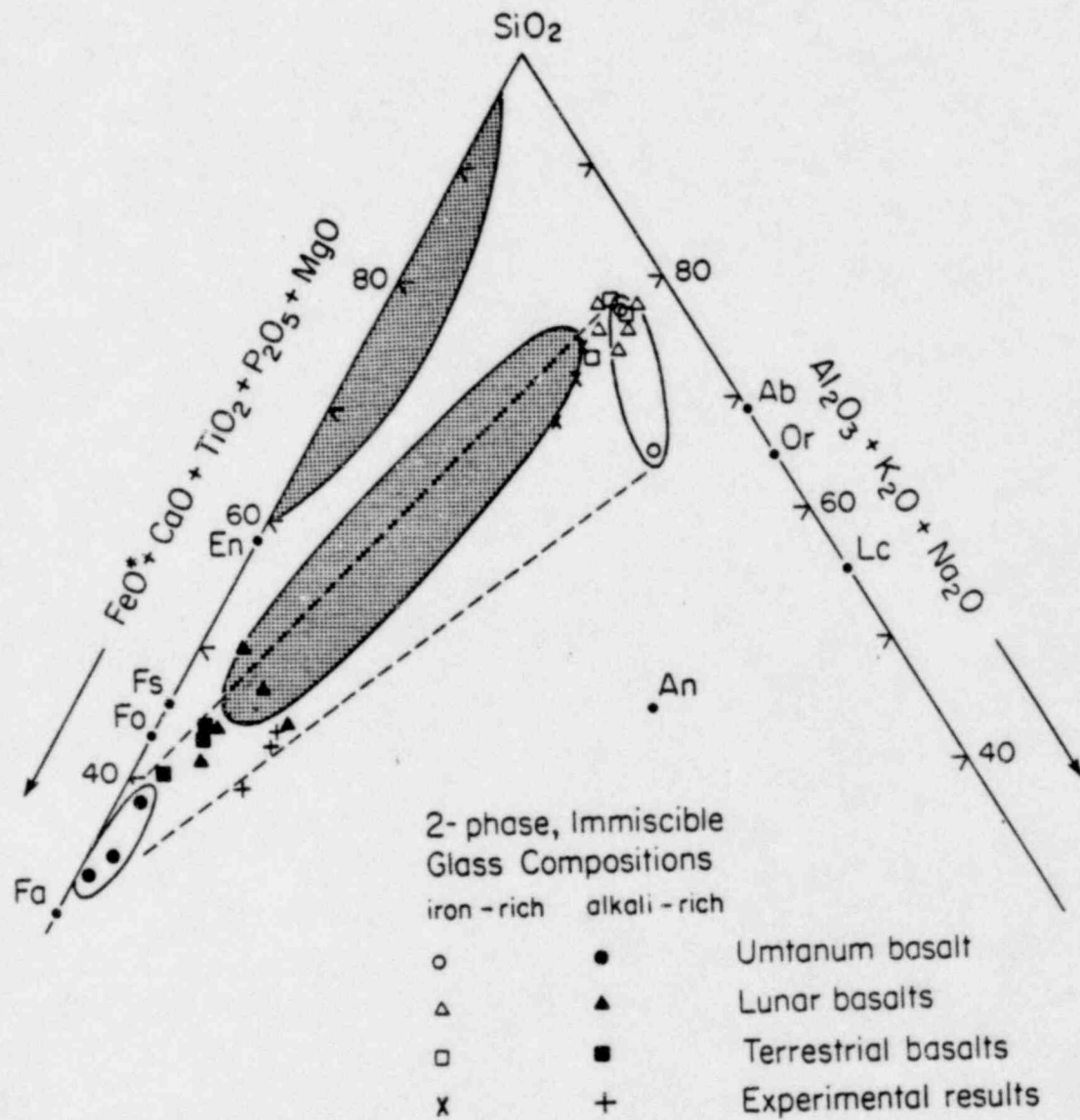|	1	2	3	4	5	6
SiO_2	29.8	30.0	77.5	65.6	36.2	32.0
TiO_2	6.4	6.8	1.0	0.9	1.0^+	8.9
Al_2O_3	0.8	1.0	14.4	17.2	2.1	1.6
FeO*	47.4	43.1	1.9	3.1	34.2	36.4
MnO	0.7	0.4	nd	nd	0.4	tr
MgO	0.8	1.0	tr	tr	2.7	tr
CaO	10.3	11.0	1.5	3.7	15.9	14.4
Na_2O	nd^θ	nd	1.2	4.4	nd	nd
K_2O	$tr^\&$	tr	2 4	5.1	0.3	1.0
P_2O_5	3.2	5.7	nd	nd	7.3	5.7
SO_2	0.6	1.0	nd	nd	nd	nd
Cl_2	tr	tr	nd	nd	tr	tr
CIPW norms (wt%) for $Fe^{3+}/Fe^{2+}=0.1$)						
Q	-	-	57	12	-	2
or	-	-	14	30	2	6
ab	-	-	10	37	-	-
an	2	3	7	12	5	2
C	-	-	7	-	-	-
di	1	1	-	-	3	-
hd	24	12	-	6	20	29
en	1	2	-	-	5	-
fs	19	44	2	1	39	26
fo	26	4	-	-	2	-
mt	8	7	-	-	6	6
il	12	13	2	2	2	17
ap	8	14	-	-	17	13
py	1	1	-	-	-	-

1, 2: homogeneous globular glasses; 3, 4: matrix glasses;

5, 6: heterogeneous globular glasses.

*Total iron as FeO

+Ti concentrated outside the area analysed within the globule

$^\theta$nd: not detected

$^\&$tr: only trace amount present

and higher Fe, Ca, Ti, P, and Mg concentrations than the published values. We suggest that our results are more reliable because all the published data were obtained using EMPA techniques, where contamination from the surrounding matrix glass is likely because of the very similar sizes of globular glasses and electron beam.

4. HYDROTHERMAL EXPERIMENTS

4.1 Methods

Hydrothermal experiments were carried out in standard Tem-Pres cold-seal pressure vessels heated in horizontal resistance furnaces with Eurotherm solid-state proportional temperature controllers. Prior to experiments, furnaces were accurately calibrated for temperature. This verified that temperature was effectively constant over the entire volume of a sample.

An experimental charge was prepared by welding approximately 0.03-0.07 g of powdered sample in gold or silver tubing, with approximately 0.02-0.1 cc of solution with composition similar to that of the groundwater at the repository (or distilled water in selected cases). Typically, three charges were loaded at the bottom of the reaction chamber. Temperature and pressure were monitored using a chromel-alumel thermocouple with a potentiometer and pressure gauges calibrated by the manufacturer. Variations in temperatures and pressures never exceeded 2%. Charges were weighed before and after experiments in order to verify that capsules remained sealed for the duration of the experiment.

4.2 Conditions for Experiments

The general range of conditions includes (a) pressures less than 1000 bars; (b) water/rock ratios approximately from 10 to 0.3; (c) times from a few

days to 18 months; (d) temperatures ranging up to 300°C, the estimated maximum value to which backfill materials are to be subjected. However, because initial experiments at or near 300°C failed to induce changes where data for geological systems indicated change should occur, experiments were undertaken at much higher temperatures (up to 460°C) and for extended time periods (up to 18 months) in order to induce reaction. The working hypothesis was that the experiments should be carried out at the limits of reaction rates, such that if reactions occurred, further experiments at progressively lower temperatures would enable limiting conditions to be defined.

Initial experiments were carried out with charges which were as simple as possible, so that if changes occurred, they could be correlated with specific starting materials. Final experiments were with mixtures of basalt and bentonite as the most probable backfill material at the BWIP site.

Experiments were therefore carried out in the following approximate sequence (Table 4.1):

Set I. Bentonite samples ENV82 1-4. These experiments were carried out using distilled water for short time periods (14-90 days) to test the stability of bentonite, and in part to test the reliability of the newly installed hydrothermal equipment. The lack of changes made it clear that higher temperatures and longer times would be necessary as defined in the following experiments:

Set II. A series of experiments involving the "pure" phases bentonite (BNC32, BND34, BNA35, BN685, BN454), illite (ILB3A, ILB3B, ILC31, ILD-32, ILA-34, IL680, IL455), and basalt (BS450, BS681, BSA-37, BSD-33, BSC-33). This sequence involved temperatures between 300 and 400°C, with times of approximately 3 months. These were carried out using a fluid whose chemistry simulated that of the ground water of the Umtanum

64

Table 4.1 Experimental run conditions and results

SET I

Sample	T (°C)	P (Bars)	WATER/ ROCK	TIME (DAYS)	CHARGE	RESULT
ENV82-2	240	260	-	14	Bentonite	No observed change
ENV82-3	240	260	-	14	"	" " "
ENV82-1	240	260	-	90	"	" " "
ENV82-4	240	260	-	90	"	" " "

SET II

Sample	T (°C)	P (Bars)	WATER/ ROCK	TIME (DAYS)	CHARGE	RESULT
BNC-32	300	300	0.44	91	Bentonite	Calcite is lost;
BND-34	300	500	0.50	71	"	Ca/K exchange
BNA-35	300	800	0.54	70	"	occurs in smectite
BN 685	360	300	2.77	97	"	Bentonite reacts;
BN 454	460	300	2.22	92	"	albite, paragonite and quartz grow
KBNA2	300	300	2.17	77	K-saturated	Bentonite survives,
KBNB8	400	300	2.22	75	bentonite	but with smaller d(001)
ILB3A	350	300	0.58	91	Illite	Berthierine grows;
ILB3B	350	300	0.53	91	"	illite is
IL 680	360	300	2.38	97	"	recrystallized;
IL 455	460	300	1.92	92	"	illite crystal-. linity improves.
ILC-31	300	350	0.40	91	Illite	No observed change
ILD-32	300	500	0.51	71	"	
ILA-34	300	800	0.51	70	"	" " "
BSA-37	300	800	0.45	70	Basalt	" " "
BSD-33	300	500	0.32	71	"	" " "
BSC-33	300	350	0.34	91	"	" " "
BS 450	460	300	2.13	92	"	Small amount of
BS 681	360	300	1.85	97	"	smectite synthesized; otherwise, no change

SET III

Sample	T (°C)	P (Bars)	WATER/ ROCK	TIME (DAYS)	CHARGE	RESULT
BN 571	300	300	1.16	584	Bentonite	No change in
BN 384	200	300	1.75	552	"	smectite beyond
BN 282	300	300	5.00	537	"	small changes in
BN 780	300	300	2.78	414	"	interlayer cation
BN 181	200	300	3.23	414	"	composition.
BN 802	300	300	9.10	432	"	Calcite dissolves.

SET III (con't.)

IL 184	200	300	2.33	414	Illite	No observed change
IL 572	300	300	9.10	432	"	
IL 389	200	300	1.23	552	"	" " "
IL 281	300	300	5.00	537	"	" " "
IL 572	300	300	1.05	584	"	Berthierine
IL 783	300	300	2.33	544	"	synthesized; Illite recrystalllized.
BS 807	300	300	10.00	432	Basalt	No observed change
BS 388	200	300	1.75	552	"	
BS 187	200	300	3.70	414	"	" " "
BS 570	300	300	1.09	584	"	" " "
BS 786	300	300	2.70	544	"	" " "
BS 284	300	300	4.54	537	"	" " "

SET IV

BB 69	400	300	5.88	81	75% basalt	Growth of wairakite;
BB 62	400	300	2.08	81	25% bentonite	no other change
BB 41	300	300	1.03	152	75% basalt	No observed change
BB 44	300	300	9.10	152	25% bentonite	" "
BQD7	300	300	1.85	334	25% basalt	No change
BQC1	400	300	1.03	280	75% bentonite	Growth of chlorite + wairakite; loss of pyroxene + smectite;
BHD4	300	300	1.15	334	50% basalt	No change;
BHC5	400	300	1.22	280	50% bentonite	Growth of chlorite + illite; loss of pyroxene + smectite + quartz;

Formation (Table 4.2). This fluid was subsequently used in all other experiments. In addition, two experiments (KBNA2 and KBNB8) were devised to test the effect of the presence of K on the inversion of smectite to illite, by using a starting material consisting of a K-exchanged bentonite. The results of these experiments showed that very little change occurred in the starting materials. Therefore further experiments were initiated:

Set III. The third and most comprehensive series of experiments involved "pure" phases as starting materials, temperatures of 200-300°C (the upper limit of the repository) but with very long time durations of up to 584 days in order to provide the longest possible times for changes to occur, as an optimum test of possible changes under laboratory conditions. Although experiments of several years duration are desirable, they are impractical given the restraints of the testing program.

Set IV. Mixtures of basalt and smectite under high temperature conditions, 300-400°C, and times ranging from 81 to 334 days.

4.3 Results

4.3.1 Set I Trial Runs

Four charges, all consisting of bentonite plus distilled water, were treated at 240°C for 14 or 90 days. These charges were in part a test of the newly acquired and calibrated hydrothermal equipment. Bentonite was chosen as it was thought to be most likely to exhibit changes. Distilled water was used, as it was desired to keep initial experiments as simple as possible in order to be able to relate changes, if any, to specific experimental parameters.

X-ray diffraction patterns of the products were effectively identical to those of the starting material. As further verification of the lack of change, TEM images were obtained. Figures 4.1a and 4.1b are lattice fringe images
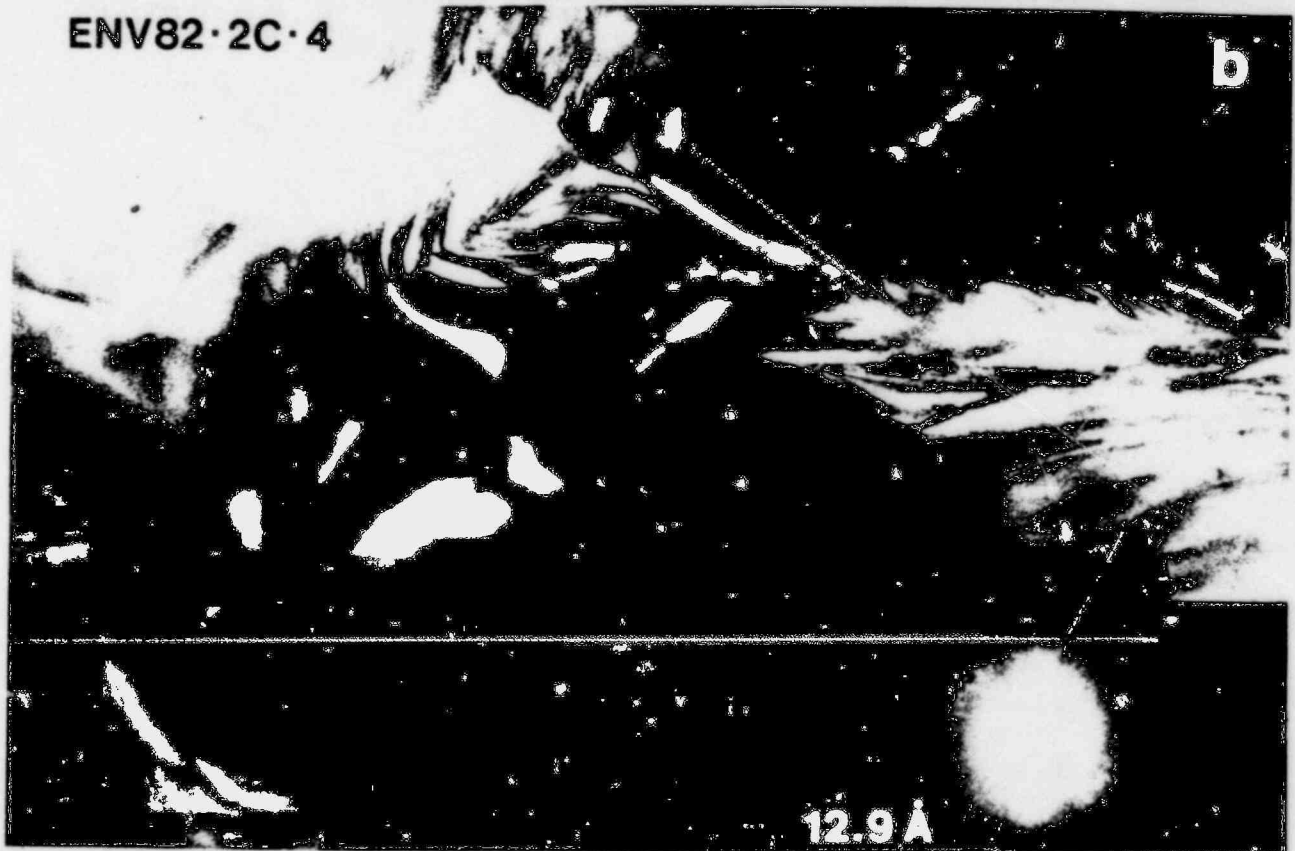
67

Figure 4.1. TEM images of bentonite from hydrothermal run ENV82-2. Only
smectite is present, with an appearance duplicating that of the starting
material.

68

Table 4.2 Chemical composition of groundwater in the Umtanum formation, Pasco Basin, Washington compared with sea water and river water compositions.

Species	1	2	3	4
Na^+	10540*	6.3	270	270
K^+	380	2.3	6	6
Ca^{2+}	400	15.0	2	2
Mg^{2+}	1270	4.1	0.3	-
H_4SiO_4	-	34.9	120	-
Cl^-	18980	7.8	190	190
F^-	1.3	-	32	32
SO_4^{2-}	2460	11.2	120	120
HCO_3^-	140	58.4	60	101
CO_3^{2-}	-	-	-	22

1: Average sea water (from Fergusson, 1982)
2: Average river water (from Fergusson, 1982)
3: Groundwater, Umtanum formation
4: simulated groundwater used in the present experiment (pH buffered to 9.5 using carbonate/bicarbonate ions)
*All figures in ppm

obtained using 001 reflections. These should be directly compared with images for the starting material as shown in Figures 3.1 and 3.2. The images of the treated and untreated structure appear to be identical. Both show anastomosing (001) layers with high levels of imperfections such as edge dislocations in the form of layer terminations. The spacings between layers are variable as a result of differential collapse of layers due to water loss in the vacuum of the TEM. However the average value for the hydrothermally treated material is 11.9 $\overset{o}{A}$, which corresponds well with the value of d(001) = 12.0 $\overset{o}{A}$ as determined from the X-ray diffraction pattern. This lack of change is not surprising in view of the short time period for the experiment (14 or 90 days) and low temperature (240°C). The experiments of Set II were therefore initiated under more stringent conditions.

4.3.2 Set II Short Term Runs

These experiments were all run for durations of 71-90 days, with temperatures at 300 to 400°C. The time periods were chosen to be as long as practical within the time constraints of this project, such that additional experiments could still be initiated based on the results of set II. The temperatures were chosen to match the maximum for the repository (300°C) or greater, in order to maximize reaction rates.

4.3.2.1. Bentonite

300°C Runs (BNC32,NBNC34,BNA35) - The XRD patterns of the hydrothermally treated bentonites show the same mineralogy as that of the untreated bentonite except for the disappearance of the calcite peaks. The d(001) value of the smectite in the run products (14.7 $\overset{o}{A}$) is significantly larger than that of the untreated bentonite (12.9 $\overset{o}{A}$), indicating a change in the character of the

70

interlayer cation(s). The STEM/AEM analyses on the treated bentonites reveal a significant increase in Ca and decrease in K, while other elements do not show detectable changes (Fig. 4.2).

360°C Run (BN685) - The products of this run shows essentially the same characteristics as those of the 300°C runs; i.e., the absence of calcite peaks and the increase in the d(001) value of the smectite (Fig. 4.3b). We suggest that the extensive exchange of Ca for K occurred in the smectite interlayer due to the increase in Ca concentration in the solution by calcite dissolution, whereas the structure of the smectite remained stable during the time period of the experiment.

460°C Run (BN454) - The XRD pattern of this run product (Fig. 4.3c) shows the presence of strong albite peaks, an increase in the relative amount of quartz versus smectite, and the appearance of a 10 $\overset{o}{A}$ phyllosilicate. Because the original solution is rich in Na but poor in K, we suggest that this 10 $\overset{o}{A}$ phase is paragonite, a Na-rich mica, instead of illite. There is still considerable unreacted smectite remaining in the charge, however, so even at 460°C reaction is incomplete.

Figure 4.4a shows the SEM images of the typical assemblage of the run product. Quartz occurs as recrystallized, euhedral aggregates masking the surface of the partially reacted smectite plate (Fig. 4.4b). Albite crystals are relatively coarse and are sparsely distributed. Paragonite (marked by the circles in Fig. 4.4a) is characterized by a platy morphology.

K-saturated samples (KBNA2, KBNB8) - Wyoming bentonite was treated by exchanging Na for K in order to produce a near end-member K-bentonite, to be used as a starting material in runs at 300 (KBNA2) and 400°C (KBNB8). Attempts were made to obtain electron diffraction patterns and lattice fringe images (obtained by imaging with 001 reflections). However, only very diffuse powder
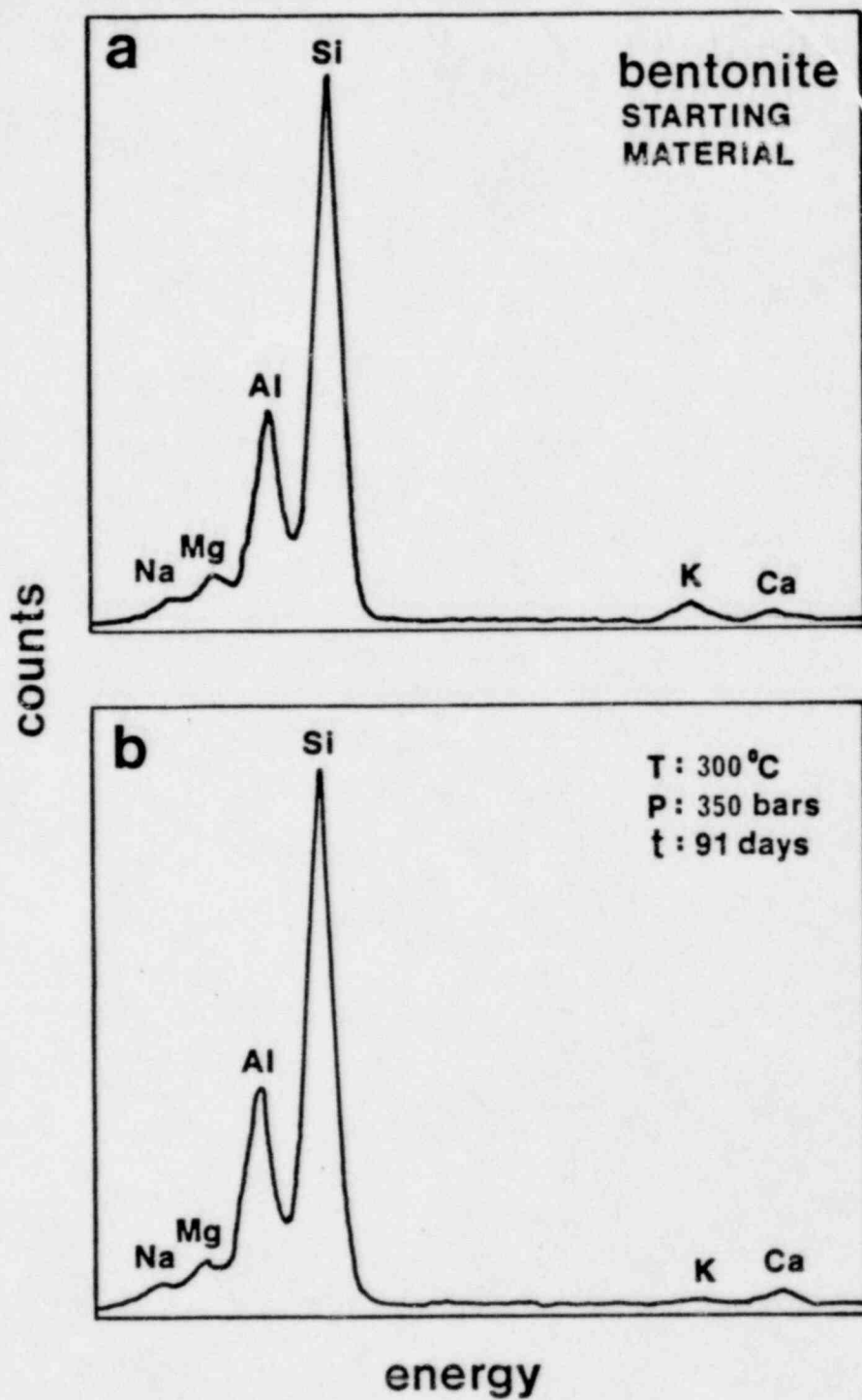
Figure 4.2. Energy dispersive X-ray spectra of bentonite for (a) starting material and (b) hydrothermally treated sample at 300°C and 350 bars for 91 days. The spectra show an increase in Ca and a decrease in K after the hydrothermal treatment.

Figure 4.3. XRD patterns of bentonite; (a) starting material, and hydrothermally treated samples in two different run conditions; (b) 360°C, 300 bars, 96.5 days and (c) 460°C, 300 bars, 92 days.
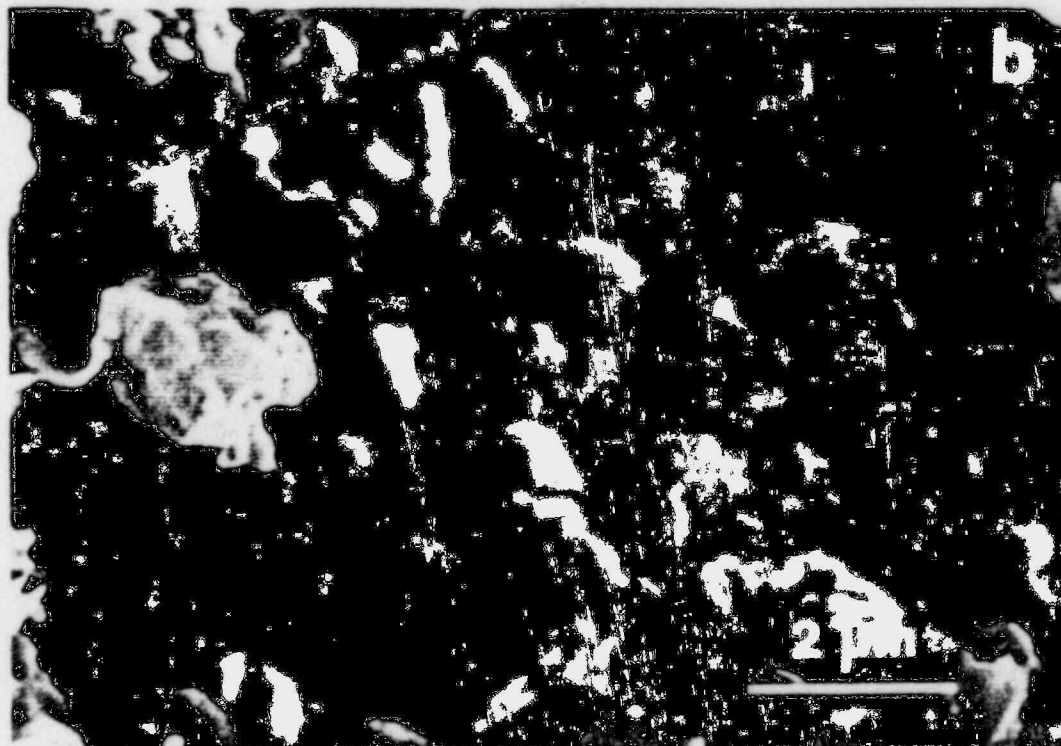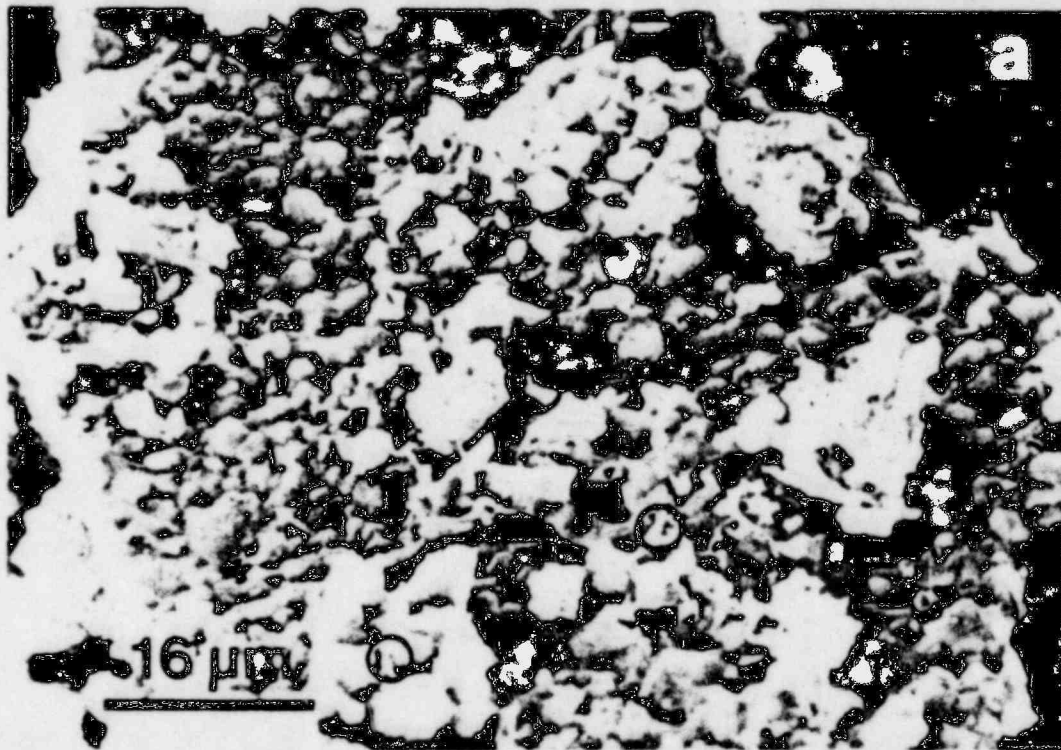
73
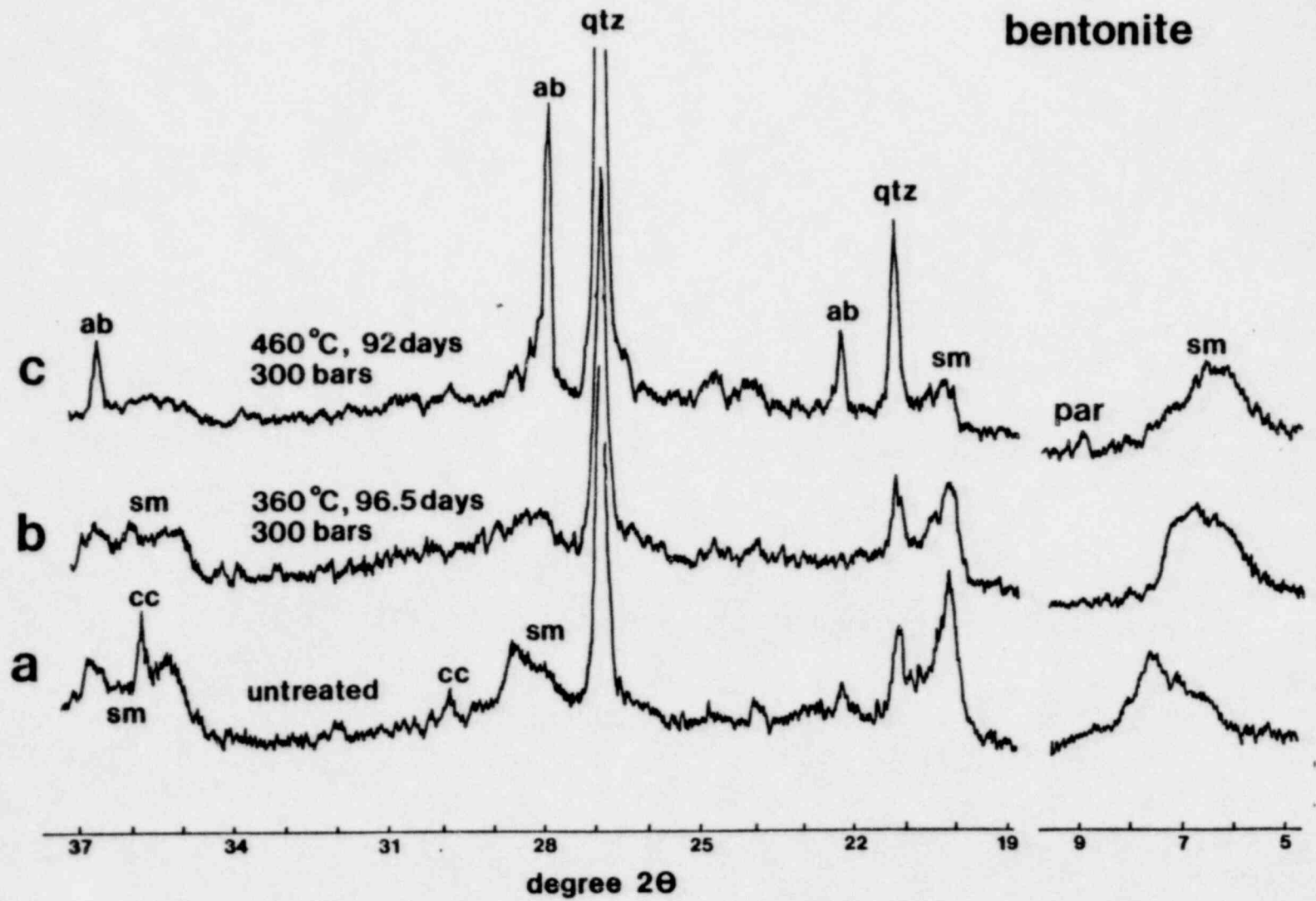
Figure 4.4. SEM photographs of run BN454 (bentonite, same sample as for
Fig. 4.3c). (a) Typical occurrence of quartz (grey), albite (white) and
paragonite (marked by circles) on a smectite surface. (b) A detailed
view of the same sample showing the morphology of crystallized aggregates
of euhedral quartz.

diffraction patterns were observed, and no lattice fringe images could therefore be obtained. The exchange process apparently resulted in separation of layers, so that the original continuous structures were broken up into units of portions of one or a few individual layers. Figure 4.5 shows the portion of the X-ray diffraction pattern which contains the characteristic 001 diffraction peak for the glycolated original and hydrothermally treated materials, and Figure 4.6 shows a larger portion of the patterns, but for unglycolated materials. The patterns for both the original and hydrothermally treated products all are similar in that K-bentonite is the principal phase. However, the 300° and 400°C run products contain a significant proportion of mixed-layer illite/smectite, indicating that there has been some conversion of smectite to illite. In addition, the 400°C run (pattern A of Figure 4.6) shows the presence of a phase having d of 7 $\overset{o}{A}$, and labelled as kaolinite (ka) or chlorite (chl). This peak is characteristic of either a 7 $\overset{o}{A}$ septechlorite or chlorite. Based on the results of TEM/AEM data from other experiments as reported below, and the conclusions of Ahn and Peacor (1985b) regarding the transformation of smectite in Gulf Coast sediments, this peak is almost certainly that of a trioctahedral septechlorite (berthierine) or chlorite. This phase results from recrystallization of smectite or transformation of smectite to illite. Its appearance is therefore compatible with the changes observed in the bentonite diffraction pattern and implies significant change in the bentonite.

4.3.2.2 Illite

300°C Runs (ILC-31, IL-D-32, IL-A-34) - These runs, at water vapor pressures ranging from 350 to 800 atm., produced no changes that were detectable using XRD techniques; i.e., the patterns for the starting and product materials were apparently identical.
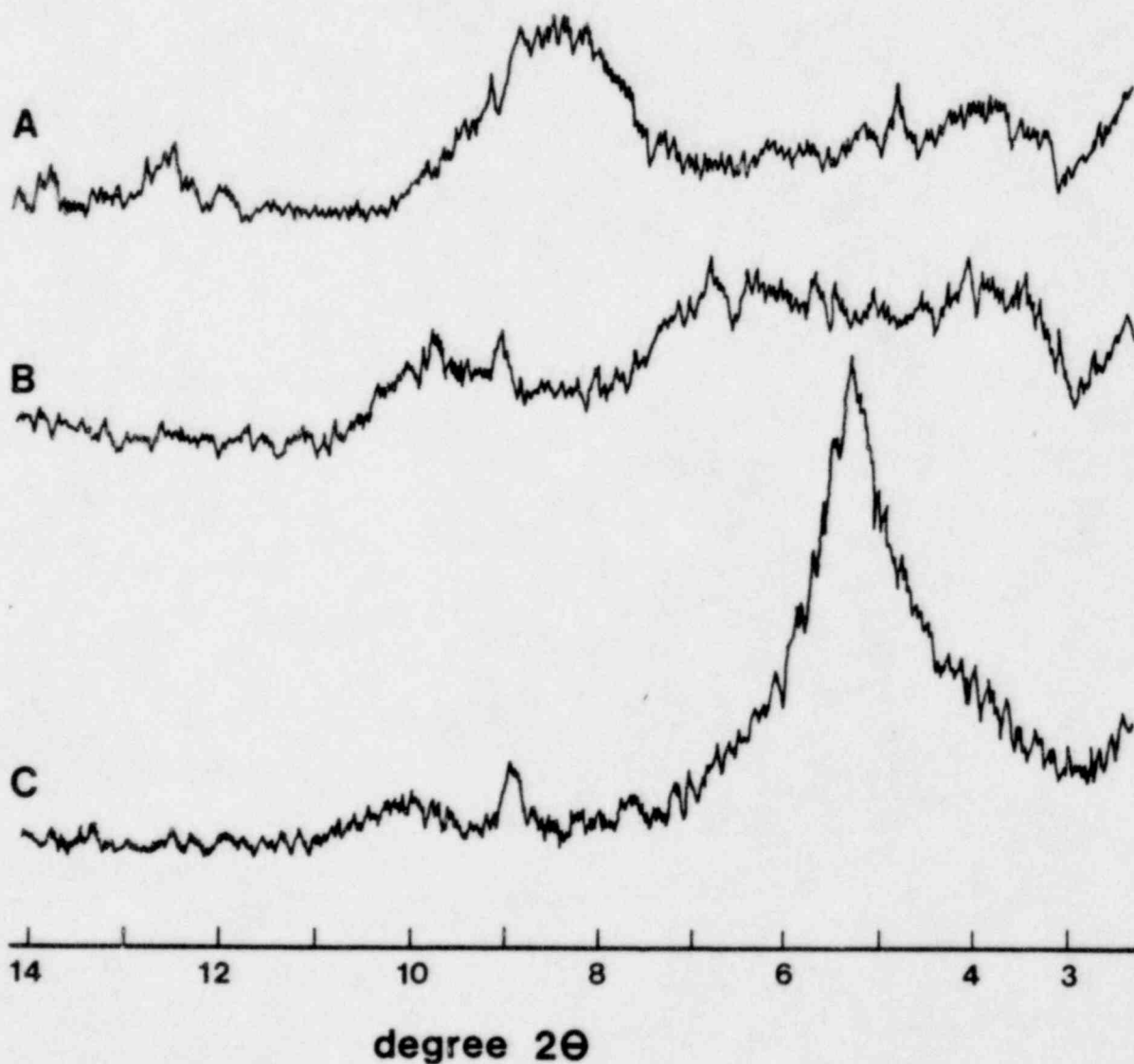
K-saturated bentonite glycolated

Figure 4.5. XRD patterns for the principal 001 peaks of glycolated, K-saturated bentonite. a. Run KBNB8 (400°C). b. Run KBNA2 (300°C). c. Starting material.

K-saturated bentonite
A: 400 °C, 75 days,
B: 300 °C, 76.5 days, 300 bars
C: untreated

Figure 4.6. XRD patterns for K-saturated bentonite, not glycolated. a. Run KBNB8 (400°C) b. Run KBNA2 (300°C) c. Starting material.

77
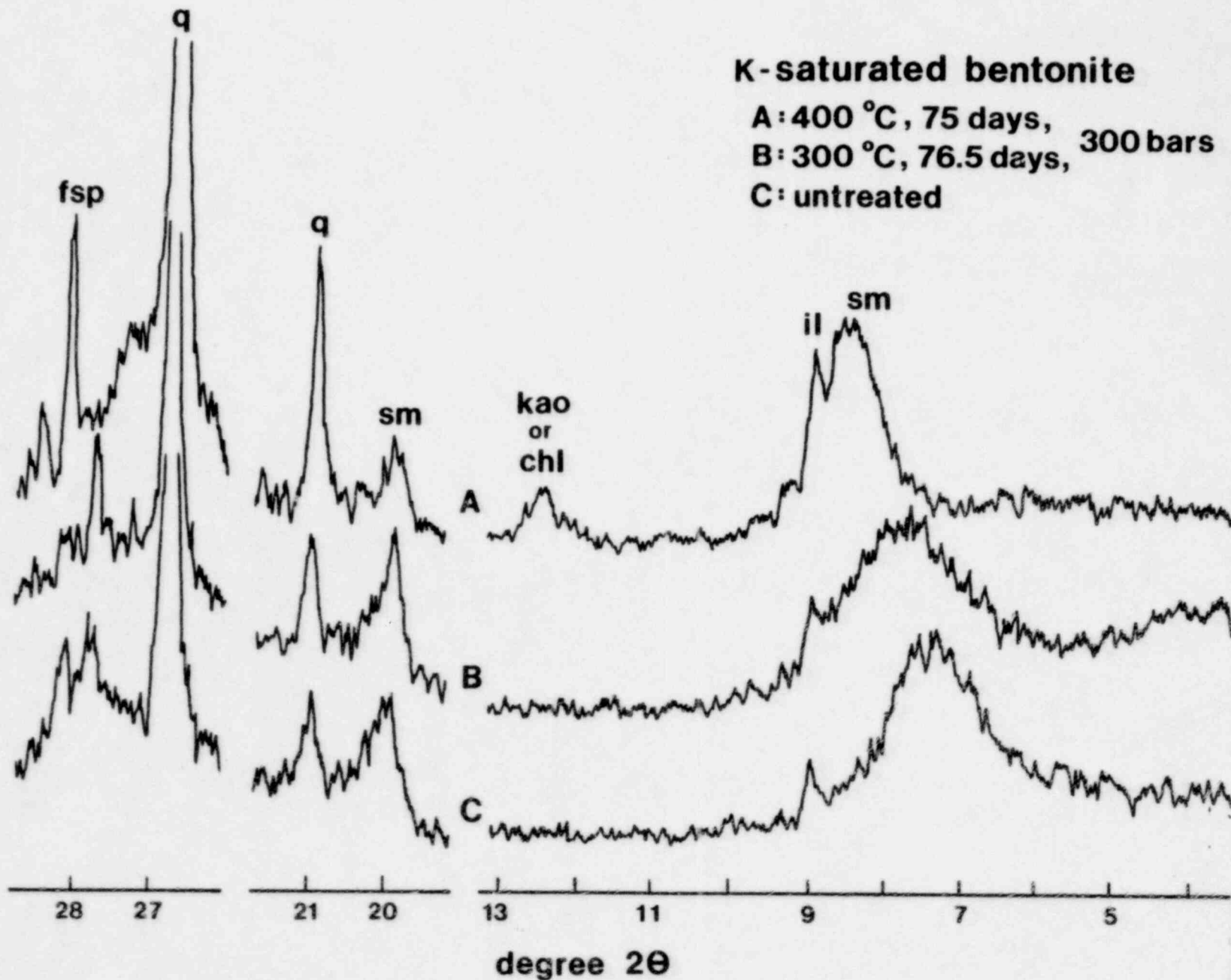
350, 360, 460°C Runs (ILB3A, ILB3B, IL680, IL455). Figure 4.7 shows XRD patterns of the starting material, and the 360 and 460° run products. The patterns for all the run products are essentially identical. They are, in turn, virtually identical to that for the starting material with one significant change. This is in the appearance of a 7 $\overset{o}{A}$ peak. XRD cannot differentiate, on this basis, between a septechlorite (e.g. kaolinite or berthierine) or a chlorite. However, for run IL783, described below, this peak is shown by TEM/AEM to be due to the trioctahedral septechlorite berthierine, and we assume the same is true in these cases. The components for this phase are derived by recrystallization of illite/smectite, and therfore it implies major recrystallization of all phyllosilicates. These relations are described and illustrated in detail below, for run IL783.

4.3.2.3. Basalt

300°C Run - There are no detectable differences between the treated basalts and the untreated basalt. The XRD patterns show dominant plagioclase (laboradorite) as well as pyroxene and magnetite peaks.

360 and 460° Runs - The only difference in XRD patterns between these two runs and that of the starting material is the appearance of a weak but definite 14 $\overset{o}{A}$ peak, indicating the production of smectite, chlorite or vermiculite as an alteration product. This is confirmed by SEM observation in which feathery clay flakes are clearly observed (Fig. 4.8). Under TEM, however, both 10 $\overset{o}{A}$ (illite, Figs. 4.9a and 4.9b) and 14 $\overset{o}{A}$ (smectite, Fig. 4.9b) lattice fringe images were observed. The 10 $\overset{o}{A}$ phase, tentatively identified as illite, occurs as discrete grains.
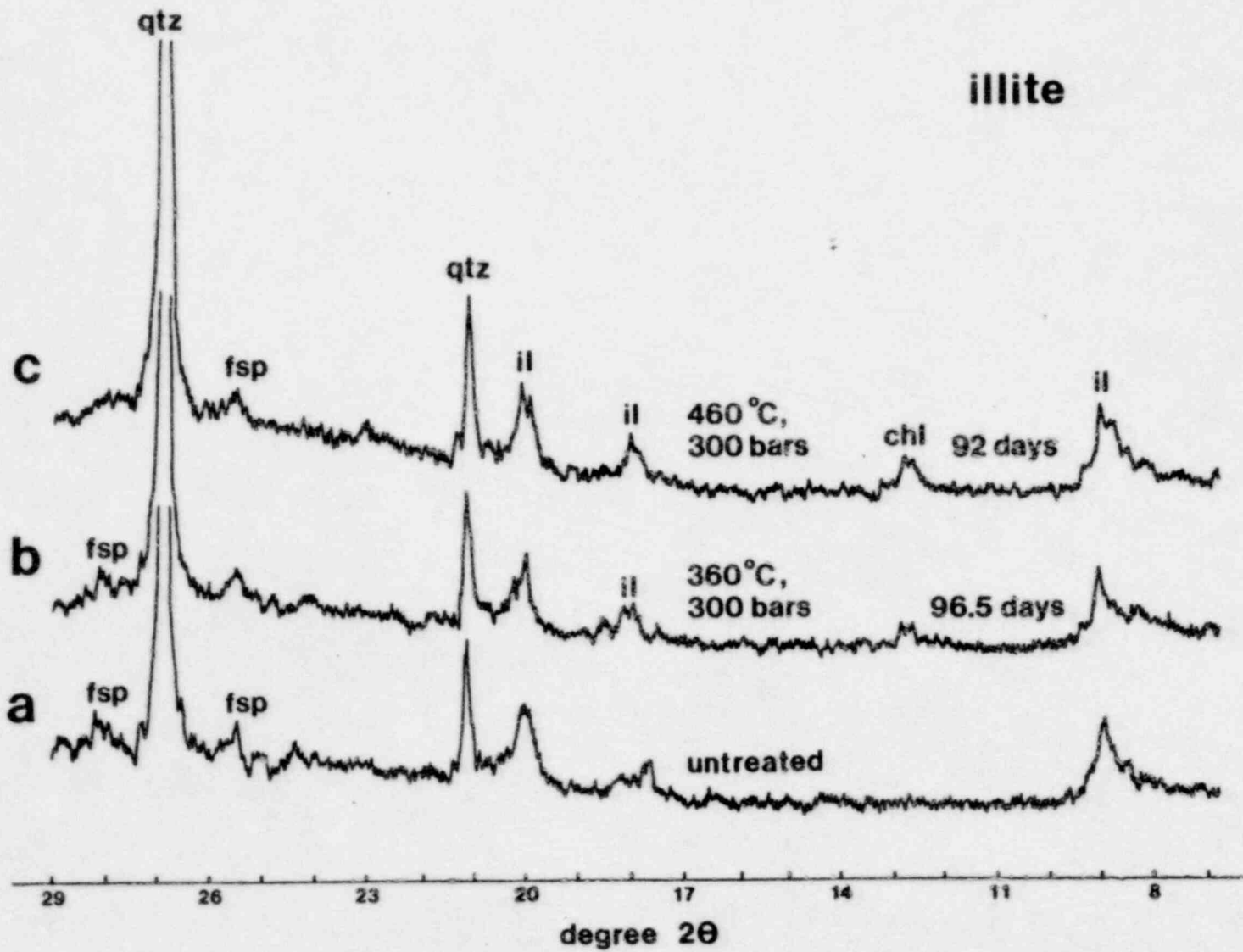
Figure 4.7. XRD patterns of illite: (a) starting material, and hydrothermally treated samples in two different run conditions; (b) 360°C, 300 bars, 96.5 days and (c) 460°C, 300 bars, 92 days.

Figure 4.8. A SEM photograph of run BS450 (basalt, same sample as for Fig. 4.7c) showing occurrences of clay minerals (flaky "feathers" at lower center).
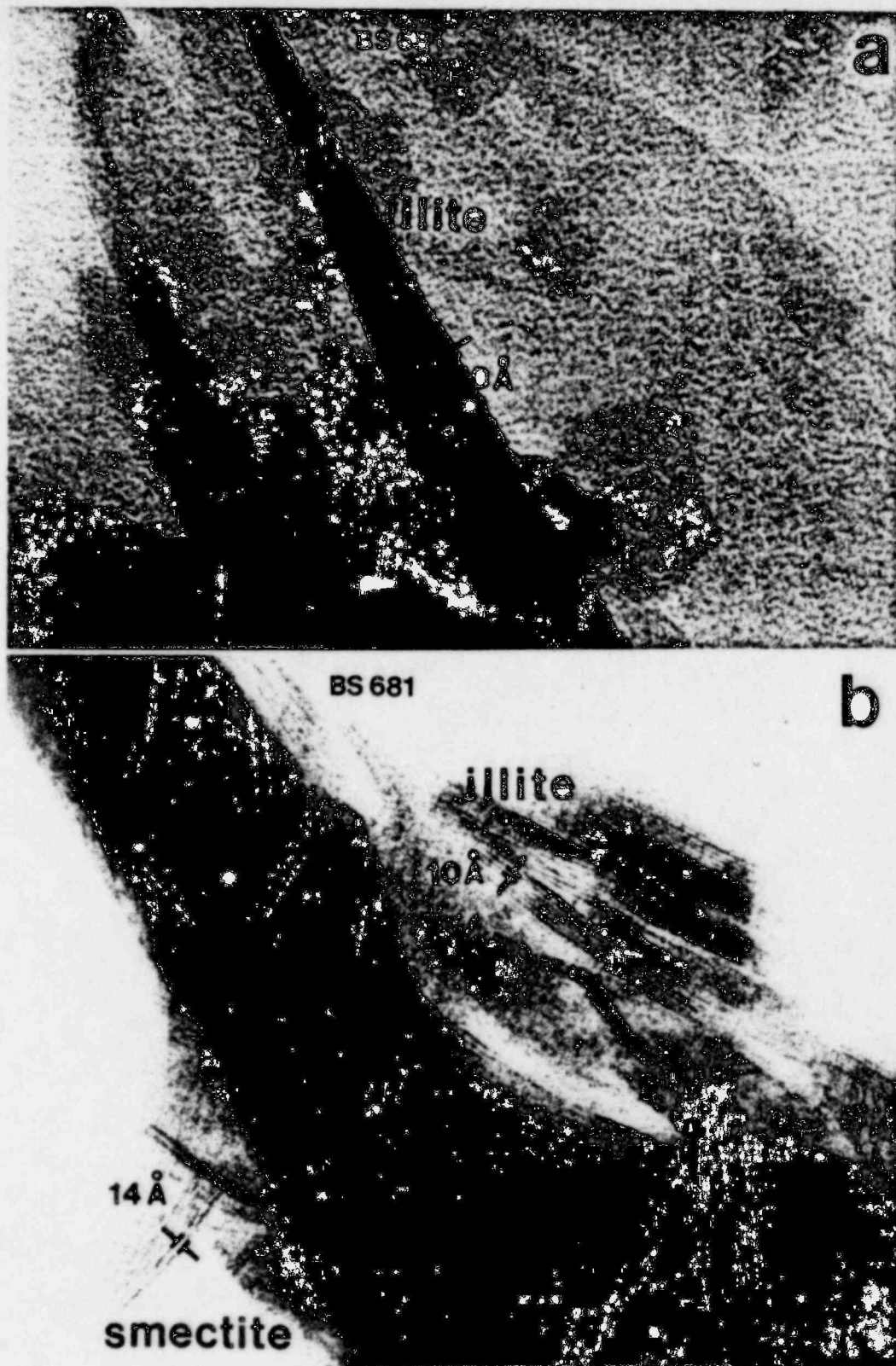
Figure 4.9. a. A TEM image of a part of basalt sample hydrothermally treated at 360°C, 300 bars for 96.5 days. The figure shows lattice fringes of straight and continuous illite 001 layers (10 A). b. A TEM image of the same sample as Figure 15a showing lattice fringes of 10 A illite and 14 A smectite layers. Illite layers are more regular and straight compared to smectite layers.

4.3.3 Set III Long Term Runs

These runs were of an extended duration of from 414 to 584 days at a temperature of 200 or 300°C with the latter as the maximum estimated for the backfill materials. This, in combination with the extraordinarily long times for the experiments (even longer times would be desirable but are not practical within the time constraints of the project) result in an optimum test of the properties of the backfill materials.

4.3.3.1 Bentonite

200°C Runs (BN384, BN 181). Other than a loss of calcite and small shifts in the d-value of the principal 001 peak (as consistent with the results described, for example, for Run BNC 32, Set II) no changes were observed; i.e. smectite remained essentially unchanged with the exception of some cation exchange.

300°C Runs (BN 282, BN 571, BN 780, BN 802). XRD patterns effectively duplicate those for 200°C. Figures 4.10 and 4.11 are TEM lattice fringe images for bentonite from Run BN 282. They should be directly compared with those of Figures 3.1 and 3.2, the starting material. These images display identical characteristics and further verify that the smectite es effectively unchanged. Figure 4.12 shows EDX spectra for the run product (the Fe peak is a contaminant). It shows that there has been no change in the Si:Al ratio, as should be true if the smectite has not undergone solution and recrystallization. However, the proportions of both interlayer Ca and Na have decreased considerably as consistent with exchange of interlayer cations. (Although the Na peak is small, it reflects a large molar proportion of Na relative to Ca and the smectite has Na as the principal interlayer cation.)
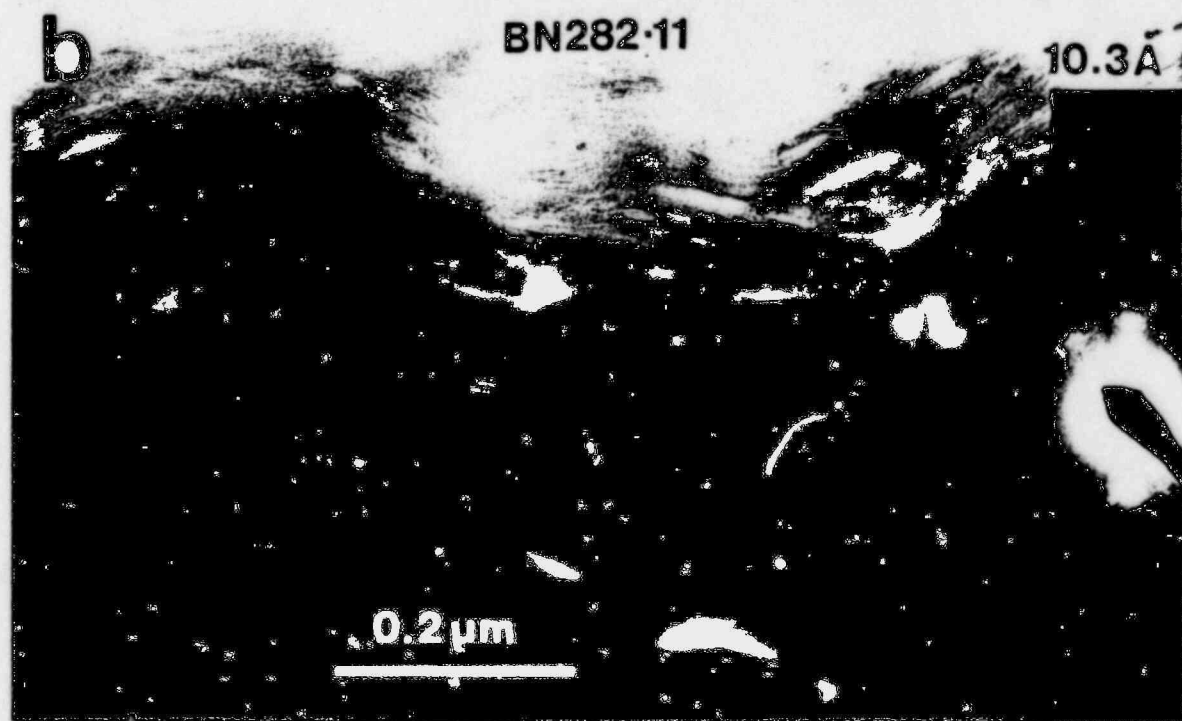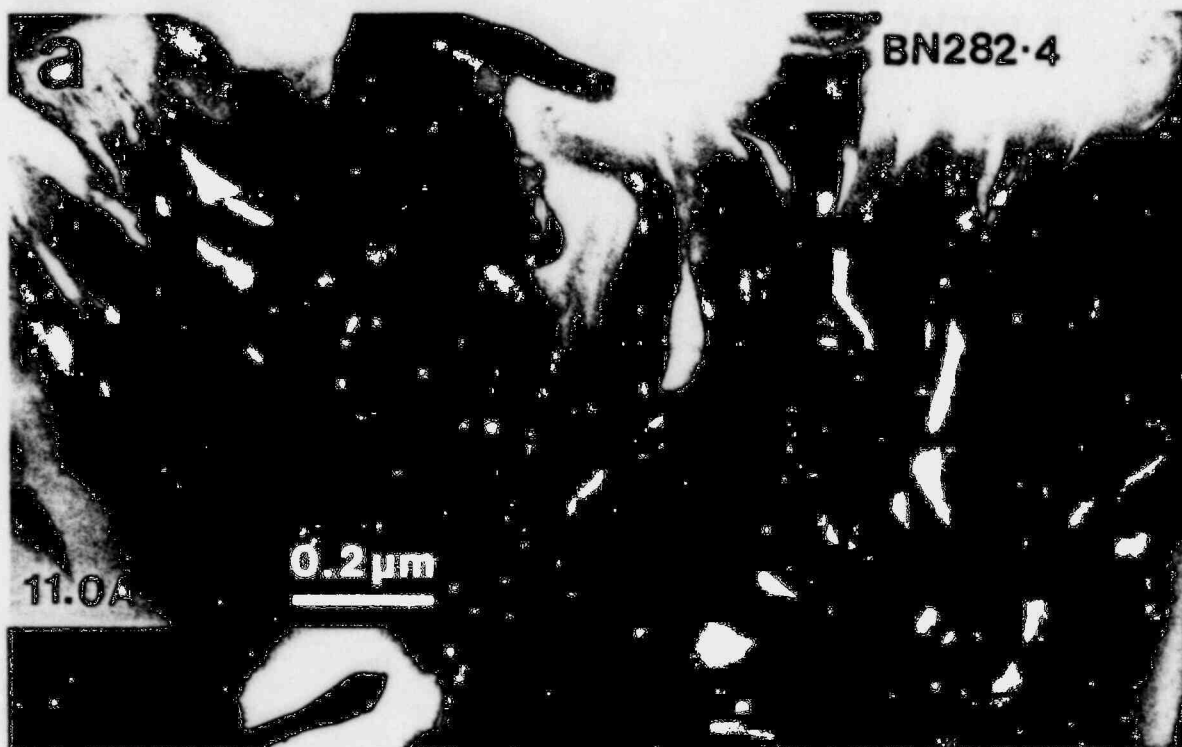
Figure 4.10. Low magnification TEM images of bentonite from Run BN282 (300°C, 537 days), showing typical bentonite texture, identical to that of starting material.
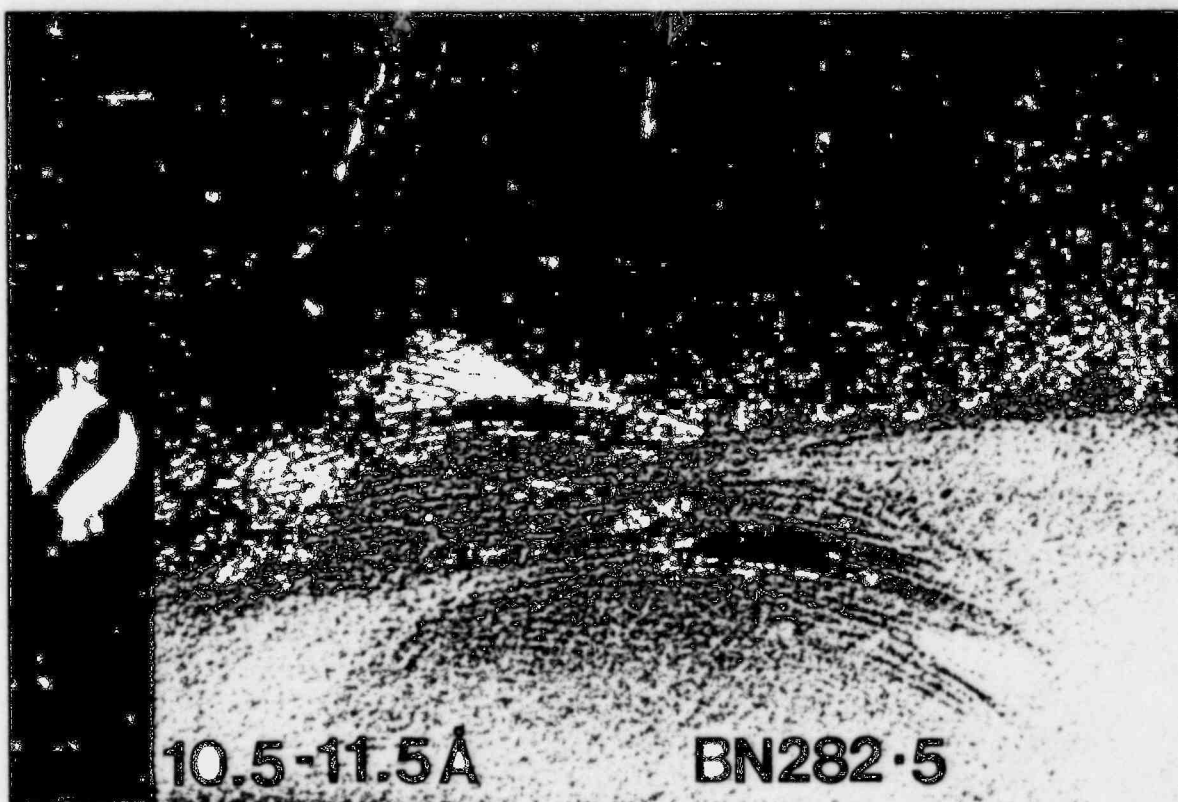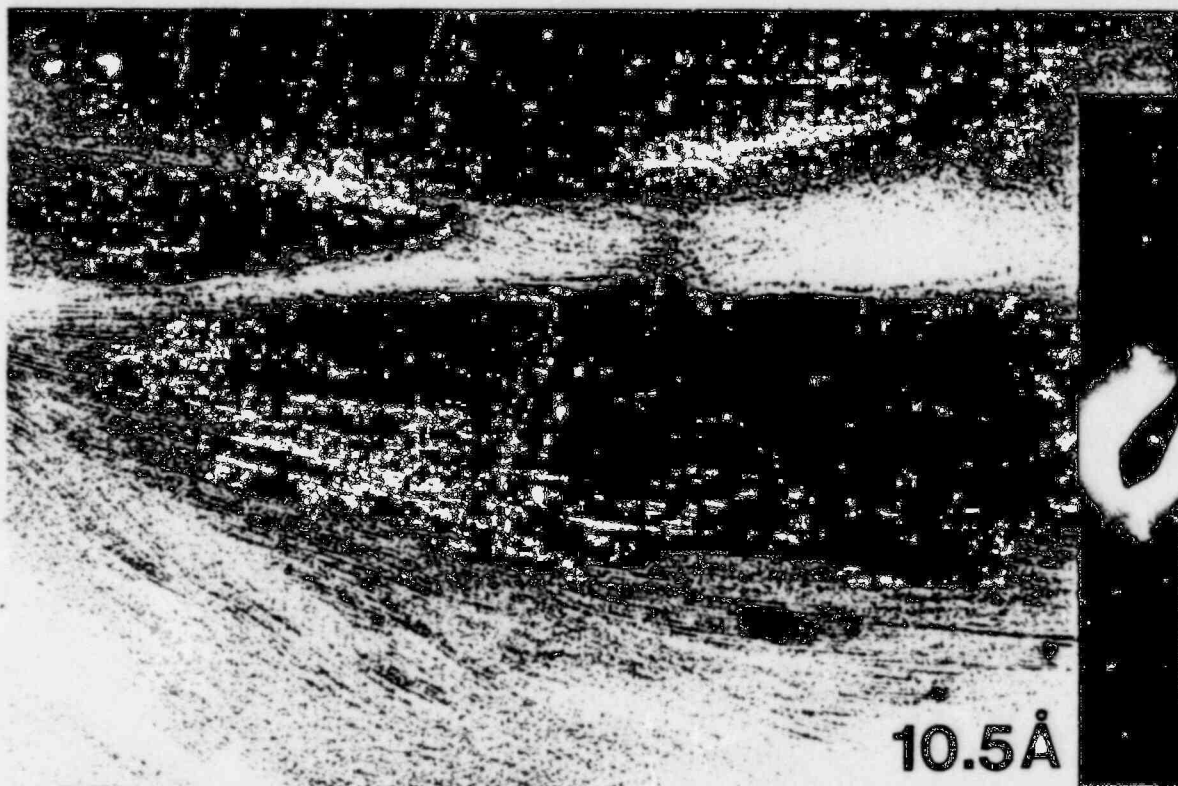
10.5Å

10.5-11.5Å   BN282·5

Figure 4.11. High magnification lattice fringe images of bentonite from
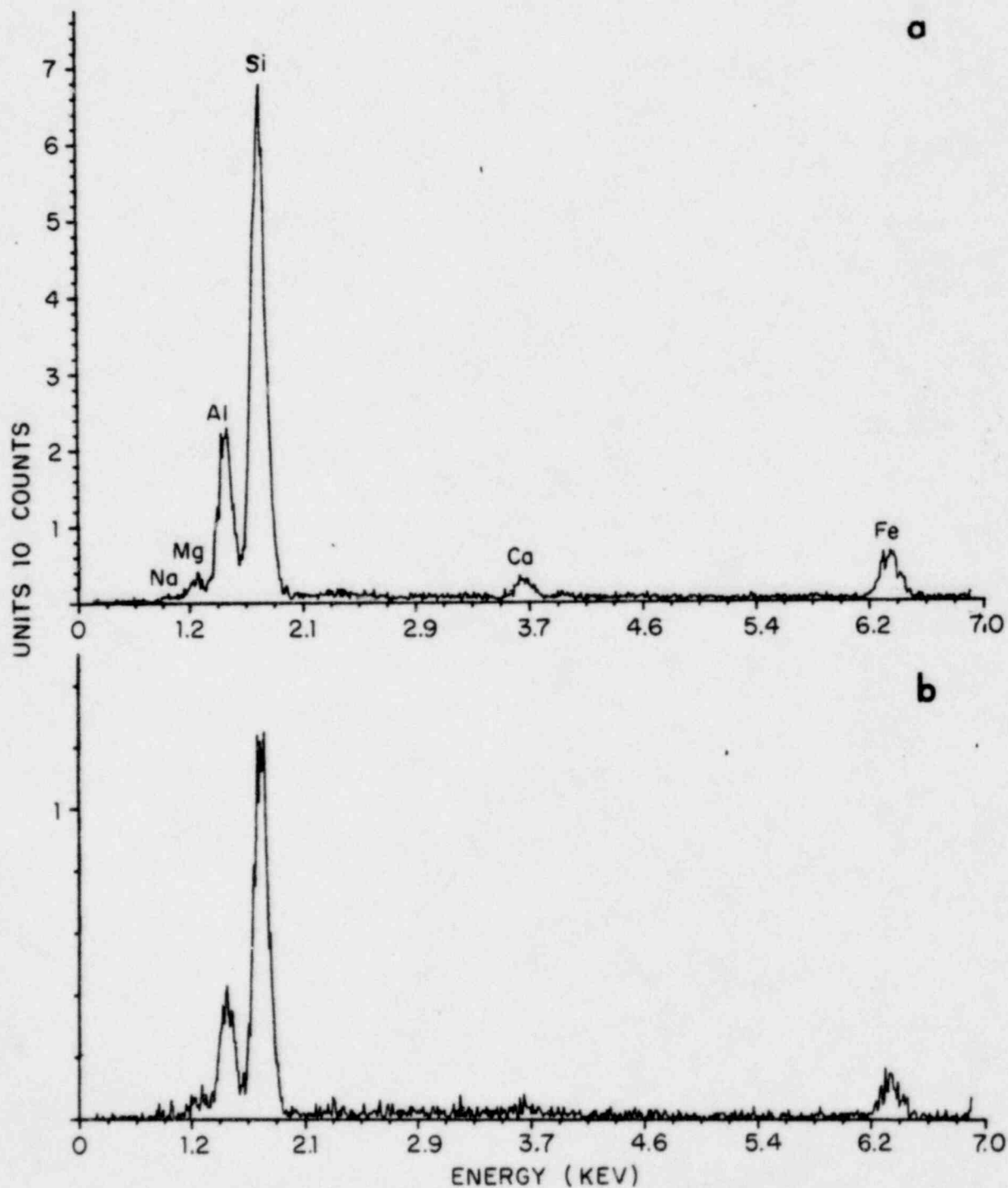   Run BN282 (300°C, 537 days).

84

Figure 4.12. EDX spectra for bentonite, obtained by AEM analysis. a. Starting material b. Product of Run BN282 (300°C, 537 days).

4.3.3.2 Illite

200°C Runs (IL 184, IL 389). XRD patterns indicate that there was no change.

300°C Runs (IL 281, IL 572, IL 783, IL 805). There was no change in Runs IL 281 and IL 805 as indicated by XRD. However, a small, new 7 Å peak appeared for Run IL 572 and a predominant 7 Å peak appeared in the XRD pattern for Run IL 783. In addition the 001 peak of illite was significantly less diffuse and asymmetric than that for the starting material, indicating that the illite has been annealed through recrystallization.

Figures 4.13, 4.14, and 4.15 are TEM lattice fringe images for Run IL 783. These should be compared with Figure 3.5 which shows the equivalent image for the starting illite. Figure 4.15 is a high magnification lattice fringe image showing that there are two kinds of phyllosilicates with layer spacings of 7 and 10 Å, respectively. As shown in Figures 4.15a and 4.15b, they occur both as separate and as intergrown packets of layers. The latter texture clearly demonstrates that they formed during the same event. Because the 7 Å phase is not present in the starting material, at least some of the illite has undergone recrystallization.

Figure 4.16a and 4.16b are EDX spectra of the original illite and that of Run IL 783. There is a clearly defined increase in both K and Al relative to Si. This is the result expected for the transition of illite toward muscovite and demonstrates that the illite has undergone annealing through recrystallization.

Figure 4.16c is an EDX spectrum of a mixture of the 7 Å phase and illite. Subtracting illite components from this spectrum shows that the 7 Å phase is rich in Mg and Fe, with minor Al in the octahedral sites. This phase is therefore berthierine. Ahn and Peacor (1986) have demonstrated that smectite,

86

Figure 4.13. Low magnification TEM image of the products of Run IL783 (300°C, 544 days), showing subhedral crystals of illite (10 A spacing) and berthierine (7 A) spacing, as identified in part with inset diffraction pattern.
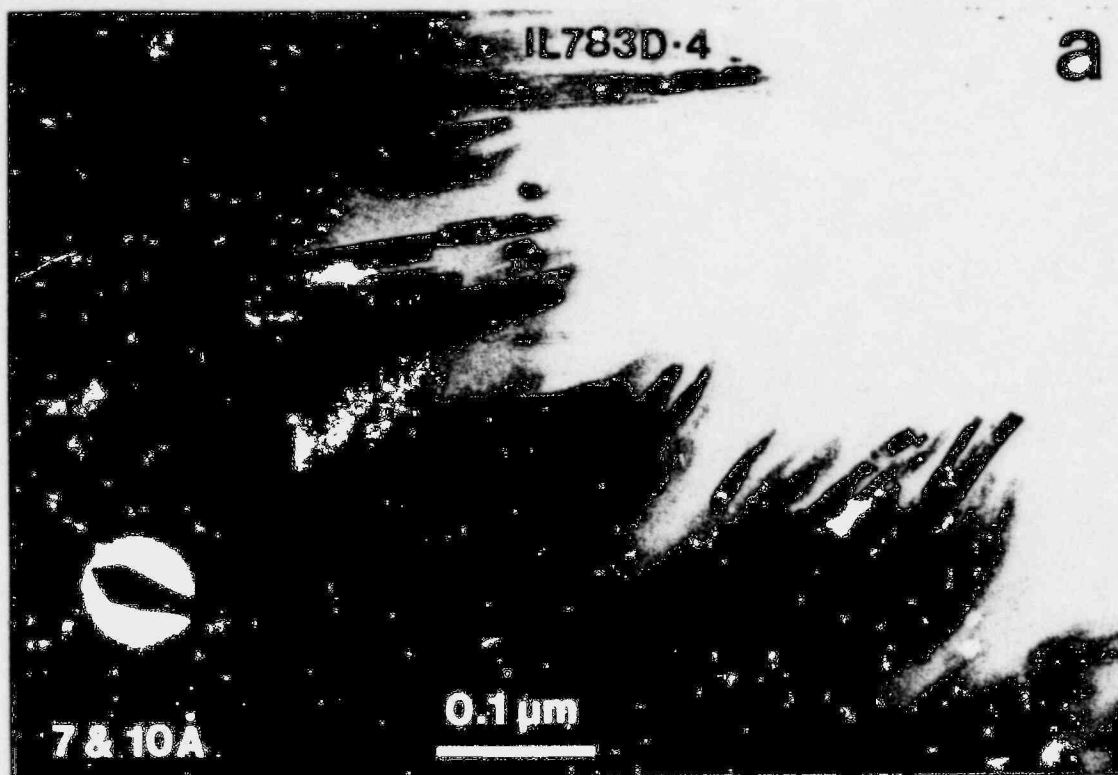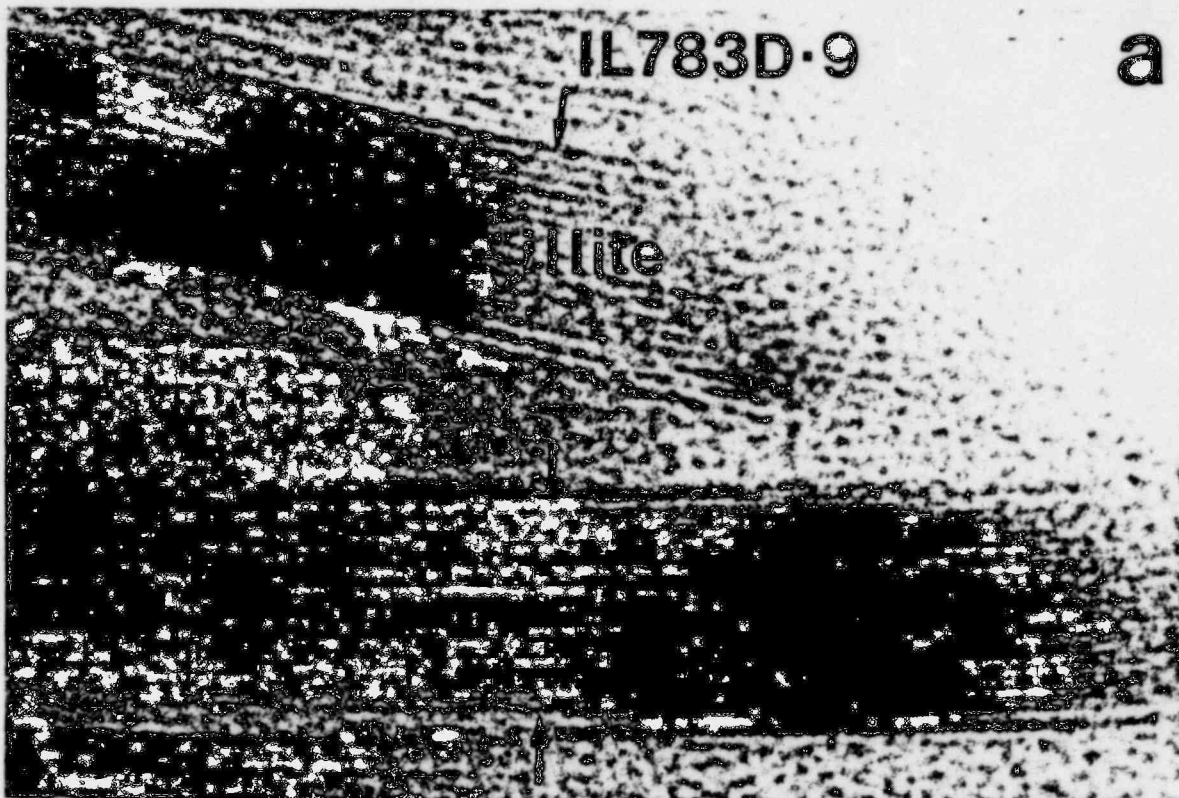
Figure 4.14. Intermediate magnification image of the products of Run IL783 (300°C, 544 days). a. Subhedral crystals of illite and berthierine. b. Subhedral crystal of illite, higher in Al and K than starting material (see analysis of this crystal, Figure 4.16b).

Figure 4.15. High resolution lattice fringe images of the products of
    Run IL783 (300°C, 544 days). a. Separate grains of berthierine and
    illite. b. Layers of illite and berthierine as part of a single grain,
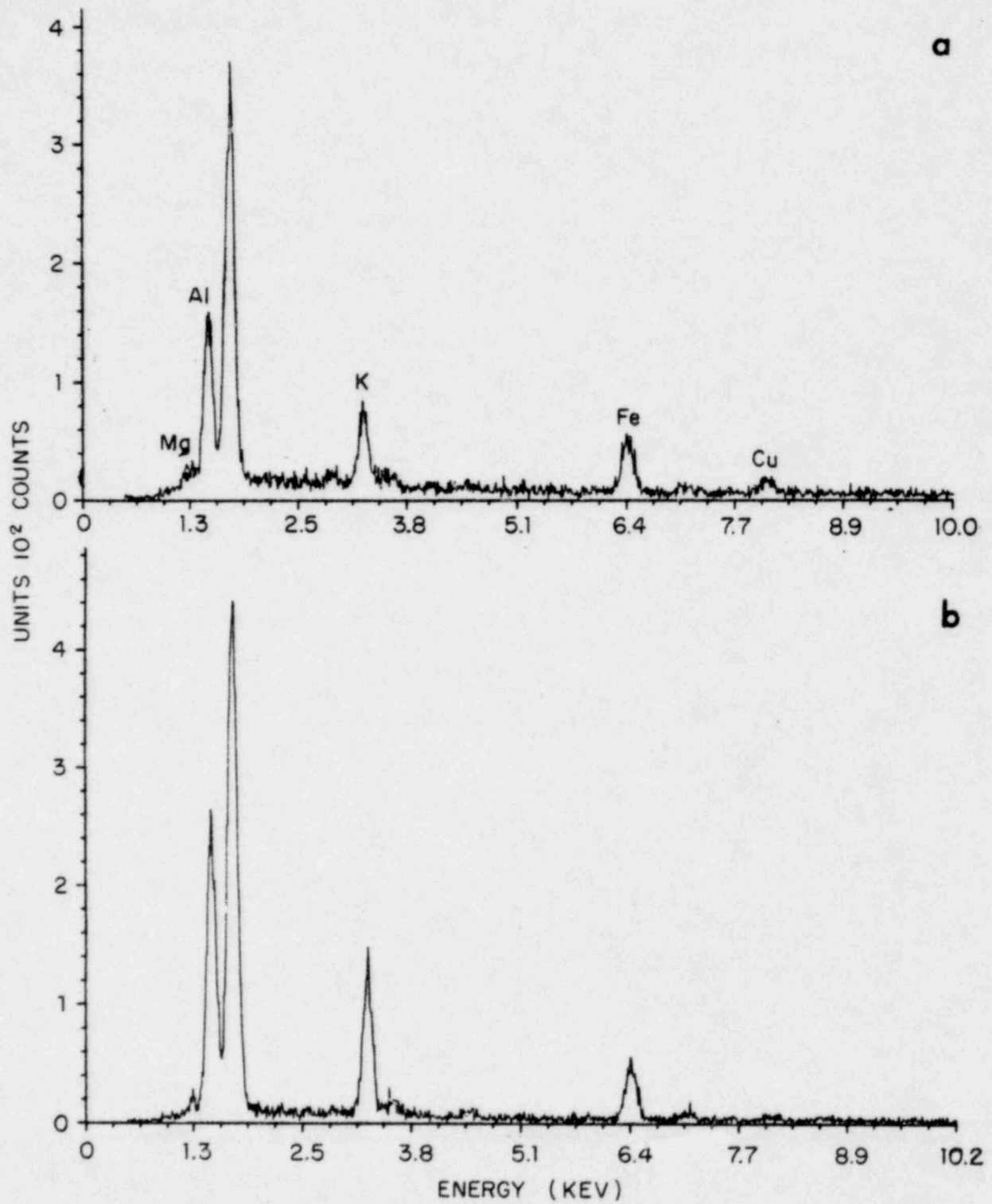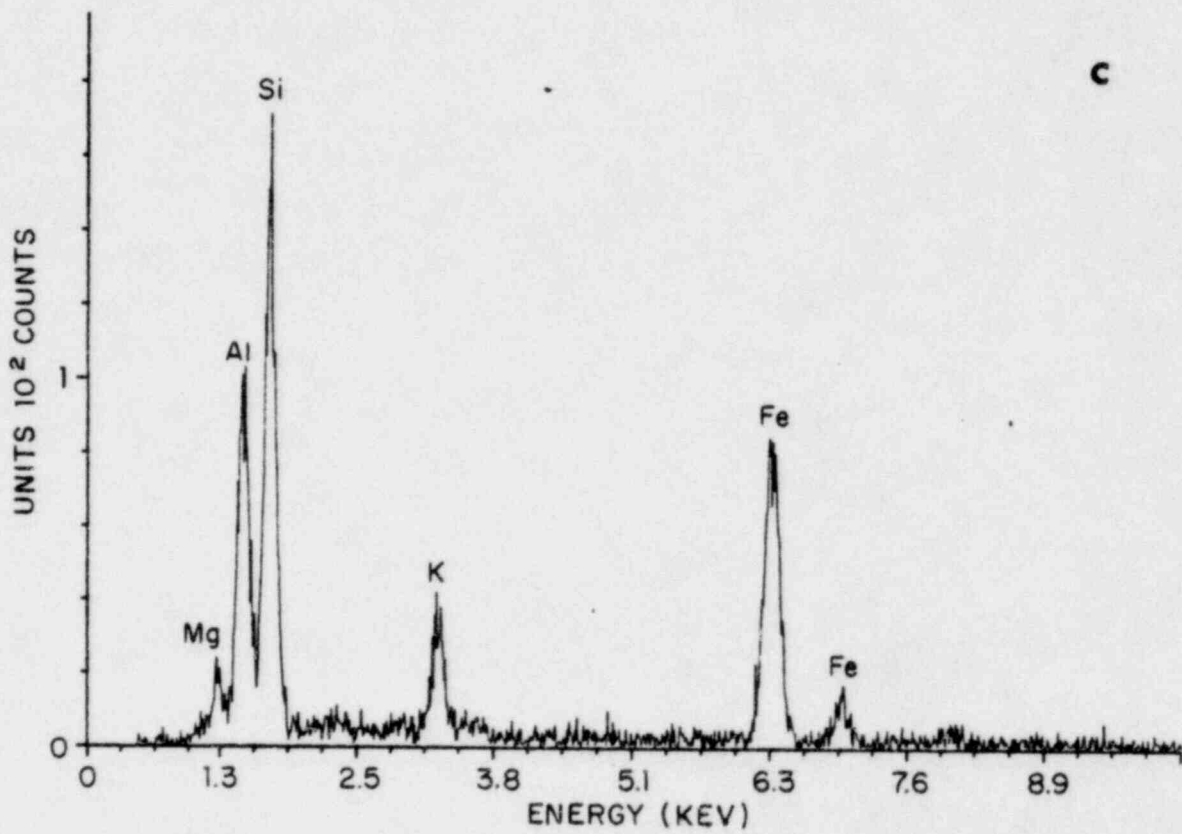   with coherent or semi-coherent interface.

Figure 4.16. EDX spectra for illite as obtained by AEM. a. Fithian illite starting material b. Illite grain shown in Figure 4.14b, from Run IL783. c. Spectrum for unresolved berthierine and illite. The high Fe and Mg are from berthierine.

90

mixed layer smectite/illite, and early-formed illite may have a considerable amount of Fe and Mg, and that the transitions to illite and toward muscovite result in separation of the Al, and Mg and Fe into separate dioctahedral (illite/muscovite) and trioctahedral (berthierine/chlorite) phases. The same process has clearly taken place in these experiments, with the Fe, Mg component of the original smectite/illite forming berthierine during the transition to more highly ordered illite.

Figures 4.13 and 4.14 show lower resolution images of the illite and berthierine. The top-central area of Figure 4.13, shows that the phyllosilicate texture has dramatically changed during the experiment. Individual subhedral, lath-like crystals of illite and berthierine are shown (the images are actually cross-sections through platy crystals, each a few hundred Angstroms in thickness) which are in sharp contrast to the textural relations of the starting material, where no subhedral to euhedral crystals are found. These crystals are strikingly similar to the illite and chlorite crystals observed for Salton Sea sediments, and Figures 2.5 and 2.6 should be directly compared. The experimental system has thus given rise to results which are texturally, structurally and mineralogically equivalent to those of the Salton Sea sediments where the water to rock ratio is unusually high for geologic materials. This further demonstrates the apparent equivalence of the Salton Sea geologic system, the hydrothermal experiments, and the parameters relating to the backfill.

4.3.3.3 Basalt

The XRD patterns of all basalt run products were effectively the same as that of the starting material for both the 200 and 300°C runs. No changes were therefore detected.

4.3.4 Set IV Basalt plus Bentonite

These runs were carried out with mixtures of bentonite and basalt, in the following proportions: (1) 75% basalt, 25% bentonite; BB41, BB44, BB62, BB69. (2) 50% basalt, 50% bentonite; BHD4, BHC5. (3) 25% basalt, 75% bentonite; BQC1, BQD7. These runs were carried out for temperatures of 300° and 400°C; the 400°C runs were carried out in order to maximize reaction rates, relative to the 300°C runs which corresponded to the maximum estimated for the repository backfill environment.

4.3.4.1 400°C Runs

Figure 4.17 shows XRD patterns for the starting materials, and run products for two different rock/water ratios at 400°C, for starting materials of 25% bentonite. The patterns demonstrate that the crystalline phases are largely unchanged, but the zeolite wairakite is present in the run product. Figures 4.18 and 4.19 are SEM images of the run products, with EDX spectra verifying the identifications in morphological criteria. The wairakite (Figure 4.18) displays a euhedral morphology of the sort that is typical of crystals that have directly crystallized from solution. Smectite is still abundant in the run products. Insofar as the starting crystalline materials have been demonstrated to be largely unchanged by treatment, yet wairakite has formed as a major phase, it is tempting to infer that the latter is largely due to the solution of the non-crystalline, glass component of the basalt. Accordingly, we carried out extensive SEM studies of both starting and product materials in an attempt to locate the sites of dissolution in the starting materials. However, those attempts were not successful. Nevertheless, we believe that reaction of glass has produced wairakite.
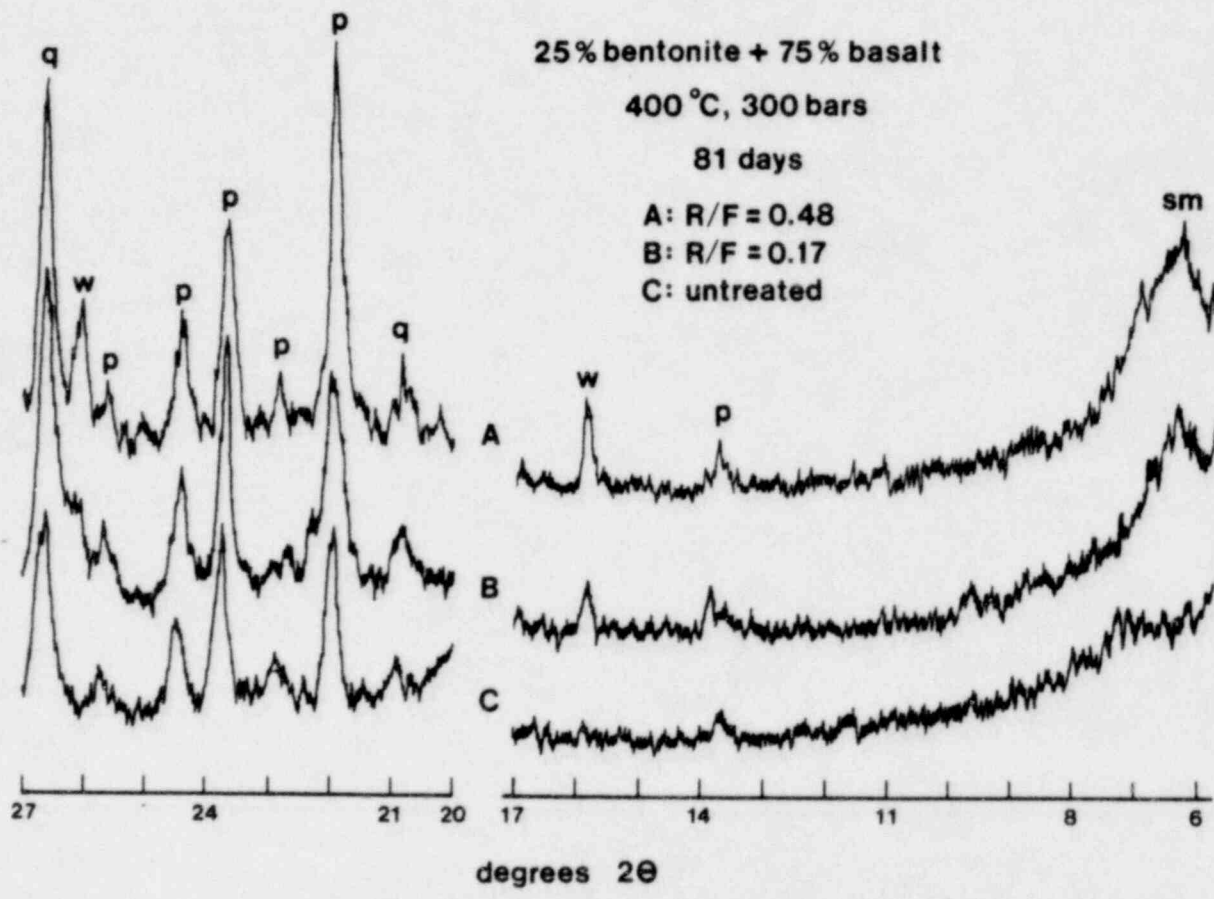
Figure 4.17. XRD patterns for 25% bentonite/75% basalt mixtures. a. Product of Run BB62 (400°C, 81 days) b. Product of Run BB69 (400°C, 81 days) c. Starting material, untreated.
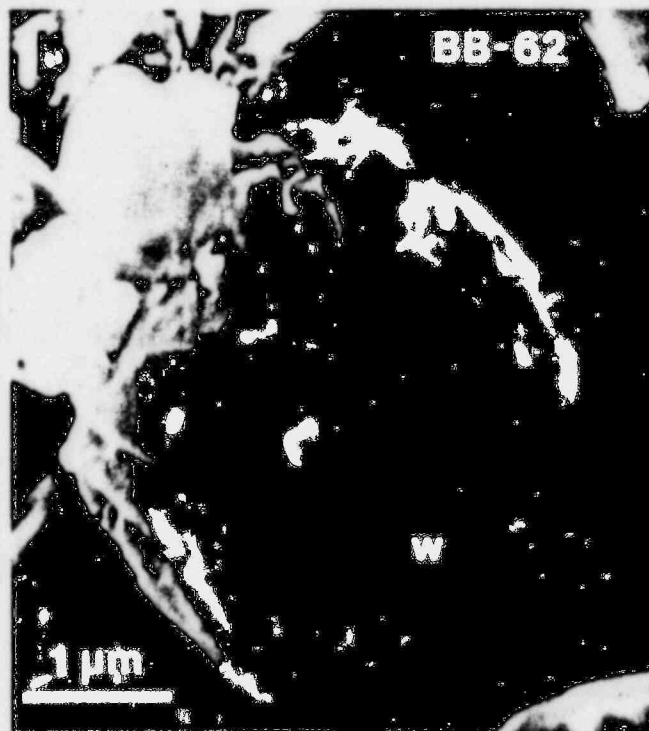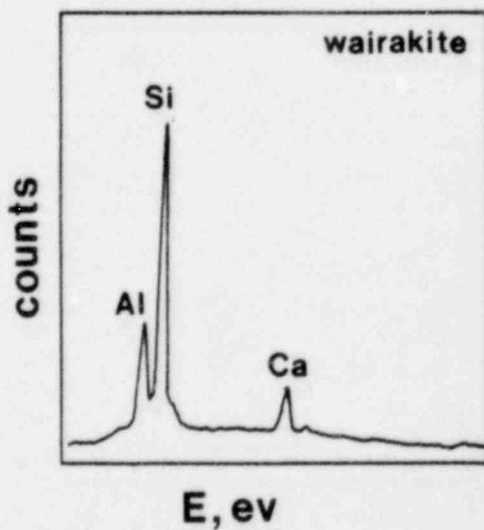
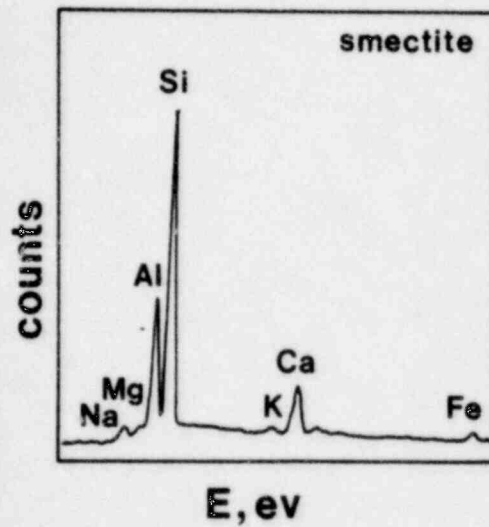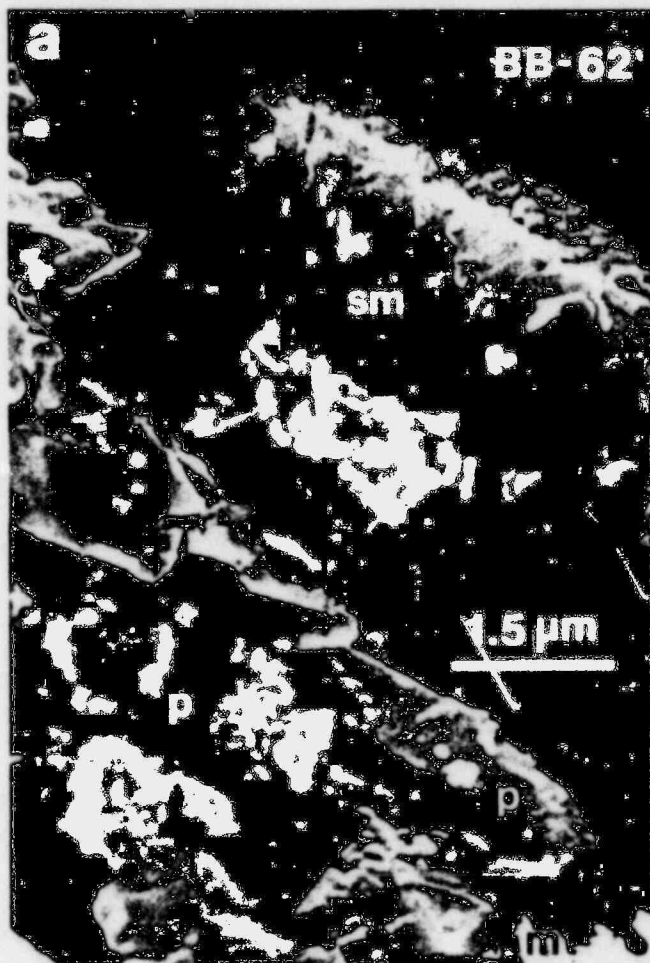Figure 4.18. SEM images and corresponding EDX spectra for smectite and wairakite from Run BB62 (25% bentonite/75% basalt; 400°C, 81 days).
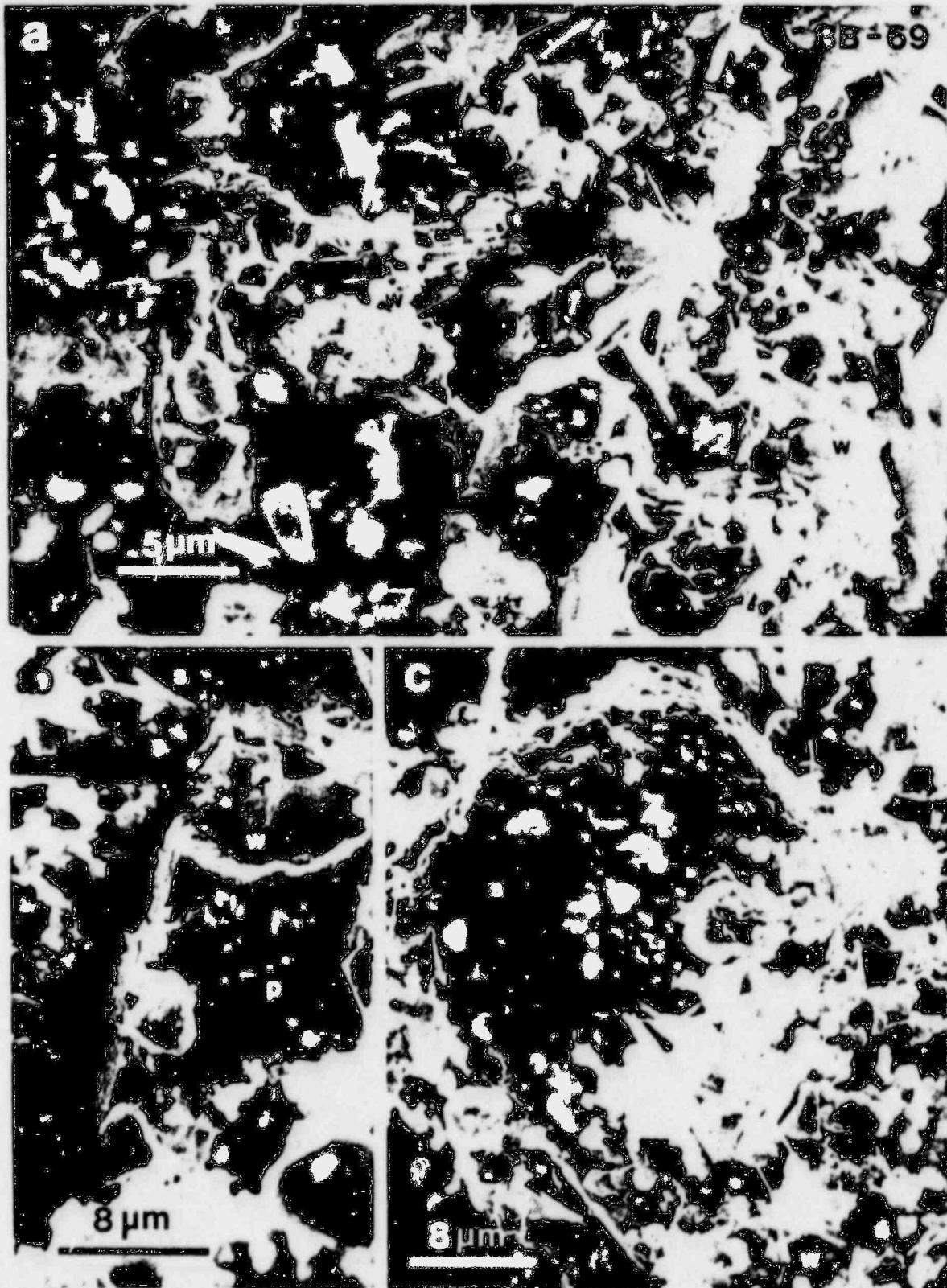
Figure 4.19. SEM images of products of Run BB69 (25% bentonite/75% basalt; 400°C, 81 days). s = smectite, w = wairakite, p = plagioclase.

Figure 4.20 shows XRD patterns for 400°C runs for each of the basalt/bentonite ratios. Pattern B (75% basalt) exhibits very little change from the starting material, except for the appearance of some wairakite, as discussed above. However, patterns A (50% basalt) and C (25% basalt) show considerable change.

Pattern C exhibits the growth of substantial proportions of chlorite and wairakite, with the loss of all or most of the smectite and pyroxene (and presumably, the glass). Plagioclase feldspar and quartz are still present in the product. The chemistries of the glass plus smectite + pyroxene reactants and chlorite plus wairakite products are, to a first approximation, correct for a mass balanced reaction.

Pattern A (50% basalt) demonstrates virtually complete change. All of the starting materials are absent, and only chlorite and illite are detectable by XRD. Figures 4.21, 4.22, and 4.23 are TEM images showing the textures at high and intemediate resolution. The illite and chlorite occur as packets of 10 and 14 Å layers, respectively. Packets of layers may be from two or three to several tens of layers in thickness. In the former case illite and chlorite occur in complex interlayered sequences; in the latter, they form individual euhedral grains.

Figure 4.23 shows illite and chlorite occurring as euhedral crystals. It is similar to Figure 4.15, which shows berthierine and illite as hydrothermal products of illite/smectite, and Figures 2.4-2.6 which the typical textures for Salton Sea phyllosilicates. Such euhedral shapes are common to all samples and we infer that they are typical of direct crystallization from solutions with high water/rock ratios - as compared to Gulf Coast type systems.

Figure 4.23 should be directly compared with that of Figure 2.3 which demonstrates illite and chlorite packets interlayered in Lehigh Gap samples.
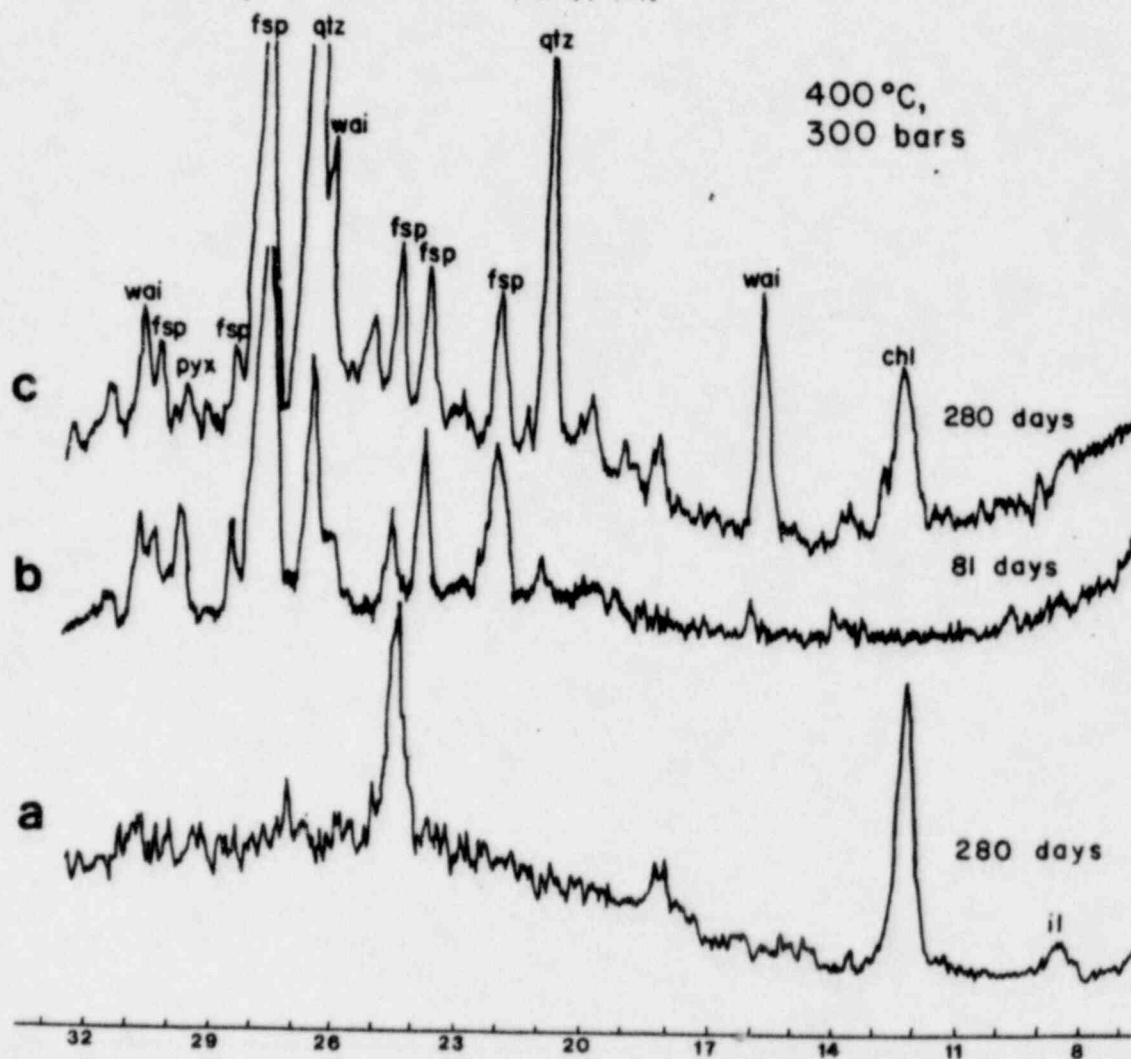
Figure 4.20. XRD patterns of products of runs with basalt/smectite mixtures
for a temperature of 400°C. a. Run BHC5 (50% basalt/50% bentonite) Peaks
correspond to chlorite and illite b. Run BB62 (75% basalt/
25% bentonite). There is a small peak for wairakite c. Run BQC1
(25% basalt/75% bentonite) wairakite and chlorite are major phases.
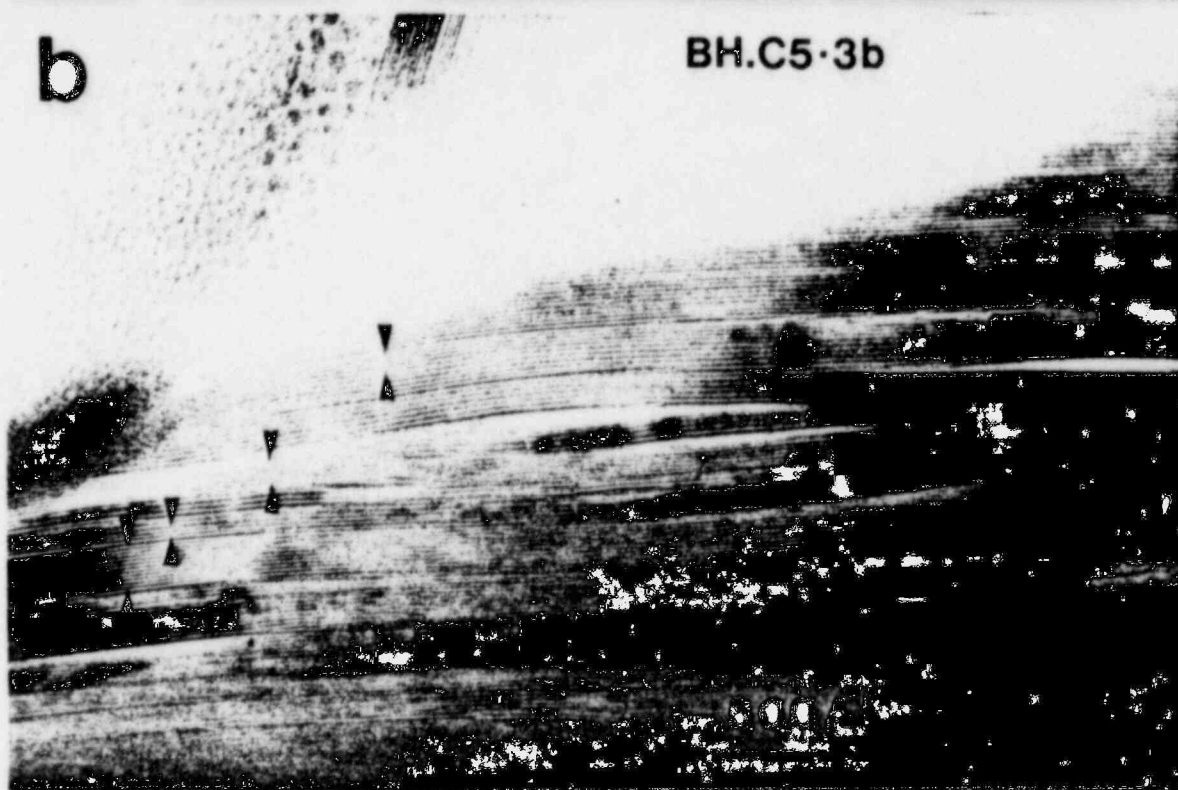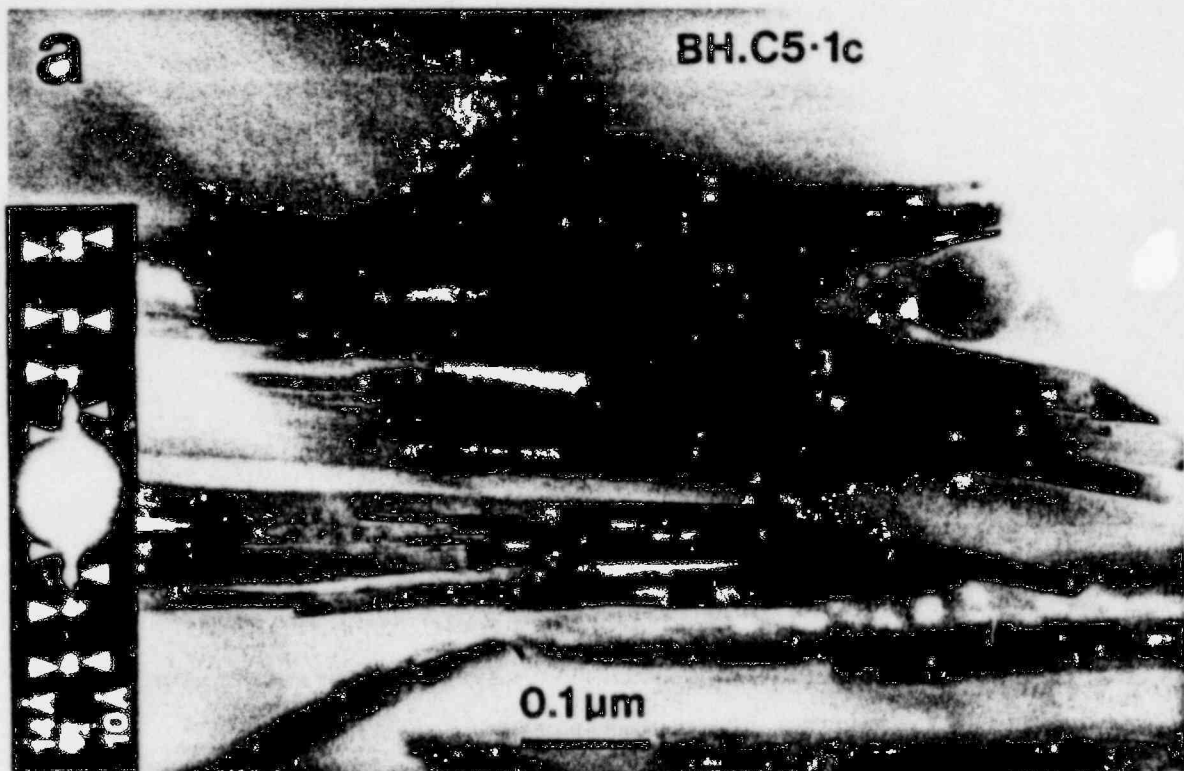
Figure 4.21. TEM images of products of Run BHC5. a. Subhedral crystals of chlorite and illite b. Mixed layering of packets of illite (between arrows) and chlorite layers.
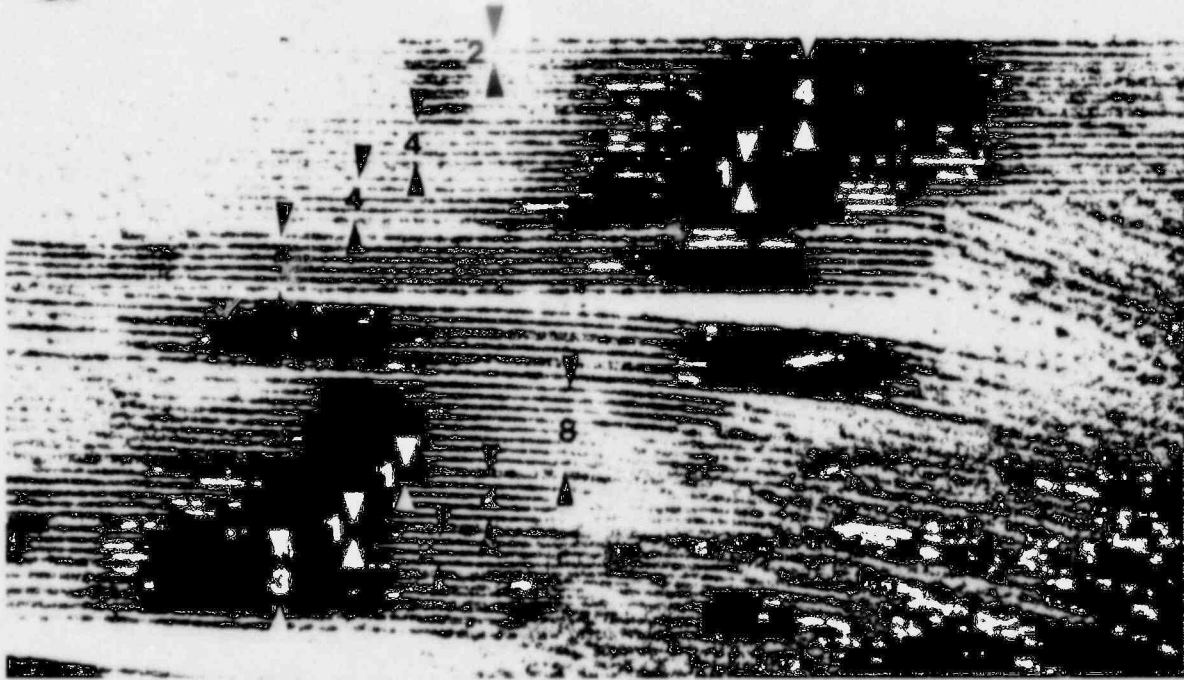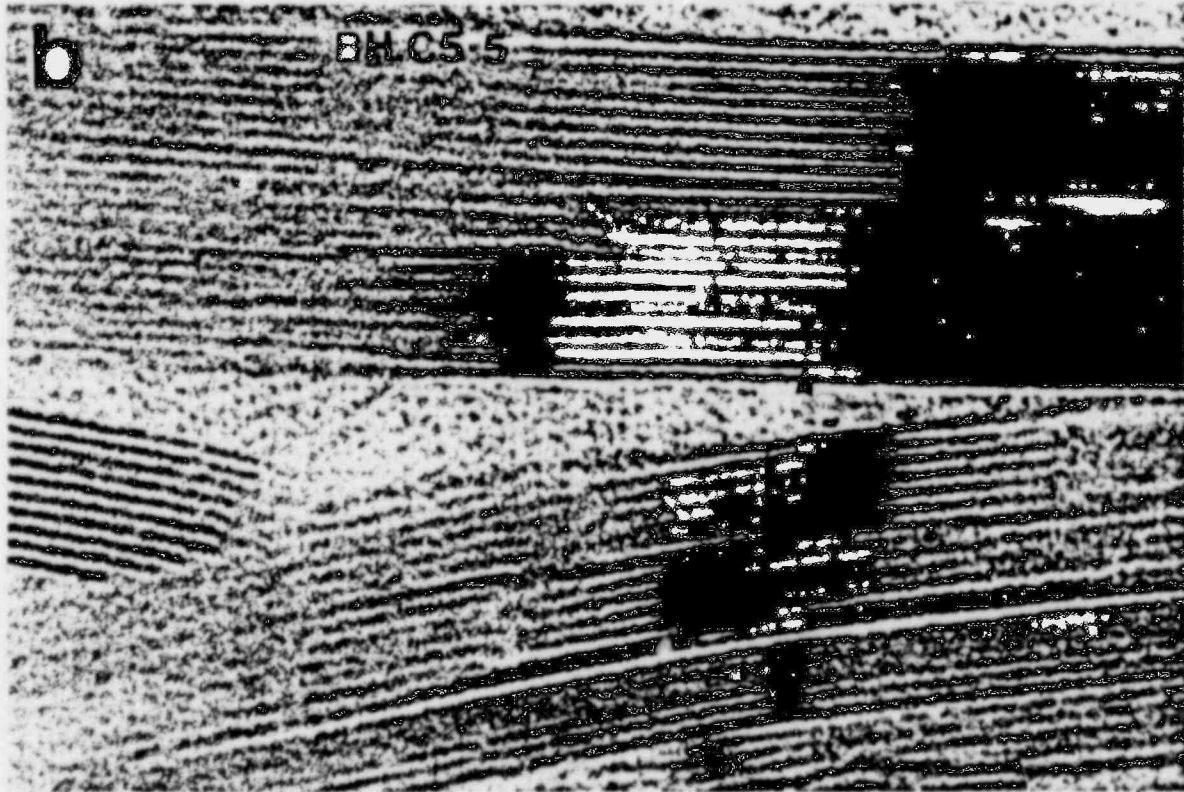
Figure 4.22. High resolution lattice fringe images of products of Run BHC5.
a. Dominant illite (black arrows) interlayered with chlorite (white
arrows). b. Chlorite with mixed layering of illite (between black arrows)
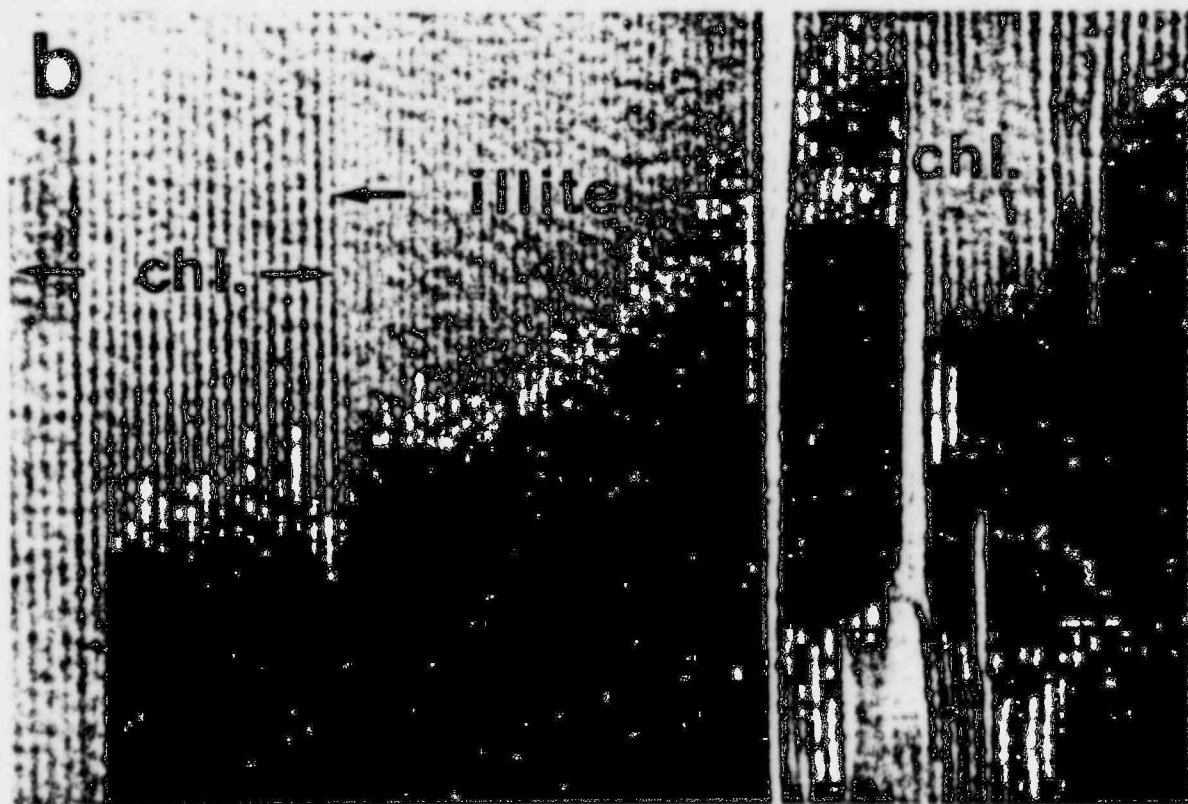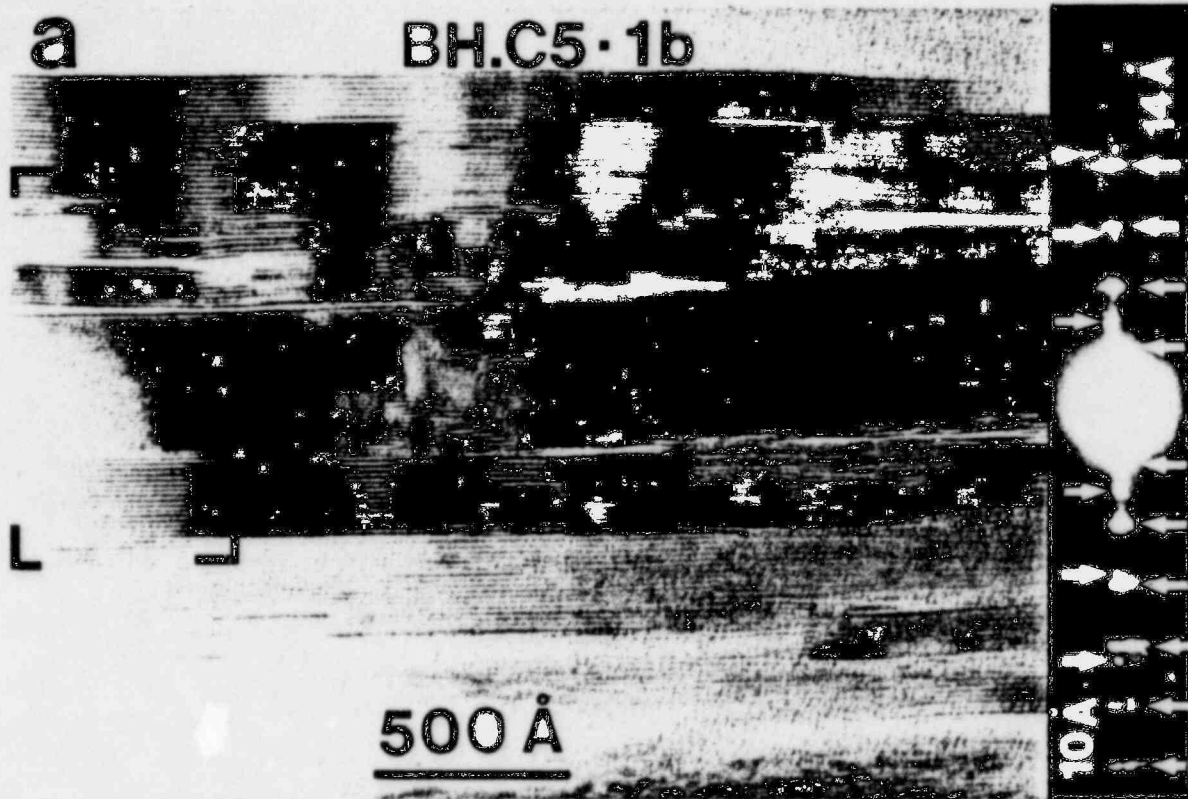
Figure 4.23. TEM images of products of Run BHC 5. Figure 4.23b is the enlarged region of 4.23a shown in brackets, and shows mixed layering of packets of illite (10 A) layers and chlorite (14 A) layers.

101

The general features shown are the same, and in a qualitative sense we could not differentiate their origins; i.e. the 400°C run has produced both phases and detailed textures that duplicate the unusual phases and textures of the analogous geologic systems.

Figure 4.24 shows AEM analytical EDX spectra for the bentonite starting material (pattern A), smectite of run BHD4 at 300°C, and the unresolved layers of illite + chlorite of run BHC5 at 400°C (pattern C). The smectite at 300°C is clearly intermediate in composition between the starting material and the reaction products illite plus chlorite. The spectra clearly confirm that the 10 Å layers of Figures 4.21, 4.22 and 4.23 are illite (the K is present in illite) and that the 14 Å layers are trioctahedral chlorite. The high proportion of illite layers require considerable K. The K of both the original solution and of the basalt glass has been entirely used in the production of illite; and only small proportions of K are sufficient to give rise to transition of the bulk of the dioctahedral component of smectite to illite.

4.3.4.2 300°C Runs

XRD patterns of the four runs at 300°C (BB41, BB44, BQD7, BHD4) exhibited virtually no change from the starting materials. The one exception was in the appearance of a very weak peak in the position of the strongest peak of wairakite for all patterns.

Figures 4.25, 4.26 and 4.27 are low to high resolution TEM images of run products of Run BHD4. These show the typical characteristics of unaltered smectite and appear to confirm a lack of reaction for at least the bulk of the smectite. However, the EDX spectrum shown in Figure 4.24 (pattern B) of that smectite clearly shows an increase in Mg and Fe relative to the starting material. Because the electron diffraction and lattice fringe images of the

102
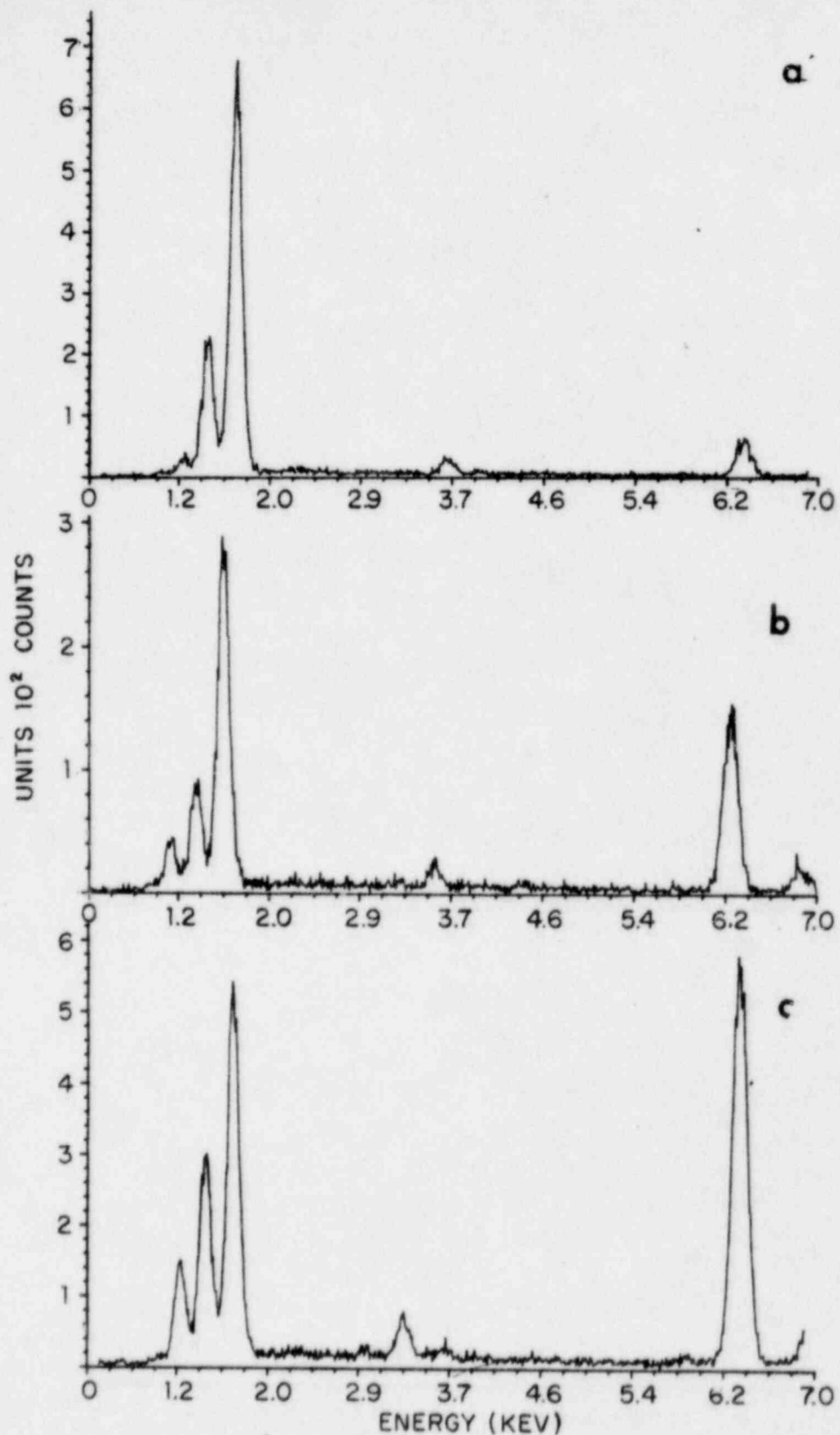
Figure 4.24. EDX spectra obtained by AEM analysis. a. Untreated bentonite
b. Bentonite from run BHD4 (50% basalt/50% bentonite, 300°C, 334 days)
showing increase in Mg and Fe. c. Unresolved illite and chlorite from
run BHC5 (50% basalt/50% bentonite, 400°C, 280 days).

103
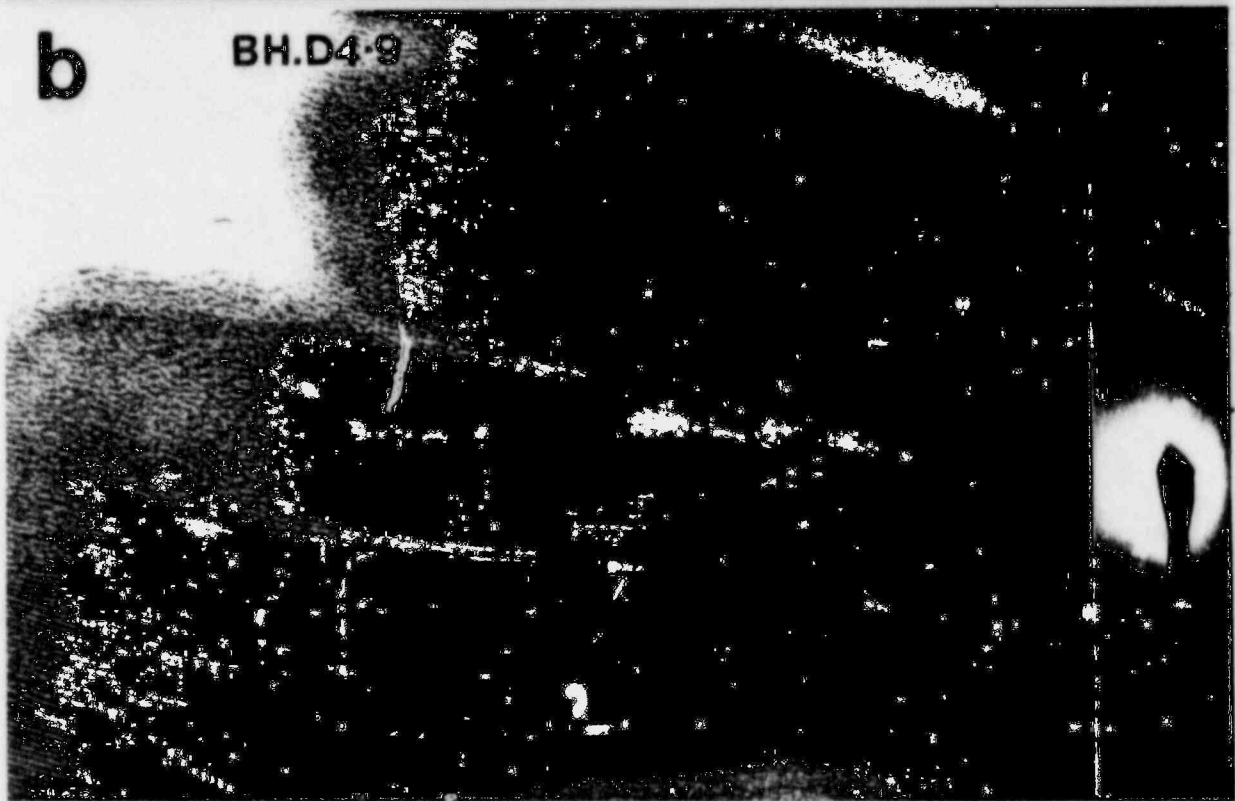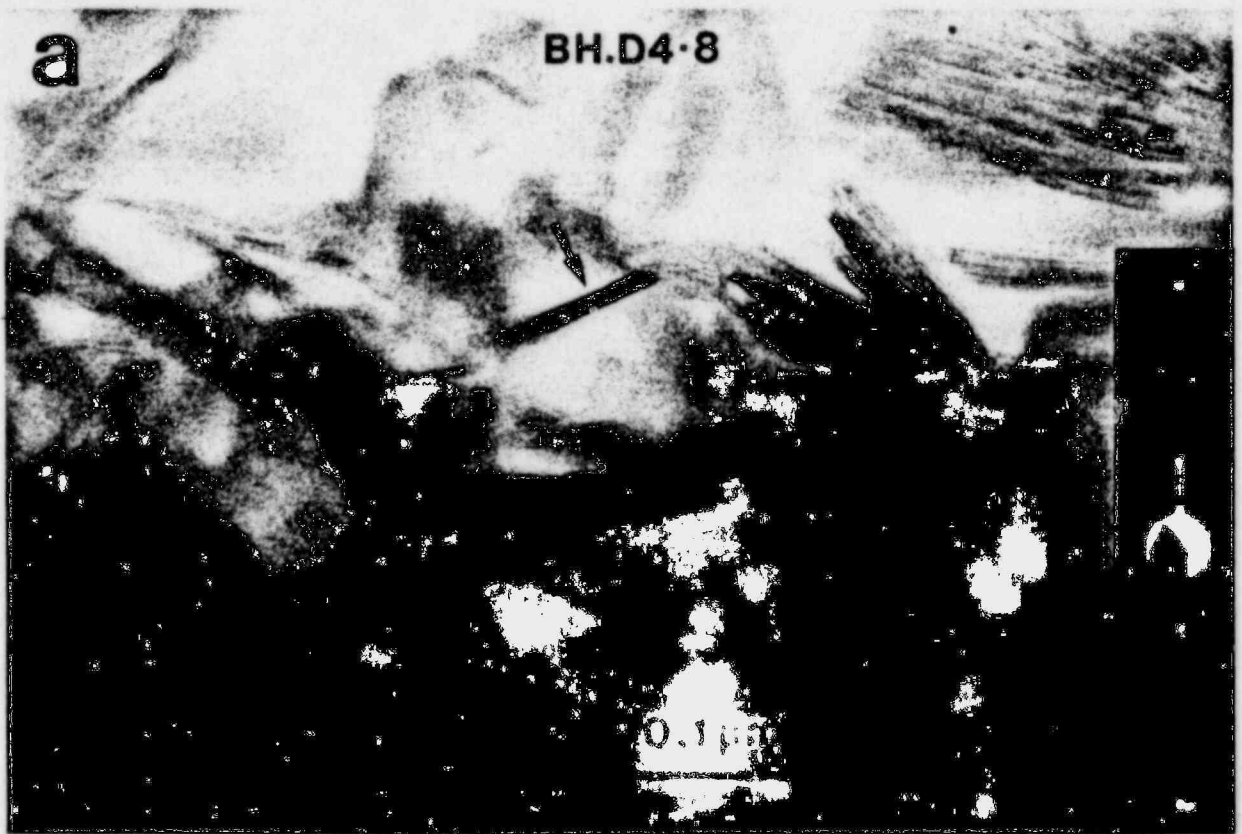
Figure 4.25. TEM images of bentonite from Run BHD4 (50% basalt/50% bentonite, 300°C, 334 days) a. Low magnification image, principally of smectite, with illite (?) indicated by arrow. b. Lattice fringe image of bentonite with typical variable layer spacings (10.9-12.1 A).
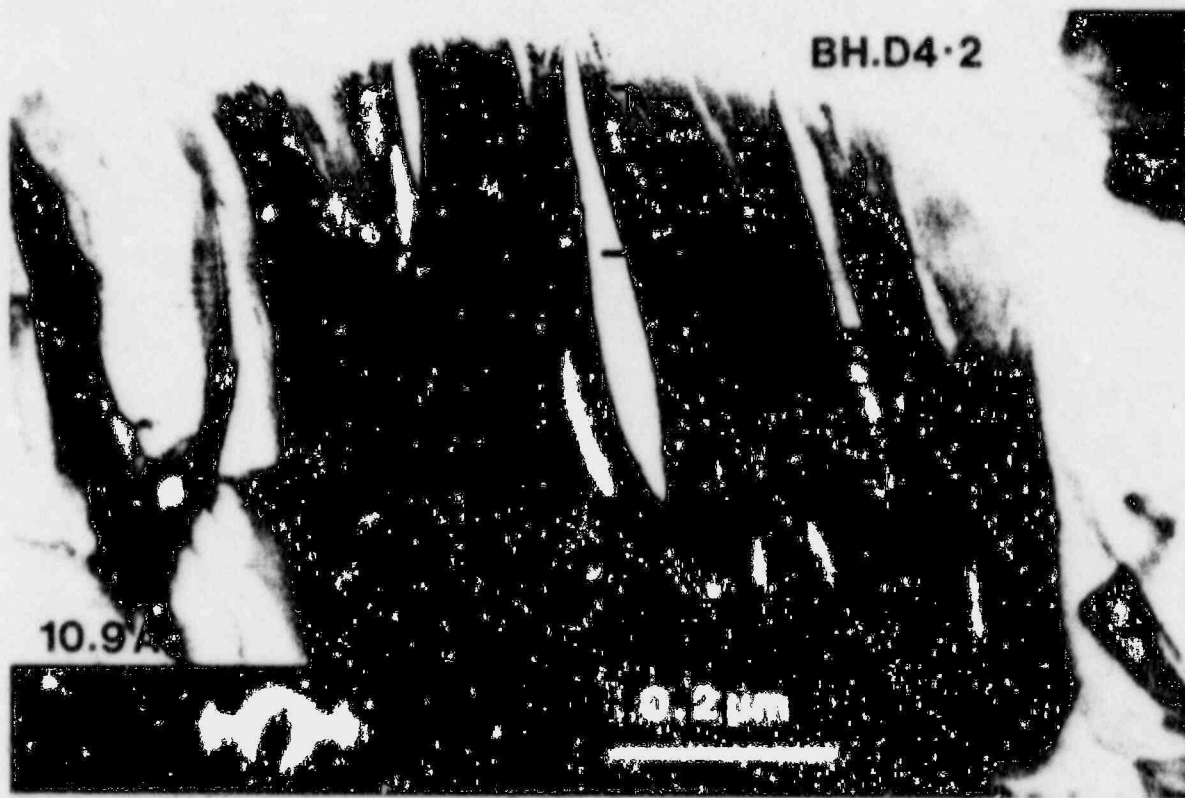
Figure 4.26. Low magnification TEM image of bentonite from Run BHD4, with appearance identical to that of starting material.
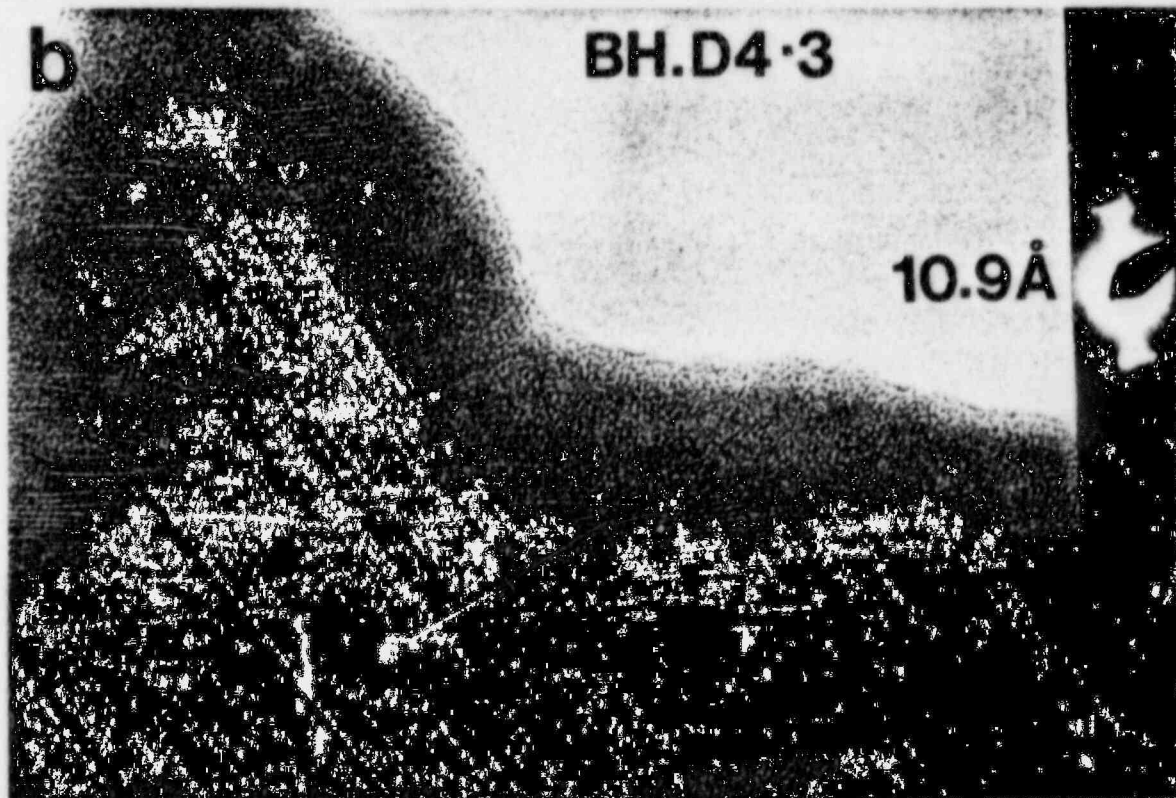
Figure 4.27. Lattice fringe images of bentonite from Run BHD4. a. high
resolution image of the area bracketed in Figure 4.26. b. Typical
bentonite which is apparently identical in appearance to untreated
bentonite.

same areas for which the EDX analyses were obtained show only smectite, we infer that the smectite has actually undergone some change through interchange of dioctahedral cations. This is surprising in that no K is evident in the analyses, as would be expected for an intermediate stage in the conversion of bentonite to chlorite plus illite. Nevertheless, it is clear that solid solution interchange has taken place without destruction of the smectite structure.

5. SUMMARY OF DATA

5.1 Analogous Geological Systems

Smectite (bentonite), when deposited in sediments and progressively buried to greater depths by overlying sediments, is subjected to increasing temperature and the effects of pore fluids in a manner analogous to conditions for the repository. Given the availability of Al and K in pore fluids (provided by dissolution of coexisting phases), smectite undergoes a continuous series of transitions through mixed-layer I/S to illite, and illite subsequently transforms toward muscovite.

All of the clay minerals are apparently metastable phases. The degree of reaction is controlled by kinetic factors. The rate-determining factor for the transition of smectite is not substitution of K in interlayer sites of smectite, although the availability of K is an essential factor in the transition to illite (a transition may occur, in the absence of K, to a phase such as kaolinite). The rate of transition is determined by reconstruction of the basic tetrahedral and octahedral layers with concomitant changes in composition of the octahedral and tetrahedral sites. The former results in a loss of Mg and Fe, originally in solid solution, to the pore solutions, which in turn may be reflected in crystallization of chlorite or berthierine. The transition of illite toward muscovite also involves at least minimal tetrahedral bond rupturing and reconstitution insofar as the proportion of Al must increase, along with addition of K in interlayer sites. This also is a sluggish process.

Because the transitions are sluggish processes, smectite and then illite may persist metastably in the geological and (backfill) environment.

108

The two reaction rate-determining factors are temperature and water/rock ratio. In the Gulf Coast system, mixed layer I/S persists to depths corresponding to temperatures approaching 200°C. In samples of shales from this system, pore space cannot be detected at the highest TEM levels, and the transition to illite is found to occur across reaction interfaces which gradually envelop original smectite grains over thousands of feet of sediment. This system is effectively closed to water, the transitions apparently taking place with vanishingly small amounts of water at the reaction interface, with increasing temperature (depth). Nevertheless, some smectite remains at temperatures approaching 200°C, and the illite at such temperatures (depths) is a relatively ideal illite; i.e. it has not transformed toward muscovite.

By contrast, pore space is abundant in the Salton Sea argillaceous sediments, where geothermal brines are actively convecting; i.e. where fluid flow is macroscopically observed, the pathways in turn are clearly discerned at TEM levels. Up to approximately 20% of such rocks is open pore space. In this environment, silicates dissolve, components are transported by convecting brines, and illite precipitates in pore space as euhedral crystals directly from solution. The illite that forms is free of smectite layers. It forms at temperatures as low as 115°C. In this open system smectite reacts by dissolution and illite forms at temperatures much below that of the Gulf Coast sediments.

The contrasting Gulf Coast (closed system) and Salton Sea (open system) systems thus clearly define the effects of mobile pore fluids in promoting reaction of the metastable phases. In addition, they illustrate the factors that control porosity/permeability and thus imply a means of affecting these variables so as to minimize reaction rates. The texture of Gulf Coast shales displays a matrix, or fabric, of clay minerals which is continuous; that is,

individual smectite or illite "grains" do not exist. Compaction and
recrystallization of original grain boundaries has produced "megagrains" of
phyllosilicates which envelop and surround grains of non-phyllosilicates (the
latter are analogous to basalt grains in a smectite matrix of backfill). Such
a matrix possesses no open pore space and constitutes a barrier through which
water cannot flow.

In order to minimize porosity/permeability in a clay-containing backfill,
and thus to reduce reaction rates, it is essential to produce such an
equivalent texture in a basalt/smectite backfill by controlling basalt grain
size, basalt/smectite ratio, and compaction of the mixture.

It is not possible to define specific temperature ranges for the
occurrence (and lack of transition) of smectite, mixed layer I/S, or illite
because of the relations described above. It part, this is also because
temperatures to which relevant geologic systems have been subjected cannot be
accurately determined in most cases. Nevertheless, the data imply that where
porosity/permeability are minimized, smectite may persist to temperatures in
excess of 100°C, mixed-layer I/S up to 200°C and illite in excess of 250°C in
appropriate geological environments.

We emphasize that these conlusions, and all of the discussion above, are
true for geological systems only, where times for reactions are in the millions
of years. Because the degree of reaction is controlled by kinetic factors, the
temperatures for which smectite and illite are unchanged may be significantly
higher in laboratory experiments, which involve times of a maximum of a few
months, or in the backfill environment for which times up to several thousand
years must be considered.

5.2 Characterization of Experimental Starting Materials

All three potential backfill materials have been found to be heterogeneous and the results for each are summarized in turn in the following:

5.2.1 Illite

The type Fithian illite actually has a considerable proportion of expandable (smectite) layers as verified by both XRD and TEM. In addition, it is compositionally heterogeneous, especially in variation in the octahedral components, Mg, Fe and Al. Thus it is locally variable in both composition and structure. Illite occurs in large volumes only as a component of shales, and although the type Fithian illite constitutes a high proportion of the sample, there is also considerable quartz, feldspar and minor calcite and chlorite. All of these occur, as shown by TEM, intimately intergrown in dominantly clay-sized grains, and without detectable pore space. At the TEM level of resolution, this material has the appearance of samples from the deepest levels of Gulf Coast shales.

5.2.2 Smectite

Although the commercial bentonite pr..... Envirogel is dominantly smectite, there are small but significan   ortions of other phases, including quartz, calcite, illite and feldspar with trace amounts of other phases. AEM analyses shows that the bentonite itself is heterogeneous in composition, both in interlayer cations (Ca, Na, K) and in octahedrally coordinated cations (Mg, Fe, Al, Ti). TEM images have defined the textural relations in that it consists of discontinuous, anastomosing layers arranged in irregular packets of only a few layers. The unconsolidated smectite consists of a high proportion of pore space in the form of space between disaggregated

111

layers and between poorly defined "grains" (packets of layers). Abundant

dislocations within packets also provide pathways for fluid and ion transport.

5.2.3 Basalt

The Umtanum basalt is a typical basalt in mineralogy and texture, with

plagioclase, pyroxene and iron oxides as the principal crystalline phases.

However, there are abundant cracks along which a variety of minerals have been

deposited, including opaline material, zeolites and iron oxides. The principal

phase of concern in the basalt is a glass which constitutes up to 25% of the

whole. This glass has been characterized in detail and found to consist of two

phases, the original liquid having been composed of two immiscible liquids.

Furthermore, AEM analysis has demonstrated that one of the glasses is rich in

K. As the glass is expected to react before the crystalline phases, this glass

is therefore a major potential source of K to contribute to the transition of

coexisting smectite to illite, and therefore to cause major changes in the

properties of a bentonite/basalt backfill.

5.3 Experiments

Experiments were carried out at temperatures between 200°C and 460°C, over

a range of water/rock ratios, and with a solution designed to match that of the

ground water in the Umtanum Basalt.

No changes were observed in all starting materials for experiments carried

out at 200°C, even though durations of some runs exceeded a year, and the

starting materials (e.g. basalt, illite) are known from a variety of other data

to be unstable under the conditions of the experiments. This is not

unexpected, as reaction rates for silicates at such low temperatures are

extremely slow. These results in no way imply that the starting materials are stable or that no change would occur over longer time periods. Indeed, the lack of change in smectite under conditions similar to those of geological systems in which smectite transforms at much lower temperatures, simply emphasizes that equilibrium was not obtained in the experiments.

Bentonite remained largely unchanged for all experiments except that at 460°C. In all other runs, the only changes were in the dissolution of the contaminating phase calcite, and in small changes in composition, especially of interlayer cations. The latter is to be expected, as exchange of interlayer cations is known to occur readily at temperatures well below those of the experiments. However, it is significant that bentonite was retained even though it is an unstable phase under the run conditions, and even though some experiments were of a duration greater than one year.

Illite samples underwent some change in runs at temperatures as low as 300°C, however, and in all runs at higher temperatures. These changes were of two types: (1) solution/recrystallization of illite/smectite, with the production of euhedral to subhedral illite, and (2) the formation of the trioctahedral phase berthierine with Mg and Fe (and other elements) having a source in solid solution in the original illite/smectite, such that Mg and Fe were provided to the fluid through the dissolution and recrystallization of the illite/smectite.

Basalt samples were unchanged in all runs at 300°C. Even in an experiment at 460°C little change could be detected.

Mixtures of basalt and smectite were effectively unchanged after durations of up to almost one year in all experiments at 300°C. However, significant changes were detected in all runs at 400°C. In a run with 75% basalt, the only change was in the synthesis of a small proportion of the zeolite wairakite, but

significant dissolution of starting phases and crystallization of new phases occurred in two runs with 50% and 75% smectite. In the latter case reaction was complete. Only chlorite and illite appeared in the run product.

6. Discussion and Synthesis of Data on Experimental and Geological
    Systems

Because reactions involving silicates are sluggish at temperatures of 300-400°C or below, and equilibrium is difficult to achieve, we have carried out experiments at temperatures as high as 460°C and for the longest possible durations under the time constraints of the contract under which this work was done (experiments of several years are desirable but impractical). Significant reactions occurred only at temperatures well above that which has been estimated as the maximum to which backfill materials will be subjected (300°C). The only changes occurring at lower temperatures involved solution of calcite and minor interlayer cation exchange of smectite. Even at 300°C changes were minimal. They included growth of wairakite in one basalt/smectite run, and solution and crystallization of illite with growth of berthierine and formation of euhedral illite. Even the latter changes did not occur in other experiments performed at nearly the same conditions, suggesting that the reactions are kinetically controlled and do not represent equilibrium conditions. Selected runs were studied in detail by TEM in order to see if subtle changes, not detectable by bulk-sensing techniques such as XRD, could be defined. However, such subtle changes were largely confined to runs for which XRD detected change; i.e. in experiments labelled as resulting in "no change", not even TEM techniques were able to detect the kind of small changes, which when extrapolated over thousands of years, might be significant. These results are compatible with the experimental results of Wood (1983) insofar as he observed only small changes in smectite and basalt systems at 300°C.

However, the changes that did occur in our experiments were those to be expected by analogy with geological systems. Given P, T, water/rock ratio and bulk composition, the mineral phases are readily predicted. The complete reaction of smectite plus basalt plus H_2O to chlorite and illite, given equilibrium conditions, is to be expected. Even the textures at the TEM level were shown to be identical to Salton Sea textures for the solution/recrystallization of illite.

The changes occurred, however, at temperatures well above those for analogous geological systems. This is precisely the result to be expected given non-equilibrium, kinetically controlled experiments. Although such experiments are necessary to confirm certain relations, and to protect against unpredictable results, the analogous geological systems are far more reliable as predictors for the stability of backfill materials.

The geological systems indicate that temperatures for reaction among the phases smectite/illite/muscovite are variable, depending in part on porosity/permeability and water/rock ratio, and also on bulk chemistry of the system. In terms of the latter variable, smectite in argillaceous marine sediments must react differently than smectite in situ in a volcanic tuff. Nevertheless, the smectite/illite/muscovite conversions occur over approximately the same temperature intervals on a global basis (taking into consideration the problems with determining actual temperatures to which rocks have been submitted - a difficult task at temperatures below 300-400°C). The Gulf Coast and Salton Sea sequences that were described in this report are especially significant as changes are thought to be occurring in those sequences today; they are now subjected to the highest temperatures to which they have ever been subjected and those temperatures are well known. An approximate temperature range for the reactions thus would be: (1) less than

115

100°C for pure smectite (2) less than 200°C for illite which retains some smectite component (3) less than 250°-300° for illite with no expandable component.

These temperatures are still only approximate and subject to variability especially with respect to kinetic factors. Mixed layer I/S occurs in the Gulf Coast at temperatures up to 200°C, yet the illite forming at 115°C in well IID #2 (Yau, pers. comm.) in the Salton Sea has no apparent expandable component. Here, too, the geological sytems imply methods for controlling the reactions. In the case of the Salton Sea argillaceous sediments, porosity (observed by TEM) is very high as is permeability, and hydrothermal brines are being actively convected through the sequence of sediments. These are prime conditions for a closer approach to equilibrium and illite therefore forms at a very low temperature (115°C). By contrast, TEM images show no pore space in Gulf Coast sediments. The clays form a continuous fabric or matrix which entirely envelops non-phyllosilicate grains, effectively producing a barrier to fluid migration. Such a fabric is essential to a backfill material if it is to serve as a barrier to fluid migration.

Reaction progress cannot be predicted quantitatively as a function of the relevant variables such as time, temperature, water/rock ratio, permeability and porosity for reasons given above; i.e. in laboratory experiments reaction rates are too slow to even permit partial reaction over the lower temperature range estimated for the repository; in natural systems, values for the appropriate variables can only be qualitatively estimated. Nevertheless, the general range of temperatures of reaction given above are appropriate for the repository, and the general effects of the significant variables are defined such that packing properties can be optimized.

REFERENCES

Ahn, J.H., Lee, J.H., Peacor, D.R. (1983) Mineralogical and textural
transitions in phyllosilicates during burial diagenesis of Gulf Coast
shales (abstr.). Geol. Soc. Amer. Abstr. Progr., 15, 512.

Ahn, J.H., Peacor, D.R. (1985) Transmission electron microscopy of diagenetic
chlorite in Gulf Coast argillaceous sediments. Clays Clay Miner., 33, 228-
236.

Ahn, J.H., Peacor, D.R. (1986) A TEM/AEM Study of the smectite to illite
transition: characterization of the phases and a model for the transition
Clays Clay Miner., in press.

Allard, L.F., Blake, D.F. (1982) The practice of modifying an analytical
electron microscope to produce clean X-ray spectra. In: Heinrich, K.F.J.
(ed.) Microbeam Analysis, 1982, San Francisco Press, 8-19.

Allpress, J.G., Hewat, E.A., Moodie, A.F., Sanders, J.V. (1972) n-beam lattice
image. I. experimental and computed images from $W_4Nb_{26}O_{77}$. Acta Cryst.,
A28, 528-536.

Anderson, J.S. (1978) Lattice imaging by high resolution electron microscopy.
The role of high resolution electron microscopy in solid state chemistry.
Proc. Indian Acad. Sci., 87A, 295-329.

Apted, M.J., Liou, J.G. (1983) Phase relations among greenschist, epidote-
amphibolite, and amphibolite in a basaltic system. Amer. J. Sci., 283-A,
328-354.

Benzel, W.M., Graf, D.L. (1984) Studies of smectite membrane behavior:
importance of layer thickness and fabric in experiments at 20°C.
Geochim. Cosmochim. Acta, In press.

Blake, D.F., Allard, L.F., Peacor, D.R., Bigelow, W.C. (1980) "Ultra-clean"
X-ray spectra in JEOL JEM--100CX. Proc. Elect. Micro. Soc. Amer., 38th
meeting, 136-137.

Blake, D.F., Isaacs, A.M., Kushler, R.H. (1983) A statistical method for the
analysis of quantitative thin-film X-ray microanalytical data. J.
Micros., 131, Part 2, 249-255.

Blake, D.F., Peacor, D.R. (1981) Biomineralization in crinoid echinoderms:
characterization of crinoid skeletal elements using TEM and STEM
microanalysis. SEM/1981, III, 321-328.

Boles, J.B., Franks, S.G. (1979) Clay diagenesis in Wilcox Sandstones of
southwest Texas: implications of smectite diagenesis on sandstone
cementation. J. Sed. Petrol., 49, 55-70.

Burst, J.F. Jr. (1959) Postdiagenetic clay mineral environmental relationships
in the Gulf Coast Eocene. Clays Clay Miner., Proc. 6th Natl. Conf.,
327-341.

Burst, J.F. Jr. (1969) Diagenesis of Gulf Coast clayey sediments and its possible relation to petroleum migration. Amer. Assoc. Petroleum Geol. Bull, 53, 73-93.

Cliff, G., Lorimer, G.W. (1972) The quantitative analysis of thin metal foils using EMMA-4 -- The ratio technique. Proc. 5th Europ. Cong. Electron Micros. Inst. Physics, London, 140-141.

Cliff, G., Lorimer, G.W. (1975) The quantitative analysis of thin specimens. J. Micros., 103, 203-207.

Dunoyer de Segonzac, G. (1964) Les argiles du Cretace superieur dans le bassin de Douala (Cameroun): Problemes de diagenese. Bull. Serv. Carte Geol. Alsace Lorraine, 17, 287-310.

Dunoyer de Segonzac, G. (1969) Les mineraux argileux dans la diagenese; passage au metamorphisme. Mem. Serv. Carte Geol. Alsace Lorraine, 29, 320 p.

Dunoyer de Segonzac, G. (1970) The transformation of clay minerals during diagenesis and low-grade metamorphism: a review. Sedimentology, 15, 281-346.

Eberl, D. (1978) The reaction of montmorillonite to mixed-layer clay: the effect of interlayer alkali and alkaline earth cations. Geochim. Cosmochim. Acta, 42, 1-7.

Eberl, D., Hower, J. (1976) Kinetics of illite formation. Geol. Soc. Amer. Bull., 87, 1326-1330.

Eberl, D., Hower, J. (1977) The hydrothermal transformation of sodium and potassium smectite into mixed-layer clay. Clays Clay Miner., 25, 215-227.

Epstein, J.B., Epstein, A.G. (1969) Geology of the Valley and Ridge province between Delaware Water Gap and Lehigh Gap, Pennsylvania. In: Subitzky, S. (ed.), Geology of Selected Areas in New Jersey and Eastern Pennsylvania and Guide Book of Excursions, New Brunswick, New Jersey. Rutgers Univ. Press, 132-205.

Eslinger, E.V., Savin, S.M. (1973) Oxygen isotope geothermometry of the burial metamorphic rocks of the Precambrian Belt Supergroup, Glacier National Park, Montana. Geol. Soc. Amer. Bull., 84, 2549-2560.

Ferguson, J.E. (1982) Inorganic Chemistry and the Earth. Pergamon Press, 400p.

Foscolos, A., Kodama, K. (1974) Diagenesis of clay minerals from lower Cretaceous shales of northeastern British Columbia. Clays Clay Miner., 32, 319-336.

Goldstein, J.I., Costley, J.L., Lorimer, G.W., Reed, S.J.B. (1977) Quantitative X-ray microanalysis in the electron microscope. In: Johari (ed.) IITRI Chicago, Ill., 1, 315-324.

Helgeson, H. C. (1968) Geologic and thermodynamic characteristics of the
        Salton Sea system. Amer. J. Sci., 266, 129-166.

Hiltabrand, R.R., Farrell, B.E., Billings, G.K. (1973) Experimeental diagenesis
        of Gulf Coast argillaceous sediment. Amer. Assoc. Petroleum Geol. Bull.,
        57, 338-348.

Holeywell, R.C., Tullis, T.E. (1975) Mineral reorientation and slaty cleavage
        in the Martinsburg Foramtion, Lehigh Gap, Pennsylvania. Geol. Soc. Amer.
        Bull., 86, 1296-1304.

Hower, J., Eslinger, E.V., Hower, M.E., Perry, E.A. (1976) Mechanism of burial
        metamorphism of argillaceous sediment: 1. mineralogy and chemical
        evidence. Geol. Soc. Amer. Bull., 87, 803-810.

Isaacs, A.M., Brown, P.E., Valley, J.W., Essene, E.J., Peacor, D.R. (1981) An
        analytical electron microscopic study cf a pyroxene-amphibole
        intergrowth. Contrib. Miner. Petrol., 115-120.

Khitarov, N. I., Pugin, V. A. (1966) Behavior of montmorillonite under
        elevated temperatures and pressures. Geochem. Int., 3, 621-626.

Kisch, H.J. (1974) Anthracite and meta-anthracite coal ranks associated with
        "anchimetamorphism" and "very-low-stage" metamorphism. I, II, III. Proc.
        K. Ned. Akad. Wet., Amsterdam, Ser. B, 77(2), 81-118.

Kisch, H.J. (1983) Mineralogy and petrology of burial diagenesis (burial
        metamorphism) and incipient metamorphism in cladistic rocks. In: Larsen,
        G. Chilinger, G.V. (eds.) Diagenesis in Sediments and Sedimentary Rocks,
        2: Developments in Sedimentology, 25B, Elsevier, 289-493.

Komarneni, S., Roy, R. (1981) Hydrothermal transformation in candidate overpack
        materials and their effects on cesium and strontium sorption. Nucl. Tech.
        54, 118-122.

Kubler, B. (1964) Les argiles, indicateurs de metamorphisme. Rev. Inst. Fr.
        Petrol., 19, 1093-1112.

Kubler, B. (1967) La cristallinite de l'illite et les zones tout a fait
        superieures du metamorphisme. In: Etages Tectoniques. A la Baconniere,
        Neuchatel, Suisse, 105-121.

Larsen, G., Chilinger, G.V. (1983) Diagenesis in Sediments and Sedimentary
        Rocks, 2: Developments in Sedimentology, 25B, Elsevier, 572 p.

Lee, J.H., Ahn, J.H., Peacor, D.R. (1983) TEM study of textural changes in
        phyllosilicates through diagenesis to low temperature metamorphism
        (abstr.). 20th Ann. Meet., Clay Miner. Soc. Progr., 41.

Lee, J.H., Peacor, D.R. (1983) Intralayer transitions in phyllosilicates of the
        Martinsburg shale. Nature, 303, 608-609.

Lee, J.H., Peacor, D.R. (1985) Ordered 1:1 interstratification of illite and chlorite: A transmission and analytical electron microscopy study. Clays Clay Miner., 33, 463-467.

Lee, J.H., Peacor, D.R. (1986) The effect of diffusion on AEM analysis for K and other elements. In prep.

Lee, J.H., Ahn, J.H., Peacor, D.R. (1985a) Textures in layer silicates: Progressive changes through diagenesis and low temperature metamorphism. J. Sed. Petrol., 55, 532-540.

Lee, J.H., Peacor, D.R., Lewis, D.D., Wintsch, R.P. (1985b) Chlorite-illite/muscovite interlayered and interstratified crystals: A TEM/STEM study. Contrib. Miner. Petrol., 372-385.

Lee, J.H., Peacor, D.R., Lewis, D.D., Wintsch, R.P. (1986) Solution-recrystallization origin of the slaty cleavage in the Martinsburg Formation at Lehigh Gap, Pennsylvania. J. Struct. Geol., in press.

Lee, J.H., Peacor, D.R., Wirtsch, R.P. (1982a) TEM and AEM study of changes in dioctahedral micas during slaty cleavage development (abstr.). EOS, 63, 468.

Lee, J.H., Peacor, D.R., Wintsch, R.P. (1982b) TEM and AEM study of interlayering and along-layer transition in tri- and dioctahedral phyllosilicates (abstr.). Geol. Soc. Amer. Abstr. Progr., 14, 544.

Lewis, D.D. (1980) An investigation of the preferred orientation of phyllosilicates in the Martinsbureg slate, Lehigh Gap area, Pennsylvania. Master's thesis, Indiana Univ., 96 p.

Liou, J.G., Kuniyoshi, Ito, K. (1974) Experimental studies of the phase relations between greenschist and amphibolite in a basaltic system. Amer. J. Sci. 274, 613-632.

Lorimer, G.W., Cliff, G. (1976) Analytical electron microscopy of minerals. In: Wenk, H.R. (ed.), Electron Microscopy in Mineralogy, Springer-Verlag, 506-519.

McDowell, D., Elders, W.A. (1980) Authigenic layer silicate minerals in borehole Elmore 1, Salton Sea Geothermal Field, California, U.S.A. Contrib. Mineral. Petrol., 74, 293-310.

McDowell, D., Elders, W.A. (1983) Allogenic layer silicate minerals in boreholes Elmore #1, Salton Sea Geothermal Field, California, Amer. Mineral., 68, 1146-1159.

Maxwell, D.T., Hower, J. (1967) High-grade diagenesis and low-grade metamorphism of illite in the Precambrian Belt series. Amer. Miner., 52, 843-857.

Moody, J.B., Meyer, D., Jenkins, J.Z. (1983) Quantitative characterization of the greenschist-amphibolite boundary in mafic systems. Amer. J. Sci. 283, 48-92.

Mottl, M.J., Holland, H.D. (1978) Chemical exchange during hydrothermal
    alteration of basalt by seawater - I. experimental results for major and
    minor components of seawater. Geochim. Cosmochim. Acta, 42, 1103-1115.

Mottl, M.J., Seyfried, W.E. Jr. (1980) Sub-sea-floor hydrothermal systems:
    rock vs. seawater dominated systems. In Rona, P.A. and Lowell, R.P.
    (eds.) Seafloor Spreading Centers: Hydrothermal Systems. Dowden,
    Hutchinson and Ross, Stroudsburg, PA. Benchmark Papers in Geology, pp.
    66-82.

Muffler, L.J.P., Doe, D.R. (1968) Composition and mean age of detritus of the
    Colorado River delta in the Salton Trough, southeastern California. J.
    Sed. Petrol., 38, 384-399.

Muffler, L.J.P., White, D.E. (1969) Active metamorphism of Upper Cenozoic
    sediments in the Salton Sea geothermal field and the Salton Trough,
    southeastern California. Geol. Soc. Amer. Bull., 80, 157-182.

Perry, E.A., Hower, J. (1970) Burial diagenesis in Gulf Coast pelitic
    sediments. Clays Clay Miner., 18, 165-177.

Perry, E.A., Hower, J. (1972) Late-stage dehydration in deeply buried pelitic
    sediments. Amer. Assoc. Petroleum Geol. Bull., 56, 2013-2021.

Pohl, D., Dickson, F.W. (1979) Basalt-seawater reactions at 400 and 500°C and
    1000 bars pressure. Implications, major element mass balances and a
    model of ore-forming processes at spreading centers. EOS, 60, 973.

Powers, M.C. (1959) Adjustment of clays to chemical change and the concept of
    the equivalence level. Clays Clay Miner., 7, 309-326.

Powers, M.C. (1967) Fluid-release mechanisms in compacting marine mudrocks and
    their importance in oil exploration. Amer. Assoc. Petroleum Geol. Bull.,
    51, 1240-1254.

Roberson, H.E., Lahann, R.W. (1981) Smectite to illite conversion rates:
    effects of solution chemistry. Clays Clay Mineral., 29, 129-135.

Roedder, E.W. (1978) Silicate liquid immiscibility in magmas and in the system
    $K_2O-FeO-Al_2O_3-SiO_2$: an example of serendipity. Geochim. Cosmochim.
    Acta, 42, 1596-1617.

Sasaki, N., Komarneni, S., Sheitz, B., Roy, R. (1982) Backfill waste
    interactions in repository simulating tests. In: The Scientific Basis
    for Nuclear Waste Management, 6, Topp, S.V. (ed.), Elsevier Science
    Publishing Co., New York.

Savage, D., Chapman, N.A. (1982) Hydrothermal behavior of simulated waste glass-
    and waste-rock interactions under repository conditions. Chem. Geol.,
    36, 59-86.

Seyfried, W.E., Jr., Bischoff, J.L. (1977) Hydrothermal transport of heavy
    metals by seawater: the role of seawater/basalt ratio. Earth Planet.
    Sci. Lett., 34, 71-79.

Seyfried, W.E., Bischoff, J.L. (1981) Experimental seawater-basalt interaction at 300°C, 500 bars, chemical exchange, secondary mineral formation and implications for the transport of heavy metals. Geochim. Cosmochim. Acta, 45, 135-147.

Singer, A., Muller, G. (1983) Diagenesis in argillaceous sediments. In: Larsen, G., Chilinger, G.V. (eds.) Diagenesis in Sediments and Sedimentary Rocks, 2: Developments in Sedimentology, 25B, 115-212.

Spear, F.S. (1980) NaSi = CaAl exchange equilibrium between plagioclase and amphibole. Contrib. Mineral. Petrol., 72, 33-41.

Spear, F.S. (1981) An experimental study of hornblende stability and compositional variability in amphibolite. Amer. J. Sci., 281, 697-734.

Steiner, A. (1968) Clay minerals in hydrothermally altered rocks at Wairakei, New Zealand. Clays Clay Miner., 16, 193-213.

Velde, B., Hower, J. (1963) Petrographical significance of illite polymorphism in Paleozoic sedimentary rocks. Amer. Miner., 48, 1239-1254.

Weaver, C.E. (1959) The clay petrology of sediments. Clays Clay Miner., Proc. 6th Natl. Conf., 154-187.

Weaver, C.E. (1961) Clay minerals of the Ouachita structural belt and adjacent foreland. In: Flawn, L.W., Goldstein, J.I., King, E.A., Weaver, C.E. (eds.) The Ouachita Belt. Univ. Texas Publ., 6120, 147-160.

Weaver, C.E. (1967) Potassium illite and the ocean. Geochim. Cosmochim. Acta, 31, 2181-2196.

Weaver, C.E., Beck, K.C. (1971) Clay-water diagenesis during burial: how mud becomes gneiss. Geol. Soc. Amer. Spec. Pap., 134, 96 p.

Weber, K. (1972a) Notes on determination of illite crystallinity. Neues Jahrb. Miner. Monatsh., 1972, 267-276.

Weber, K. (1972b) Kristallinitat des Illits in Tonschiefern und andere Kristerien schwacher Metamorphose in nordostlichen Rheinischen Schiefergebirge. Neues Jahrb. Geol. Palaeontol. Abh., 141, 333-363.

Wintsch, R.P. (1978) A chemical approach to the preferred orientation of mica. Geol. Soc. Amer. Bull., 89, 1715-1718.

Wood, M.I. (1983) Experimental Investigation of sodium bentonite stability in Hanford basalt. In: Brookens, D.G. (ed.), Scientific Basis for Nuclear Waste Management. Elsevier, New York.

Yau, L.Y.C., Lee, J.H., Peacor, D.R., McDowell, D. (1983) TEM study of illite diagenesis in shales of the Salton Sea geothermal field, California (abstr.). 20th Ann. Meet., Clay Miner. Soc., Progr., 42.

Yoshida, T. (1973) Elementary layers in the interstratified clay minerals as revealed by electron microscopy. Clays Clay Miner., 21, 413-420.

DISTRIBUTION   LIST

K. S. Kim (10)
U.S. Nuclear Reg. Commission
Washington, DC 20555

G. F. Birchard
U.S. Nuclear Reg. Commission
Washington, DC 20555

K. R. Goller
U.S. Nuclear Reg. Commission
Washington, DC 20555

F. A. Costanzi
U.S. Nuclear Reg. Commission
Washington, DC 20555

R. E. Browning
U.S. Nuclear Reg. Commission
Washington, DC 20555

J. T. Greeves
U.S. Nuclear Reg. Commission
Washington, DC 20555

T. C. Johnson
U. S. Nuclear Reg. Commission
Washington, DC 20555

M. Tokar
U.S. Nuclear Reg. Commission
Washington, DC 20555

Waste Management Subcommittee
ACRS
U.S. Nuclear Reg. Commission
Washington, DC 20555

D. Stahl
Battelle Columbus Lab.
505 King Avenue
Columbus, OH 43201

M. J. Steindler
Argonne National Lab.
Argonne, IL 60439

P. Soo
Brookhaven National Lab.
Upton, NY 11973

R. Williams
EPRI
P. O. Boc 10412
Palo Alto, CA 94301

Ray Walton
U.S. Dept. of Energy
Washington, DC 20545

D. H. Alexander
U.S. Dept. of Energy
Washington, DC 20545

Michael Smith
BWIP
Rockwell Hanford Operation
Richland, WA 99352

D. E. Clark
ONWI-Battelle
505 King Avenue
Columbus, OH 43201

J. E. Mendel
MCC-PNL
P. O. Box 999
Richland, WA 99352

J. McElroy
PNL
P. O. Box 999
Richland, WA 99352

A. G. Crott
ORNL
P. O. Box X
Oak Ridge, TN 37830

K. W. Stephens
The Aerospace Corp.
Suite 400
955 L'Enfant Plaza, S.W.
Washington, DC 20024

D. R. Peacor (50)
University of Michigan
Ann Arbor, MI 48109

1. REPORT NUMBER (Assigned by TIDC, add Vol. No., if any)
NUREG/CR-4585

2. TITLE AND SUBTITLE	3. LEAVE BLANK
Investigation of the Stability of Clay/Basalt Packing Materials	

4. DATE REPORT COMPLETED	
MONTH	YEAR
January	1986

5. AUTHOR(S)
D.R. Peacor, E.J. Essene, J.H. Lee

6. DATE REPORT ISSUED	
MONTH	YEAR
March	1986

7. PERFORMING ORGANIZATION NAME AND MAILING ADDRESS (Include Zip Code)	8. PROJECT/TASK/WORK UNIT NUMBER
Department of Geological Sciences University of Michigan Ann Arbor, Michigan 48109	9. FIN OR GRANT NUMBER
	A-2239

10. SPONSORING ORGANIZATION NAME AND MAILING ADDRESS (Include Zip Code)	11a. TYPE OF REPORT
Division of Radiation Programs and Earth Sciences Office of Nuclear Regulatory Research U.S. Nuclear Regulatory Commission Washington, D.C. 20555	Topical Report
	b. PERIOD COVERED (Inclusive dates)
	1982 - 1985

12. SUPPLEMENTARY NOTES

13. ABSTRACT (200 words or less)

Geological systems analogous to proposed packing materials have been reviewed and investigated and approximate temperature limits for smectite, mixed layer smectite/layer smectite/illite and illite have been found to be 100, 200, and 250 C, respectively. All phases are metastable, with reaction rates being controlled by factors influencing kinetics, principally temperature and rock/water ratio. Even over geological time periods the phases may exist metastably at low temperatures with low water/rock ratios. Experiments with bentonite/basalt mixtures confirm that there is little change at 300 C and below in simulated packing conditions for experimental durations of up to a year and a half. Data are consistent with a lack of equillibrium, such that experimental reactions occur at much higher temperatures than in geologic systems, and cannot be used to reliably predict the state of such systems over long time periods. Analysis of geologic systems suggests that a suitable continuous clay matrix can minimize the degree of transition of clays and clay/basalt mixtures.

14. DOCUMENT ANALYSIS - a. KEYWORDS/DESCRIPTORS	15. AVAILABILITY STATEMENT
High-level waste Waste package Packing/backfill materials	Unlimited
b. IDENTIFIERS/OPEN-ENDED TERMS	16. SECURITY CLASSIFICATION
	(This page)
	Non-classified
	(This report)
	Non-classified
	17. NUMBER OF PAGES
	18. PRICE

DO NOT PRINT THESE INSTRUCTIONS AS A PAGE IN THE NUREG REPORT

INSTRUCTIONS

NRC FORM 335, BIBLIOGRAPHIC DATA SHEET, IS BASED ON GUIDELINES FOR FORMAT AND PRODUCTION OF SCIENTIFIC AND TECHNICAL REPORTS, ANSI Z39.18–1974 AVAILABLE FROM AMERICAN NATIONAL STANDARDS INSTITUTE, 1430 BROADWAY, NEW YORK, NY 10018. EACH SEPARATELY BOUND REPORT—FOR EXAMPLE, EACH VOLUME IN A MULTIVOLUME SET—SHALL HAVE ITS UNIQUE BIBLIOGRAPHIC DATA SHEET.

1. **REPORT NUMBER.** Each individually bound report shall carry a unique alphanumeric designation (NUREG) assigned by the Division of Technical Information and Document Control, ADM, in accordance with American National Standard ANSI Z39.23–1974, Technical Report Number (STRN). Use uppercase letters, Arabic numerals, slashes, and hyphens only, as in the following examples: NUREG-0100, NUREG/CP-0010, NUREG/CR-0100, and NUREG/BR-0010. For reports in a series add Vol., Supp., Revision, and Addendum, when necessary. Add contractor cross-reference identification number (if any) below NUREG number, e.g., PNL-XXXX, SANDXX-XXXX, SAI-XXXX.

2. **TITLE AND SUBTITLE.** Title should indicate clearly and briefly the subject (coverage) of the report; including any subtitle to the main title. When a report is prepared in more than one volume, repeat the primary title, add volume number and include subtitle for the specific volume. Use upper and lower case letters, but capitalize computer code names. Do not use acronyms and initialisms in titles; may be added in parenthesis.

3. **LEAVE BLANK.**

4. **DATE REPORT COMPLETED.** Each report shall carry a date indicating month and year project/task completed.

5. **AUTHOR(S).** Give name(s) in conventional order (e.g., John R. Doe, J. Robert Doe). List author's affiliation if it is different from the performing organization.

6. **DATE REPORT ISSUED.** Each report shall carry a date indicating month and year published.

7. **PERFORMING ORGANIZATION NAME AND MAILING ADDRESS.** Give name, street, city, state, and ZIP code. List no more than two levels of an organizational hierarchy. Display the name of the organization exactly as follows: Division, Office, Organization or Government agency, and address.

8. **PROJECT/TASK/WORK UNIT NUMBER.** Use the project, task and work unit numbers under which the report was prepared (if any).

9. **FIN OR GRANT NUMBER.** Insert the FIN or grant number under which report was prepared.

10. **SPONSORING ORGANIZATION.** List NRC Division, Office, U.S. Nuclear Regulatory Commission, Washington, DC 20555.

11. a. **TYPE OF REPORT.** State draft, final, preliminary, topical, technical, regulatory, quarterly, etc., and, if applicable, inclusive dates.

    b. **PERIOD COVERED.**

12. **SUPPLEMENTARY NOTES.** Enter information not included elsewhere but useful, such as: Prepared in cooperation with . . . Presented at conference of . . . To be published . . . Docket No. . . . When a report is revised, indicate whether the new report supersedes or supplements the older report.

13. **ABSTRACT.** Include a brief (200 words or less) factual summary of the most significant information contained in the report. If the report contains a significant bibliography or literature survey or multiple volumes, mention it here. Abstract is to be prepared by author or project manager.

14. **DOCUMENT ANALYSIS**

    a. **KEY WORDS/DESCRIPTORS.** Select from the Energy Data Base Subject Thesaurus, DOE/TIC-700R R-5, the proper authorized terms that identify the major concept of the research and are sufficiently specific and precise to be used as index entries for cataloging.

    b. **IDENTIFIERS AND OPEN-ENDED TERMS.** Use identifiers for project names, code names, equipment designators, etc. Use open-ended (keywords) terms written in descriptor form (14a) for those subjects for which no descriptor exists in the thesaurus.

15. **AVAILABILITY STATEMENT.** Denote public releasability, for example "unlimited", or limitation for reasons other than security.

16. **SECURITY CLASSIFICATION.** Enter U.S. Security Classification in accordance with U.S. Security Regulations (i.e., unclassified).

17. **NUMBER OF PAGES.** Leave blank. (Added by NTIS)

18. **PRICE.** Leave blank. (Added by NTIS)